

# The Extraterrestrial Particles Collector

a project presented to  
The Faculty of the Department of Aerospace Engineering  
San José State University

in partial fulfillment of the requirements for the degree  
**Master of Science in Aerospace Engineering**

by

**Volodymyr Zhukov**

May 2025

approved by  
Dr. Yawo Ezunkpe  
Faculty Advisor



**San José State**  
UNIVERSITY

© 2025  
Volodymyr Zhukov  
ALL RIGHTS RESERVED

# ABSTRACT

## **The Extraterrestrial Particles Collector**

Volodymyr Zhukov

Extraterrestrial materials have always interested scientists and researchers worldwide. They can uncover information about the origin and chemistry of celestial bodies and even life in the solar system. Access to the extraterrestrial materials is very limited and cannot be easily obtained. At the same time, they are always present in the atmosphere in small amounts, slowly descending into lower layers where they mix with terrestrial dust. The amount of extraterrestrial materials increases several times during meteor showers, while their source is also known.

This report covers the project development of the Extraterrestrial Particle Collector probe to attempt to allow the collection of extraterrestrial dust in the high atmosphere, before it gets contaminated with terrestrial dust. It starts with an overview of the previous collector design and its test results, followed by a literature review related to the origin of extraterrestrial particles and their primary sources, existing methods of collecting extraterrestrial particles, the physics of micrometeorite particle behavior, and engineering systems implemented into the drone. It is followed by an overview of the project objectives, methodology, mission statement, stakeholders, and concept exploration.

Using principles of system engineering, the probe is designed at a high level as a system with specific functional and non-functional requirements before it is divided into smaller subsystems, components, and parts with their own requirements. The probe is designed part by part, where each part is analysed as it is designed before being assembled to form components and then subsystems until the system is ready to be tested. The components, subsystems, and system were then verified and validated to make sure that they correspond to the requirements set for them. The project is concluded with some words on its outcome and work that should be done in the future.

## Acknowledgments

I would like to thank Professor Yawo Ezunkpe for being my project advisor, Professor Maria Chierichetti, and Dr. Nikos Mourtos for their guidance during my master's project development. I also would like to thank Rae Chavaux, Tom Rouse, and Erick Charlton for being part of this project in the past and for helping me to develop its first generation.

I would also like to acknowledge my parents, Oleksandr Zhukov and Valentina Zhukova, for believing in me and helping all of this happen.

# Table of Contents

<b>The Extraterrestrial Particles Collector.....</b>	<b>3</b>
<b>ABSTRACT.....</b>	<b>5</b>
<b>The Extraterrestrial Particles Collector.....</b>	<b>5</b>
<b>Acknowledgments.....</b>	<b>6</b>
<b>Table of Contents.....</b>	<b>7</b>
<b>List of figures.....</b>	<b>9</b>
<b>List of Tables.....</b>	<b>11</b>
<b>Symbol.....</b>	<b>12</b>
<b>1. Introduction.....</b>	<b>1</b>
1.1. Motivation.....	1
1.2. The First Extraterrestrial Particles Collector.....	2
1.3. Old Design Description.....	3
1.4. Drawbacks Of The Old Design.....	7
1.5. Literature Review.....	11
<b>2. Project Objective and Methodology.....</b>	<b>42</b>
2.1. Project Objective.....	42
2.2. Methodology.....	42
<b>3. Mission Statement, Stakeholders, and Concept Exploration.....</b>	<b>46</b>
3.1. Mission Statement.....	46
3.3. Stakeholders.....	46
3.4. General Concept.....	47
3.5. Trade Studies.....	48
3.6. Alternative Subsystem Concepts.....	49
<b>4. Concept of Operations.....</b>	<b>51</b>
4.1. Ground Infrastructure.....	52
4.2. The Rocket.....	55
4.3. Flight Plan.....	56
<b>5. System Requirements.....</b>	<b>59</b>
5.1. Functional Requirements.....	59
5.2. Non-Functional Requirements.....	60
<b>6. Component Design.....</b>	<b>61</b>
6.1. Structure.....	61
<b>7. Final EPC System Design.....</b>	<b>95</b>

7.1. EPC System Design Description.....	95
7.2. EPC System Operation Concept.....	96
<b>8. Manufacturing and Assembly.....</b>	<b>97</b>
8.1. Parts Manufacturing.....	97
8.2. Component Assembly.....	104
8.3. Subsystem Assembly.....	107
8.4. System Assembly.....	108
<b>9. Verification and validation.....</b>	<b>108</b>
9.1. Component Verification and Validation.....	108
9.2. Subsystem Verification and Validation.....	109
9.3. System Verification and Validation.....	110
<b>10. Project Outcome and Future Work.....</b>	<b>111</b>
10.1. The Outcome.....	111
10.2. Future Work.....	111
<b>References.....</b>	<b>113</b>
<b>Appendix A - Component geometries and CFD simulation results for component analysis</b>	<b>116</b>
<b>Appendix B - Parts in Slicer Before Manufacturing.....</b>	<b>121</b>

## List of figures

Figure 1.1 - On the left is the rocket with the probe next to the rocket. On the right is the rocket assembly with probe loading on the rail.....	3
Figure 1.2 - At the top is the old MMC probe in complete assembly. At the bottom are the CFD analysis results of the geometry.....	4
Figure 1.3 - On the left is the blueprint for the collector chamber assembly. On the right is the working principle of the collector chamber.....	6
Figure 1.4 - On the left is the rotor computer and custom board on the plastic model of the MMC. On the right is the Kate-3 on the MMC and the forward section with dummy chambers.....	6
Figure 1.5 - From above, the entire MMC probe assembly in the exploded view. From below, the CAD model of the rocket assembly with the MMC probe and sections nomenclature.....	7
Figure 1.6 - On the left is the aft section with a working GPS after the crash landing. On the right, the forward section is crushed into a few pieces near the round crater, a few meters away from the aft section.....	8
Table 1.1 - Drawbacks of the old design.....	10
Figure 1.7 - Aerosol Number Density/cm <sup>3</sup> during a meteor shower.....	12
Figure 1.8 - Average temperature profile for the lower layers of the atmosphere.....	15
Figure 1.9 - Total mass influx of particles on earth by mass given by sources [4] and [23].....	18
Table 1.2 - The diameter and maximum concentration of particles for independent flow.....	19
Figure 1.10 - Particle moving through the air, which is also moving(29).....	21
Figure 1.11 - Drag coefficient of a sphere versus Re (29), with separation into 5 commonly divided flow regimes..	21
Table 1.3 - Dynamic shape factors, averaged over all orientations(29).....	24
Figure 1.12 - On the left, cyclone collector particle separation. In the middle, a mist eliminator with one curve and two collection openings. On the right, cascade impactor: schematic diagram, showing trajectories of particles of three different diameters (29).....	25
Figure 1.13 - Secondary electron images. (a) Anhydrous CP IDP. (b) Hydrated CS IDP. (c) Single-mineral forsterite grain with adhering chondritic material. (d) Optical micrograph of giant cluster IDP in silicone oil on ER2 collection flag [30].....	26
Figure 1.14 - V-shaped delivery process diagram for system engineering.....	27
Table 1.4 - Hardware nomenclature in the system development [34] from the top to the bottom level, where 1 is the top level and 5 is the bottom level.....	28
Figure 1.15 - Inlets with different spillage [35].....	30
Figure 1.16 - Compressible flow functions vs Mach number[35].....	31
Figure 1.17 - Inlet spillage [35].....	32
Figure 1.18 - Command module aerodynamics.....	34
Figure 1.19 - An example of the existing types of gears used in one system.....	37
Figure 1.20 - An example of a planetary gear with a smaller sun gear.....	38
Table 1.5 - The material characteristics and cost estimation for the materials available for the project.....	40
Figure 1.21- The diagram of the axial compressor used in turbojet engines.....	41
Table 4.1 - Table of trade studies of the EPC project.....	48

Figure 4.1 - Concept of operation.....	51
Figure 4.2 - The map of the FAA launch site [40].....	52
Figure 4.3 - Launching rails at the FAR launch site in the Mojave Desert. Baxter 60-Foot T-Rail at the left and Microcosm 60-Foot T-Rail at the right.....	53
Figure 4.4 - Buried in the ground bunker at the FAA launch site.....	54
Table 5.1 - Functional Requirements.....	59
Table 5.2 - Non-Functional Requirements.....	60
Figure 6.1 (At the left is the sketch; At the right is the geometry of the first design).....	64
Figure 6.2 - At left is the sketch; At the right is the geometry of the second design.....	65
Figure 6.3 - At the left is the sketch; At the right is the geometry of the third design.....	65
Table 6.1 - The analysis of 4-inch long nosecone configurations with variable curvature radius.....	65
Figure 6.4 - CFD analysis of the nosecone.....	67
Table 6.2 - The analysis of 4-inch long nosecone configurations with variable curvature radius and central nosecone feature at the distance from the exit...	67
Table 6.3 - The analysis of 4-inch long nosecone configurations with variable curvature radius and central nosecone feature at the distance from the exit...	68
Figure 6.5 - CFD analysis of the collector unit.....	71
Figure 6.6 - Iteration 6 of cylindrical single opening per stage collector design geometry and with one hundred 5-micrometer diameter particles injection.....	72
Figure 6.7 - Iteration 6 of cylindrical multiple opening per stage collector design geometry and with one hundred 5-micrometer diameter particles injection.....	73
Figure 6.8 - Iteration 1 of extruded-washer shaped with multiple openings per stage collector geometry and with one hundred 5-micrometer diameter particles injection.....	74
Figure 6.9 - The final iteration of the collector unit adapted for the rest of the probe assembly.....	75
Figure 6.10 - The NACA 65-series airfoils analyzed for the compressor.....	77
Fig 6.11 - The NACA airfoil sketch with a one-unit length and extruded shape with one rounded edge.....	78
Figure 6.12 - The sketch of the designed epicyclic gear with all measurements in inches and the 3d assembly of the single stage of the gearbox system.....	80
Figure 6.13 - The assembly of three three-stage planetary gearbox after several iterations of physical model testing... 81	81
Figure 6.14 - Nosecone subsystem components separately and in assembly.....	82
Figure 6.15 - The initial 3D model of the turbine part.....	85
Figure 6.16 - The shaft design with connectors.....	86
Figure 6.17 - The geometry of the airbrake with attachment to the tail and gearbox.....	87
Figure 6.18 - The blade position and sizing on the turbine.....	88
Figure 6.19 - The assembly of the stabiliser.....	89
Figure 6.20 - The sealing principle when intake is open on the left, and when intake is closed on the right.....	90
Figure 6.21 - SG90 Micro Servo Motor.....	91
Figure 6.22 - The main body part at the top contains electronics and the collector unit, and the tail connector secures the collector unit and the stabiliser.....	92
Figure 6.23 - Arduino Nano BLE 33.....	93
Figure 6.24 - SparkFun OpenLog and MicroSD.....	93
Figure 6.25 - Featherweight GPS transmitter and receiver.....	94
Figure 7.1 - The external geometry of the assembled EPC probe system.....	96

Figure 7.2 - Section view of the assembled EPC probe system.....	96
Figure 8.1 - Example of part slicing and 3D printing on Nosecone Part 1.....	99
Table 8.1 - Nosecone component parts dimensions and parameters.....	99
Table 8.2 - Compressor component parts dimensions and parameters.....	100
Table 8.3 - Gearbox component parts dimensions and parameters.....	101
Table 8.4 - Body Frame component parts dimensions and parameters.....	102
Table 8.5 - Collector Unit component parts dimensions and parameters.....	102
Table 8.6 - Stabilizer component parts dimensions and parameters.....	103
Figure 8.** - The nosecone component assembly without stators.....	104
Figure 8.** - The compressor component assembly with rotor blades).....	105
Figure 8.** - The gearbox inside the nosecone from the top and the bottom.....	105
Figure 8.** - The assembly of the collector unit.....	106
Figure 8.** - The nosecone subsystem assembly.....	107
Figure 8.** - The body frame subsystem assembly.....	107
Figure 8.** - The stabilizer subsystem assembly.....	108
Figure 8.** - The assembled EPC probe.....	108
<b>Figure 9.1 - Force testing for the nosecone.....</b>	<b>109</b>
<b>Figure 9.2 - The testing handle for the gearbox.....</b>	<b>109</b>

## List of Tables

Table 1.1 - Drawbacks of the old design.....	10
Table 1.2 - The diameter and maximum concentration of particles for independent flow.....	19
Table 1.3 - Dynamic shape factors, averaged over all orientations(29).....	24
Table 1.4 - Hardware nomenclature in the system development [34] from the top to the bottom level, where 1 is the top level and 5 is the bottom level.....	28
Table 1.5 - The material characteristics and cost estimation for the materials available for the project.....	40
Table 4.1 - Table of trade studies of the EPC project.....	48
Table 5.1 - Functional Requirements.....	59
Table 5.2 - Non-Functional Requirements.....	60
Table 6.1 - The analysis of 4-inch long nosecone configurations with variable curvature radius.....	65
Table 6.2 - The analysis of 4-inch long nosecone configurations with variable curvature radius and central nosecone feature at the distance from the exit.....	67
Table 6.3 - The analysis of 4-inch long nosecone configurations with variable curvature radius and central nosecone feature at the distance from the exit.....	68
Table 8.1 - Nosecone component parts dimensions and parameters.....	99
Table 8.2 - Compressor component parts dimensions and parameters.....	100
Table 8.3 - Gearbox component parts dimensions and parameters.....	101
Table 8.4 - Body Frame component parts dimensions and parameters.....	102
Table 8.5 - Collector Unit component parts dimensions and parameters.....	102
Table 8.6 - Stabilizer component parts dimensions and parameters.....	103

## Symbol

Symbol	Definition	Unit
T	Temperature	K/C
p	Pressure	KPa
h	Altitude	m
c	Mass concentration of the particles	Unitless
$c_{number}$	Particle number concentration	Unitless
$D_p$	Diameter of the particles	m
$C_D$	Drag coefficient for a particle based on frontal area	Unitless
$\vec{U}$	Carrier fluid velocity	m/s
$\vec{v}$	Particle velocity	m/s
$\vec{v}_r$	Relative velocity of particle	m/s
Kn	Knudsen number	Unitless
C	Chord Length	in
C	Cunningham Slip Factor	Unitless
Cg	Center of gravity	m
Cp	Center of pressure	m
r	Radius of gear	m
z	Number of teeth	Unitless

<b>Greek Symbols</b>		
$\rho$	Density	kg/m <sup>3</sup>
$\rho_p$	Particle density	kg/m <sup>3</sup>
$\mu$	Dynamic viscosity	Pa*s
$\nu$	Kinematic viscosity	m <sup>2</sup> /s
$\lambda$	Mean Free Path	m
$\omega$	Angular Velocity	deg/s
<b>Acronyms</b>		
EPC	Extraterrestrial Particles Collector	
NACA	National Advisory Committee for Aeronautics	
GPS	Global Positioning System	
LiFePO <sub>4</sub>	Lithium Iron Phosphate	
LTO	Lithium Titanate	
NiMH	Advanced Nickel-Metal Hydride	
Li-Ion	Lithium Ion	
V&V	Verification and Validation	

# 1. Introduction

## 1.1. Motivation

### 1.1.1. The Scientific Need

Every day, the Earth gains tons of extraterrestrial materials. All this material comes in different forms and is slowed down by the Earth's atmosphere. Some, as meteoroids burning through the skies to the point of impact, while most of them get to the Earth as dust. The tons of dust are being slowed down in the atmosphere, and extraterrestrial materials gradually make their way to the ground to be mixed with the rest of the particles that once came to the Earth the same way, but are going to be forever changed due to the chemistry on Earth. From those tons, we can rarely gather more than several particles using expensive collection systems. It makes extraterrestrial particles very limited and inaccessible to many researchers. In addition, there are not enough samples gathered in total, especially considering the composition of those extraterrestrial materials may differ drastically for a short period, depending on the time of the year. Our current rates of gathering those materials are not sufficient to satisfy the scientific interest of those, who don't have access to expensive sample collection missions, and creating a collection method that could be cheap, accessible, and working at any desired time from almost any point of earth could increase access to extraterrestrial materials and let to more scientific data gathered from them.

### 1.1.2. Engineering Challenge

Creating a new engineering system that is able to collect extraterrestrial material mid-air is a challenge that has many different solutions, with advantages and disadvantages. While existing solutions can complete the task of collecting material, they are not able to achieve some of the requirements to be used by a broader number of researchers or for specific cases. The systems are usually expensive and require the usage of very limited and high-maintenance specialized equipment, or require a lot of time for collection and resources for recovery. Some methods lack decontamination or are impossible to use over certain areas of the atmosphere. Thereby, there is a chance to try to solve an existing challenge differently, look to other ways to

complete the task, and try to make it in a way that can be used to increase accessibility of extraterrestrial material to the scientific community.

### 1.1.3. Personal Motivation

I am motivated to work on this project because of my previous experience with developing extraterrestrial material collectors, which was not successful. I believe that the accumulated knowledge and experience gathered throughout the development of the previous system allow me to approach the same problem with a better understanding of how to perform the task and make the system perform better while being more reliable, practical, and accessible. In addition, learning more and experiencing the creation of payloads and probes will benefit my future career in the space industry.

## 1.2. The First Extraterrestrial Particles Collector

In the first weeks of September 2023, I was introduced to Erick Charlton, and together with Tom Rouse and Rae Chauvaux, who joined soon after we started to work on the Micrometeorite Collector project (From now on MMC). Several consecutive months were spent on research, meetings with people in the field from SETI and NASA, and discussions on the nature of the project and how we wanted it to be done. It was decided to design a probe that could fit in a two-stage sounding rocket that Tom Rouse, without help, will design and assemble, while I will be focused on the probe design, analysis, and assembly. From December to February, I spent time on design, analysis, and parts search, and after approval of the final design by the team, I began to assemble it with Rae Chavaux. It took two months to complete the probe and test its mechanical and recovery systems. On April 27, 2024, during the Lyrid meteor shower, it was launched on two-stage rockets in the Southern California desert. The rocket trajectory got way too inclined, and instead of reaching 100,000+ ft as was simulated, it flew on an angled ballistic trajectory, barely reaching 35,000 ft. The probe was ejected at apogee as intended, stabilized, and flew down on its own, crashing into the sand close enough to get a GPS signal from where it landed and recover it.



Figure 1.1 - On the left is the rocket with the probe next to the rocket. On the right is the rocket assembly with probe loading on the rail

### 1.3. Old Design Description

The Probe that was built for this mission previously was a 25-inch-long, 3.9-inch-diameter probe, designed to withstand loads associated with an energetic launch. The self-stabilizing design comprises a 7-inch-long forward section and an 18-inch aft section. The total weight of the probe was 3.96 pounds. The forward section houses the airflow manager, four collection chambers with dual-layer cascading impactors, the protective rotor door assembly, the rotor computer, and the power source. The aft section contains the flight electronics, air brakes, and recovery system, which consists of a deployment charge and parachute.

The main idea behind the probe's geometry was to provide the highest possible area of intake allowed by the launch vehicle for the airflow manager to capture as many particles as possible, and self-stabilize the probe in vertical orientation, where the intake surface had the smallest angle difference from airflow direction. The only feature that did not follow the main idea was an opening at the side of the forward section and an airbrake disc that served the function of letting the shock cord through the probe to connect the nose cone to the second stage of the rocket.

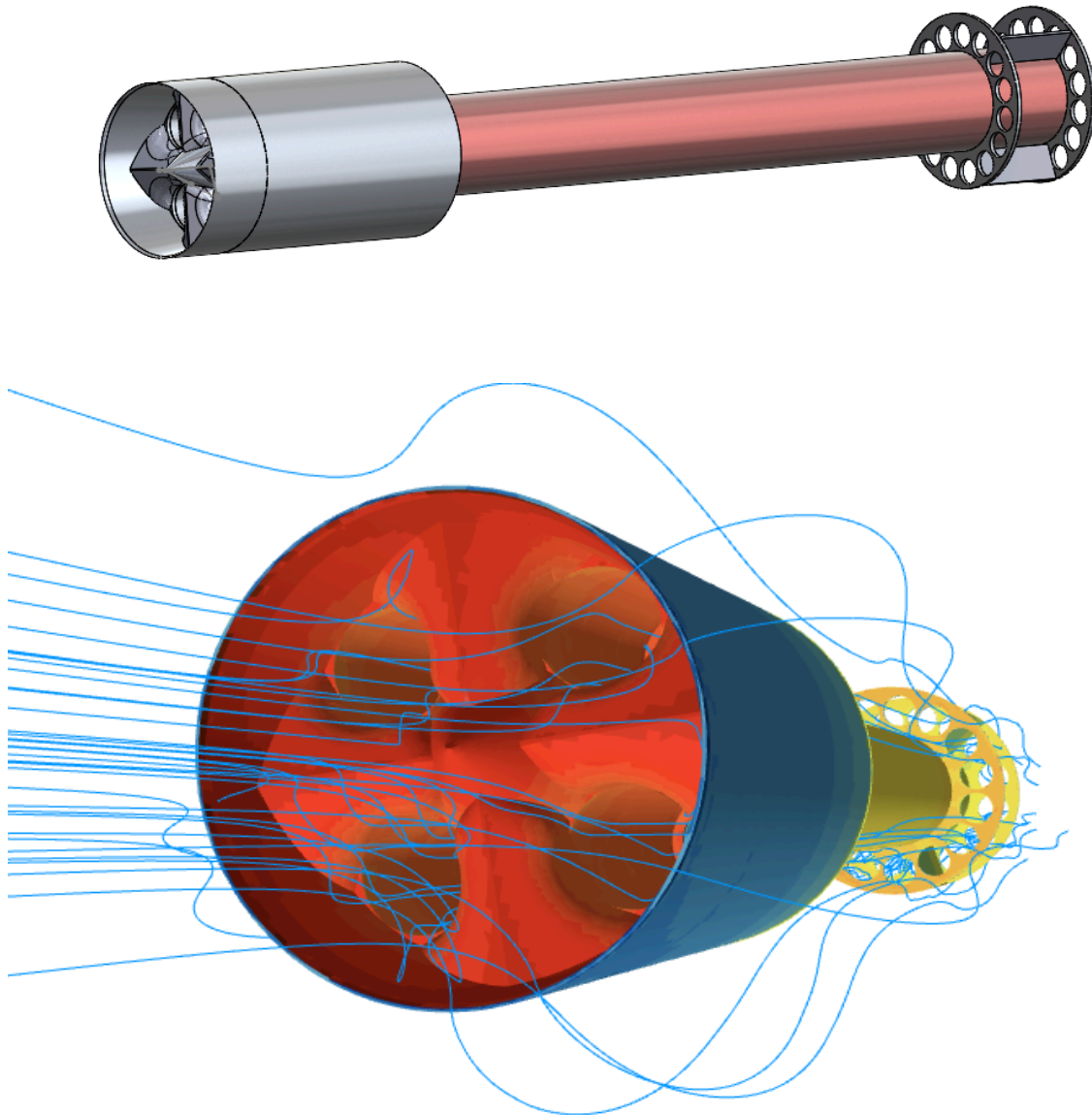


Figure 1.2 - At the top is the old MMC probe in complete assembly. At the bottom are the CFD analysis results of the geometry

Computational analysis and CFD modeling have been used to design the MMC to achieve two objectives: maintain a self-stabilizing descent and maximize sampling volumes. To tune the MMC's design for optimal flight stability and collection performance at high and low altitudes. The MMC was designed to dampen both post-deployment tumbling and during descent oscillations caused by turbulence. This is accomplished by balancing the nose with the tail

section drag. Additionally, the airflow manager, air brakes, and body tube were modeled for their influences on stability.

The Airflow Manager directs the atmosphere being sampled toward four 1.1-inch-wide collection chambers, each housing dual-layer impact collectors. As the MMC falls, high-speed air is entrained around the collection plates/targets. Heavier, high-mass particles collide with and stick to the 1st collector plates, which are covered with viscous silicone oil. Smaller, lighter particles tend to deflect around the first plate, but some could strike the second. The smallest particles and dust would still leave the collector chamber uncollected.

Before and after the collection, the collection chamber could be accessed by opening its structure. It was necessary for the application of the silicon oil of a certain viscosity, which was the main method to collect and contain the gathered material in the non-reactant surroundings, and to let easy access to the collected material for future study in the lab, where the entire probe should have been delivered prior breaking the seal. Dr. Marc Fries provided the proper silicon oil for the collector chamber in the Astro Material Acquisition and Curation Office at NASA Johnson Space Center.

To seal and unseal the collector chamber during the flight, it was supported with a rotational mechanism that would rotate all four chambers between the two possible positions and back in this order: 1. Closed position to stay sealed before flight, 2. Open position to start collection after deployment, 3. Closed position during descent when a certain altitude is reached. To make this possible the old MMC probe was supplied with the Greartisan DC 12V 10RPM rotor in the middle, an Arduino Nano computer programed with a custom code controlling the rotation using signals from the flight computer during certain events of descent, and a power supply of replaceable batteries enough to stay on for many hours before flight while being loaded into the rocket. To perform such clockwise, counterclockwise rotation using a connection to the rotor, an additional custom-made board was made using several transistors to enable reverse mode whenever the computer sends a signal of a certain command in the sequence.

All of it was controlled by the Kate-3 transmitter signals that were programmed to occur at specific moments of the flight, registered by changes in trajectories and the GPS location of the probe. The Kate-3 transmitter is both a GPS and a flight computer, which means it has a Pyro board that can send signals by increasing voltage to the pyro charges for different events during the flight, programmed beforehand. Signals are sent by the wires, directly connecting the flight computer with the rotor computer by two signal wires and two ground wires, while the deployment charge of the recovery system was connected with just one signal and ground wire. The wires to the rotor computer had to go through the special opening in the collection chamber space, where they were rotating, in a way not to obstruct rotation.

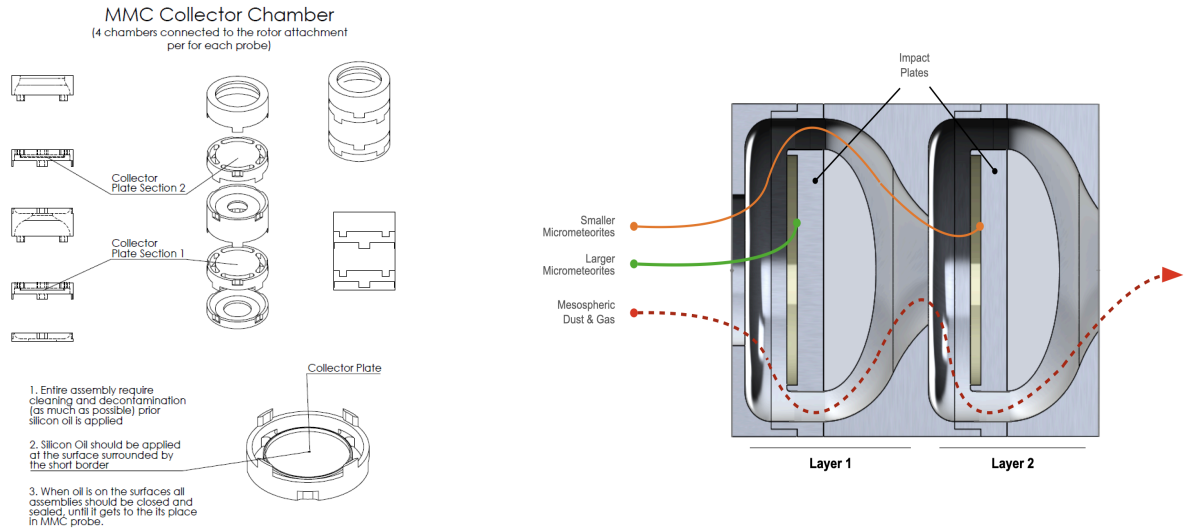


Figure 1.3 - On the left is the blueprint for the collector chamber assembly. On the right is the working principle of the collector chamber



Figure 1.4 - On the left is the rotor computer and custom board on the plastic model of the MMC. On the right is the Kate-3 on the MMC and the forward section with dummy chambers

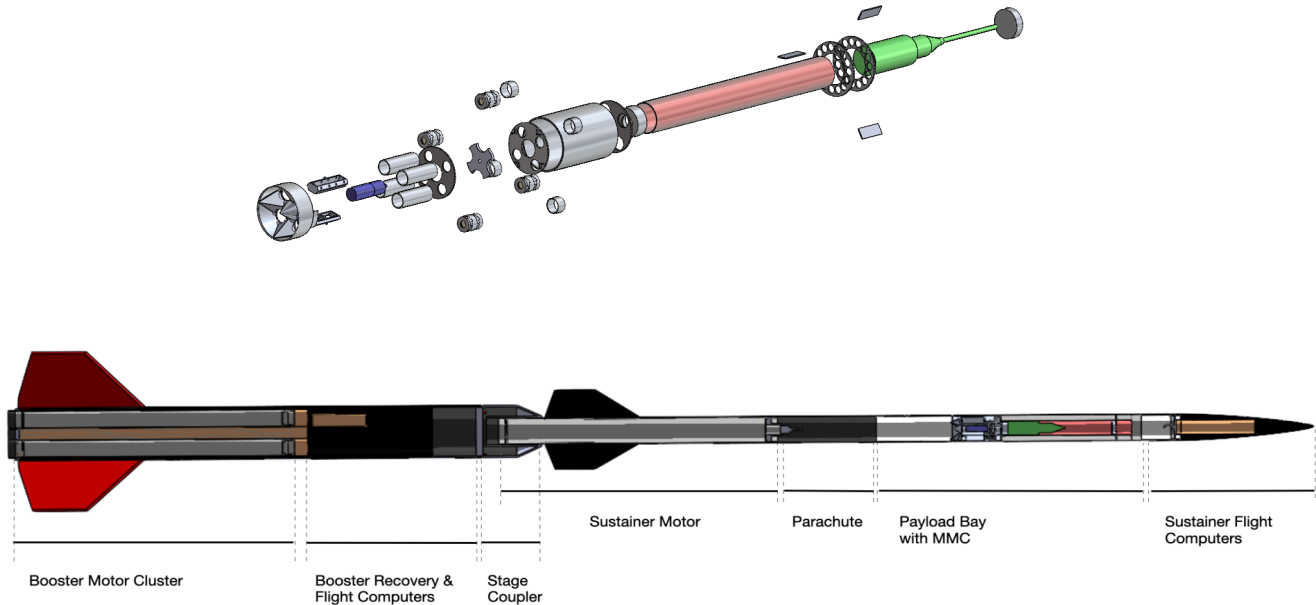


Figure 1.5 - From above, the entire MMC probe assembly in the exploded view. From below, the CAD model of the rocket assembly with the MMC probe and sections nomenclature

The description given above is enough to understand the assembly features and working principle of the old MMC probe and its components. However, it was necessary to properly describe the problems with the design that were found during the assembly and operation of the old MMC design.

## 1.4. Drawbacks Of The Old Design

The two pictures below were taken at the MMC probe's landing point. Despite the incorrect flight performance of the rocket resulting in possible deployment at high velocity, the probe should have survived it much better than it did in reality. It suggests that the drawbacks of the old design were numerous.



Figure 1.6 - On the left is the aft section with a working GPS after the crash landing. On the right, the forward section is crushed into a few pieces near the round crater, a few meters away from the aft section.

The old design was the first attempt to do anything like that, and it was the first test of a system similar to this. It was not clear what problems could have occurred when the system was done. There was no internal data recording of flight parameters inside the probe, which made the problem of figuring out what went wrong with the probe harder. However, some known drawbacks or features could have been done in a better way to improve the analysis, testing, and performance of the system.

The first and main possible reason for the wrong recovery system deployment was the wiring of the internal systems. Due to the location of different subsystems, the wiring had to go through the entire probe, and due to the specifics of assembly, it had several connectors between sections. It was done poorly and could have a weak strength. That could have been not enough, and it disconnected during high-G linear and angular dynamics. The ascent or deployment at a much higher horizontal velocity than what was expected resulted in very high forces during deployment. Another big drawback of the probe's function was the lack of redundancy.

Due to limited resources, space, and time, it had only one component for each system, which could have drastically decreased its reliability and could have affected the final result. Disconnection or improper work of any of the components of the Flight Computer, GPS, or recovery system could result in the wrong operation or non-deployment of the recovery parachute.

It is known that the GPS signal from the probe was not received a few seconds after launch, and while it was operating after landing, it is unknown if it was able to register its location during the flight and send signals to the recovery system. The GPS signal in the probe was also influenced by the metal parts of the probe. Despite the transmitter being at least two inches away from any metal parts, as recommended by its creator in one of the numerous discussions. The signal certainly interfered to some degree, and likely did not have a connection to reach the receiver until it landed.

The position of internal systems and collection chambers required the collection chamber section to be opened shortly before the launch, which could have very negatively affected the results of the collection by contaminating it with a large amount of dust in a very dry location at the final assembly of the system. While it would not critically compromise the collection, it could lead to high amounts of terrestrial particles in the collector chambers, which would make the goal of finding extraterrestrial particles in silicon oil more difficult.

The intake area, although it was limited by the rocket size, was too small to collect a substantial amount of micrometeorites during flight. Depending on the altitude of deployment, it could gather just a few extraterrestrial particles that would stick to its chamber surfaces. The efficiency of the collection could be higher if the drawback of high total pressure at the intake, resulting in the loss of potential airflow containing particles, could be resolved.

The recovery deployment method could possibly be harmful to the parachute integrity. It could be a result of high packing density and an insufficient protection layer.

Certain structure components manufactured out of aluminum were much stronger than would be needed. While making the structure very reliable, it results in a higher mass of the probe, which in turn makes it harder to manage stability on the rocket and to slow down the probe in low-pressure atmosphere layers after deployment.

The probe also had non-accessible electronics after sealing, which made it harder to operate during preparations. It could only be accessed before collection chambers were inserted, and could not be opened as soon as they were inside, to avoid contamination. All systems had to work for several hours way before the probe was launched, draining the power supply. As a result, the power system of certain components was sufficient to work for several hours, which might not have been enough due to long preparations or delays at the launch site. For the GPS and recovery system, a separate, reliable power supply was used.

Finally, the way the probe interacted with the second stage of the rocket influenced the final geometry. For the second stage to stay in one connected assembly, the shock cord had to pass through the collector probe. It was done by utilizing the cut on the side of the body and airbrake, which can be visible in Figures 1.1, 1.8, and 1.12. The attempt to close this opening from the external side airflow was not successful and had to be removed at the final assembly. While it was an acceptable solution, it was located in a previously designated place and did not cause any problems with other subsystems. In future designs, it would be preferable to fully isolate the shock cord opening from other systems, especially the collector chamber, since contamination due to side airflow was an issue.

To structure the described known drawbacks of the old design with their reasons and affected performance, they will be put together in the table below.

Table 1.1 - Drawbacks of the old design

	<b>Drawback</b>	<b>Possible problems caused by a drawback</b>
1	No long-term data recording	After the flight test, the analysis is very limited
2	Wiring planning and quality	Harder to assemble and possible discontinuity in connections at high forces
3	Redundancy	Lack of redundancy decreases the chance of proper mission operation
4	Reliability of the recovery system	Decreased chance of probe recovery during flight
5	GPS signal interference	Possible problems with GPS-dependent flight events, no real-time probe data, and geolocation issues after landing
6	Internal systems location	Convenience of assembly and simplicity of use, increased time of preflight preparations, and possible wiring issues
7	Contamination risk	Decreased chance of mission outcome, difficulty in post-flight sample analysis
8	Overweight structure system	Decreased apogee altitude, rocket stability issues, and higher flight velocity after deployment
9	Accessibility	Longer preparation, contamination risk, and higher power supply requirements
10	Short power supply	Decreased chance of proper mission operation, possible shutdown of subsystems before landing
11	High intake pressure	Reduced efficiency of sample collection
12	Shockcord pass	Possible contamination or deployment issues

While making a new system entirely avoiding previous drawbacks might not be possible, the correction and additional work on the drawbacks above could significantly improve the overall performance and reliability of the system. Thereby, the new design should include solutions and better reasoning behind certain design decisions, following the requirements and the feasibility of the extraterrestrial material collection mission using large-scale amateur rockets.

## 1.5. Literature Review

For a better understanding of the development of the new collection system, it is necessary to review topics directly related to its application conditions, subject, other existing methods, and engineering systems and principles that can be used.

### 1.5.1. Genesis and Nature of Extraterrestrial Dust

At any time, the atmosphere contains extraterrestrial dust, as well as dust from terrestrial sources. This dust can be created in a few ways, but usually, it happens when a meteoroid small enough to enter the atmosphere but does not reach the ground. Those meteoroids can be big enough to reach relatively dense atmospheric layers, heat up, and evaporate, leaving a tail of particles behind. The meteoroids as large as 200 metric tons can evaporate before reaching atmospheric layers below 50 kilometers, converting their entire mass into extraterrestrial particles. Some small enough meteoroids, usually several hundredths of a gram, can slow down before reaching high enough temperatures, and slowly descend unchanged through the atmosphere until they reach the ground[2][3]. While it might be surprising, most of the extraterrestrial mass influx is happening due to particles of the size of around two hundred micrometers or less, while massive meteoroids can temporarily take over for short durations of time[4]. The total extraterrestrial mass influx from all kinds of sizes can differ significantly depending on the Earth's orbital position relative to meteor structures, such as meteor showers.

### 1.5.2. Meteor Showers

During meteor showers, the flux of extraterrestrial materials can increase up to  $10^5$  from its normal levels for a few hours [2]. Thereby, meteor showers present an increased interest as a source of extraterrestrial particles for short-duration missions designed to collect them. The total amount of meteor showers is still being cataloged; however, by the estimation from 2016, it was proven that the existence of at least one hundred twelve meteor showers, thirty-two of which have known parent bodies, and five hundred sixty-three more are in the working list. The meteor showers also possess an additional interest because they can reveal more data about the past of the solar system [5][6], while for this project, they drastically increase the amount of extraterrestrial particles for a short duration of time, with higher chances of capturing a particle with a known origin. While all meteor showers result in a higher influx in the Earth's atmosphere, some of them that bring a much higher influx might be favorable targets for extraterrestrial particle collection, with the biggest of them being the Perseid meteor shower [8], and the Geminids as the second biggest. The known big meteor showers also relate to such meteor showers as Quadrantid, Lyrids, Eta Aquariids, Delta Aquariids, Alpha Capricornids, Orionids, Taurids, Leonids, and Ursids, as marked by the American Meteor Society. The list is not limited to those, while other, smaller, meteor showers are also creating an additional influx of

extraterrestrial matter, although in smaller volumes [5]. An interesting aspect of meteor showers is also their period. Each meteor shower appears at a certain time of the year, as the Earth goes around its orbit, which gives a foreknown time to observe or collect material from each of them. Most of them usually last for one to two days, until the intensity of the additional influx decreases again to normal levels[9].

### 1.5.3. Aerosols in Atmospheric Layers

Another convenient feature of the particles in the atmosphere is that particles of certain sizes and densities are much more abundant at certain levels of the atmosphere than others, while one of them, so-called the Stratospheric Aerosol Layer, aka Junge Layer, at the altitude of around twenty kilometers on average accumulates higher presence than other layers around it, while being high enough to reduce amount of particles of terrestrial origin reaching such heights[7][10]. While the total density of the particles at different atmospheric layers changes, it can be concluded that the highest density of extraterrestrial particles of submicrometer size can be detected at altitudes below twenty-five kilometers in regions at average longitudes and during the biggest meteor showers[11].

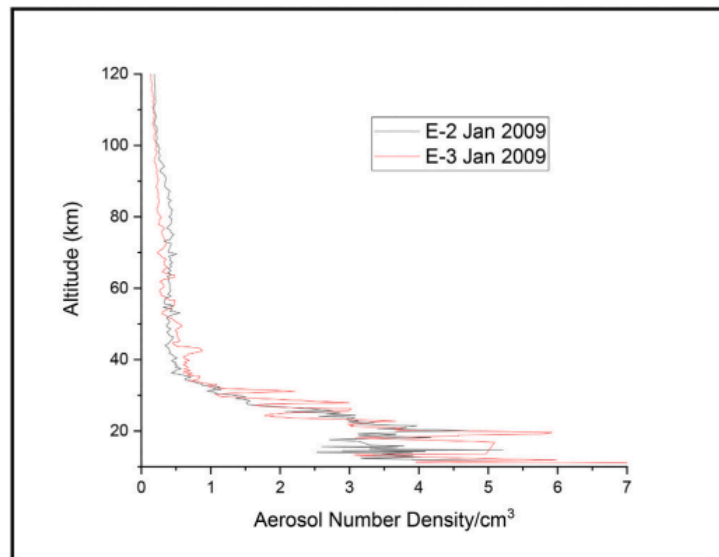


Figure 1.7 - Aerosol Number Density/cm<sup>3</sup> during a meteor shower

### 1.5.4. Existing Collection Methods

There are different ways of collecting extraterrestrial particles in the air or even in space. It is worth going over them to see how they are working, not to reinvent the wheel, and to see if

some parts of already existing systems can be used as legacy systems with proven concepts and as sources of data.

#### 1.5.4.1. Collection in Space

The interest in collecting and analyzing extraterrestrial particles inspired many scientists and teams to attempt their collection both in the atmosphere and beyond the Karman line. Several experiments were conducted in space using aerogels of very low density. Aerogel plates, being exposed to space in low Earth orbit for many months, were able to collect some particles of different sizes. The purity of aerogel and the very low amount of terrestrial particles make this method of collection very clean, while it is very long and expensive to position collection modules or satellites in orbit and recover them. One of the first experiments of such kind was conducted using a space shuttle for deployment and recovery of the aerogel plates[12], while another used a module attached to the international space station, and aerogel plates were exposed to the open space for a few years, and then analyzed, resulting in more than 300 identified impacts over three years [13][14]. While collection located in space is certainly the cleanest way to collect extraterrestrial particles, the duration and impossibility of quick analysis of impacts make it almost impossible to tell with certainty the meteor shower from which certain particles could originate.

#### 1.5.4.2. Collection by Plane

Another method of collection of particles is plane collection, using aircraft able to fly up to sixty thousand feet in height in the stratosphere to perform collection on special collection pylons, covered with viscous silicon oil in relatively clean conditions[15][16][17]. While the collection using such a method is much higher than any other method, aircraft are not able to reach layers of atmosphere around twenty kilometers and above, where the Junge layer is located at average longitudes. Operating such planes can be very costly and result in around 12 particles per collector[15].

#### 1.5.4.3. Collection by Balloon

One more way used to collect particles is stratospheric balloons, capable of operating at altitudes higher than twenty kilometers. Such balloons can provide a good platform for long-duration missions and stay in the stratosphere for days. The collection will depend on the hardware used and the altitudes of operation[1]. Such a way can make a medium or long-duration collection in relatively clean conditions, resulting in a high amount of particles due to the amount of air that is going through the collector over the span of days. The negative side of the collection using stratospheric balloons is a significant limit on payload mass and the

absence of controllability. The balloon will be directed wherever the wind is blowing and will require other vehicles to recover the payload, possibly from very distant and isolated locations.

#### 1.5.4.4. Collection Using Rockets

The last existing method of airborne collection right now is collection using rockets, which is the fastest way, taking from five to twenty minutes from the launch to landing. The sampling rocket flies through all the layers of the atmosphere below the designated altitude twice, while doing it at very high velocities, creating a possibility of particle fracture. While it depends on the method of collection, high velocities make the collection of the smaller particles more complicated, due to the influence of the strong aerodynamic forces around the rocket and instruments on particles. It also requires a rapid system of enabling and disabling collection to avoid contamination in the lower atmosphere [18][19][20]. The rocket collection is very similar to the one used in this project.

#### 1.5.5. Atmospheric Layers and Conditions

Earth's atmosphere has major 5 layers that differ in their conditions. Since the particles start to slow down significantly at an altitude of around 100km, any layer above it will not influence particle behavior, and thereby we need conditions of 3 lower layers of the atmosphere.

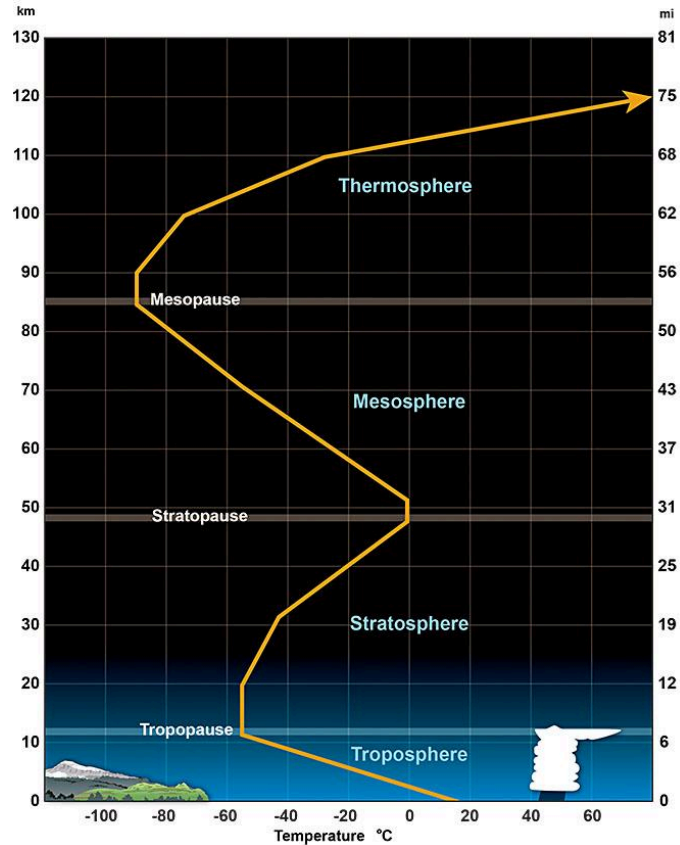


Figure 1.8 - Average temperature profile for the lower layers of the atmosphere

#### 1.5.5.1. Troposphere

Earth's troposphere extends from Earth's surface to, on average, about 12 kilometers, with its height lower at Earth's poles down to 6 km and higher at the equator, up to 18-20 km. This layer holds about 99 percent of all water vapor and aerosols. In the troposphere, temperatures typically go down the higher you go, since most of the heat found in the troposphere is generated by the transfer of energy from Earth's surface. The temperature on average ranges from 17°C at sea level to -51°C at the tropopause. The troposphere is the densest atmospheric layer, compressed by the weight of the rest of the atmosphere above it. Most of Earth's weather happens here, and almost all clouds that are generated by weather are found here.[26][27]

#### 1.5.5.2. Stratosphere

Located between approximately 12 and 50 kilometers (ranges with latitude). In this region, the temperature increases with height. Heat is produced in the process of the formation of ozone, and this heat is responsible for temperature increases, from an average of -51°C at the

tropopause to a maximum of about  $-15^{\circ}\text{C}$  at the top of the stratosphere. This increase in temperature with height means warmer air is located above cooler air. This prevents convection as there is no upward vertical movement of the gases. The stratosphere is nearly cloud- and weather-free, but polar stratospheric clouds are sometimes present in its lowest, coldest altitudes. It's also the highest part of the atmosphere that jet planes can reach. [26][27]

#### 1.5.5.3. Mesosphere

Located between about 50 and 85 kilometers above the Earth's surface, the mesosphere gets progressively colder with altitude. The top of this layer is the coldest place found within the Earth system, with an average temperature of about  $-85^{\circ}\text{C}$ , while the bottom can heat up due to reasons described before, up to  $-15^{\circ}\text{C}$ . The very scarce water vapor present at the top of the mesosphere forms noctilucent clouds, the highest clouds in Earth's atmosphere. Most meteors burn up in this atmospheric layer. Sounding rockets and rocket-powered aircraft can reach the mesosphere. [26][27]

#### 1.5.5.4. Atmospheric Conditions Equations

The equations for temperature and pressure for this atmosphere differ depending on altitude, and are not always directly related to the atmospheric layer. The equations given below are for certain altitude ranges at normal atmospheric conditions for the metric system, generated by the model developed from atmospheric measurements that were averaged and curve-fitted. [28]

##### **Density for any altitude**

$$\rho = p/[0.2869 * (T + 273.15)] \quad (1.1)$$

##### **For altitudes below 11,000 meters**

$$T = 15.04 - 0.00649 * h \quad (1.2)$$

$$p = 101.29 * [(T + 273.15)/288.0]^{5.256} \quad (1.3)$$

##### **For altitudes between 11,000 and 25,000 meters**

$$T = -56.46 \quad (1.4)$$

$$p = 22.65 * e^{(1.73 - 0.000157 * h)} \quad (1.5)$$

##### **For altitudes from 25,000 meters and above**

$$T = -131.21 + 0.00299 * h \quad (1.6)$$

$$p = 2.488 * \left(\frac{T+273.15}{216.6}\right)^{-11.388} \quad (1.7)$$

Where  $\rho$  is density in  $\text{kg/m}^3$ ,  $T$  is temperature in Celsius,  $p$  is pressure in KPa, and  $h$  is altitude in meters.

Those equations are valid for altitudes higher than 25 000 meters, they are not valid for very high altitudes, reaching mesosphere and higher, since temperature starts to decrease again, so it is safe to assume they are valid for up to 50 000 meters, which is higher than the expected altitude of this project.

### 1.5.6. Behavior of Particles

#### 1.5.6.1. The Abundance of Extraterrestrial Particles

The behavior of the particles varies significantly due to their sizes and composition. All of the methods described above depend on so-called Inertial collection techniques. It is a way to collect particles using their mass, which is substantially higher than the mass of gas particles surrounding them. [21][22] The behavior of the particles greatly depends on their mass, shape, and density. From previous research, up to two-thirds of a mass influx of extraterrestrial materials have a weight between  $10^{-6}$  and  $10^{-3}$  gram, and a radius between 49 micrometers and 490 micrometers[24]. The data collected with LDEF spacecraft and analyzed further suggest that the most abundant size of the particles counted by total mass influx is around 200 micrometers, and weights around  $1.5E-5$  grams, while most submillimeter particles size and weight by total mass influx stays in the range from 100 to 300 micrometers, with weight from  $1.5E-6$  gram to  $1.4E-4$  gram, and average density of a particle of  $2.5-2.8 \text{ g/cm}^3$  [4][23]. Particles of such size also lose their velocity at the atmosphere entry so rapidly and in rare atmospheres that they do not experience enough heating to evaporate, and stay in a similar composition through their descent[2]. Other data shows an altitude of around 18 kilometers, and the concentration of particles of submicrometer size is higher than in other layers below, especially during meteor showers. Even though submicrometer-size particles account for a small percentage of total mass influx, such regions of high concentration also possess an interest, since they are located in reachable layers of the atmosphere, and may have a higher number of particles of much smaller mass, and collection in those regions will increase the chances of extraterrestrial material retrieval.

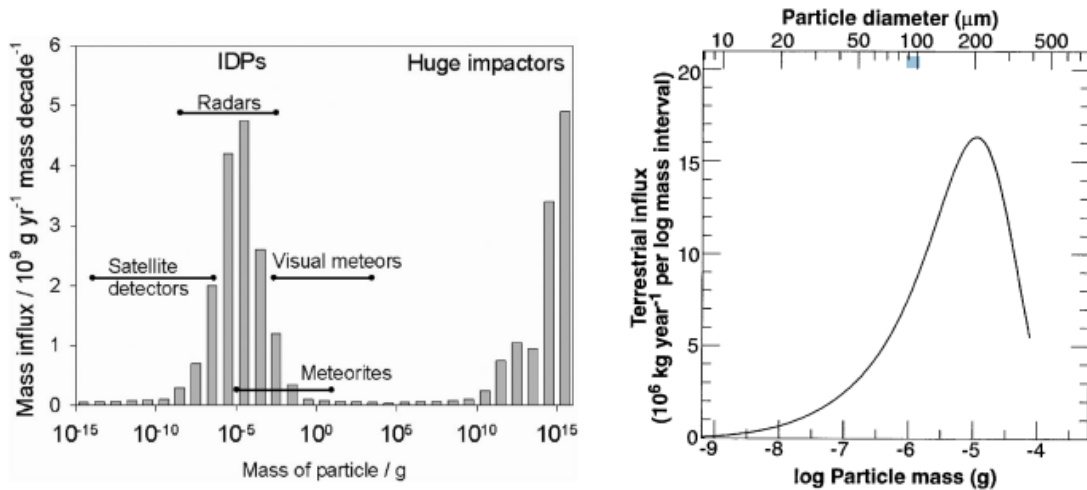


Figure 1.9 - Total mass influx of particles on earth by mass given by sources [4] and [23]

### 1.5.6.2. Atmospheric Behavior of Extraterrestrial Particles

When particles enter the atmosphere and slow down, they start their descent from the upper atmospheric layers to the ground. Since the size and diameter of the particles interesting for collection is now more understandable as particles in the range of 100-300 micrometers, with a density of 2.5-2.8 g/cm<sup>3</sup>, as well as submicrometer particles in Junge layers, it is important to understand the behavior of such particles in the atmosphere and if it varies with atmospheric layers. It is hard to analyze all of the parameters of particles of such a small size with all the turbulence of the atmosphere however one of the most important parameters that can be analyzed and approximated is how long the particles stay airborne and if there are any layers of the atmosphere, where particle concentration of similar size and density may vary. Cosmic particles can stay in the air for several hours to many weeks, but particles of a size larger than 10 micrometers usually settle within a day[7][25].

### 1.5.6.3. Particle Dynamics in Moving Fluids

To design the collection method for particles, it is crucial to understand the particle dynamics in moving air. The motion of particles will depend on the velocity of the flow, particle inertia, and aerodynamic drag. The particle size is the decisive factor in determining particle motion. The concentration of particles can also determine the behavior of particles in the airflow, due to their ability to interact with each other and flow, making trajectory prediction extremely complicated. It is possible to decrease the complexity of calculations if it is possible to prove that the concentration of particles is too low to significantly influence the flow of particles and that the particles don't influence the flow.

The specific value of concentration will depend on the particle size and number per unit of volume, and if the influence of particle interaction is not significant. As a general rule, the

particles in flow are considered not to influence the flow if the average distance between particles is ten times or more larger than the particle diameter. The significance of influence can be quantified using the following equation.

$$\frac{4\pi\rho_p}{3c} = \frac{n}{c_{number} D_p^3} \quad (1.8)$$

Where  $\rho_p$  is particle density,  $c$  is the mass concentration of the particles,  $c_{number} = n_t/V$  is the particle number concentration,  $D_p$  is the diameter of the particles, and  $n$  is the number of particles for the volume taken. The easiest shape to analyze would be a cube of a size where only 8 particles can fit at the corners. If the result of the equation above is less than the length of the cube side to the power of 3, it means that the particles in the flow move independently, and it is possible to calculate the trajectory of a single particle. We can use the following equation for monodisperse aerosol to find if particles in the flow move independently or not.

$$\frac{4\pi\rho_p}{3c} < (L/D_p)^3 \quad (1.9)$$

Taking the average density of particles to be maximum at  $2800 \text{ kg/m}^3$  found in previous research, and the largest expected particle diameter  $D_p$  to not exceed 200 micrometers, giving the desired distance between particles to be  $L = 2$  centimeters. The left-hand side has a variable  $c$  which can be found, and a value of  $c$  can tell if particles in the flow are far away from being dependent, or need more estimations. For the right-hand side, using the general rule in that case,  $L/D_p$  is equal to 10, and the right side of the equation is equal to 1000. Plugging all the numbers and calculating  $c$  for the worst case, tells that being approximately  $17.6 \text{ kg/m}^3$  it is way higher than it possibly can get in earth's atmosphere containing dust, and since density also decreases as altitude increases, the flow can be assumed to be independent, which allows to calculate the trajectory of each particle. It can also be calculated and checked using the table below with precalculated values.

Table 1.2 - The diameter and maximum concentration of particles for independent flow

$D_p$ ( $\mu\text{m}$ )	$c_{number}$ (particles/ $\text{m}^3$ )
1	$8 \times 10^{15}$
10	$8 \times 10^{12}$
100	$8 \times 10^9$

The next step is to find a way to calculate the trajectory of a single particle in a size, density, and shape range found before. To calculate the change in motion of the particle, we need to find the sum of forces acting on it.

$$m_{particle} a = \sum F = F_{gravity} + F_{drag} \quad (1.10)$$

#### 1.5.6.3.1. Gravitational Force

The net gravitational force is equal to the weight of the particle minus the buoyancy force on the particle, where the buoyancy force is equal to the weight of the air displaced by the particle.

$$F_{gravity} = m_{particle}g - m_{air}g = \pi \frac{D_p^3}{6} (\rho_p - \rho)g \quad (1.11)$$

For a spherical particle, where  $g$  is the acceleration of gravity,  $\rho$  is the density of the air, and  $\rho_p$  is the density of the particle. The density of a particle is typically 1,000 times greater than the density of air. Thus, the force of buoyancy on a particle is often neglected compared to its weight.

$$F_{gravity} = m_{particle}g - m_{air}g \simeq \pi \frac{D_p^3}{6} \rho_p g \quad (1.12)$$

#### 1.5.6.3.2. Aerodynamic Drag

$$F_{Drag} = -C_D \frac{\rho}{2} \frac{\pi D_p^2}{4} (\vec{v} - \vec{U}) \left| \vec{v} - \vec{U} \right| = -C_D \frac{\rho}{2} \frac{\pi D_p^2}{4} (\vec{v}_r) \left| \vec{v}_r \right| \quad (1.13)$$

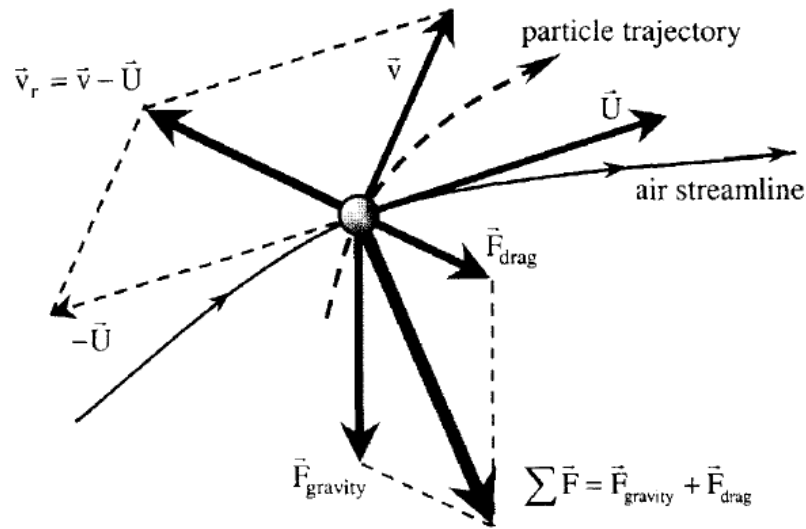
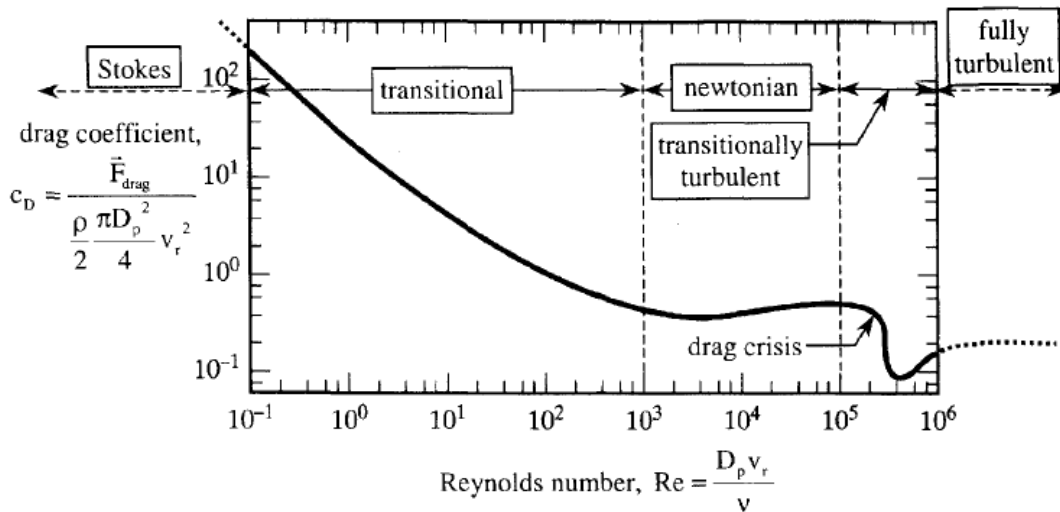


Figure 1.10 - Particle moving through the air, which is also moving(29)

$$\vec{v}_r = \vec{v} - \vec{U} = \vec{i}(v_x - U_x) + \vec{j}(v_y - U_y) + \vec{k}(v_z - U_z) = \vec{i}v_{rx} + \vec{j}v_{ry} + \vec{k}v_{rz} \quad (1.14)$$

$$|\vec{v}_r| = |\vec{v} - \vec{U}| = \sqrt{(v_x - U_x)^2 + (v_y - U_y)^2 + (v_z - U_z)^2} = \sqrt{v_{rx}^2 + v_{ry}^2 + v_{rz}^2} \quad (1.15)$$

$\vec{U}$  = carrier fluid velocity,  $\vec{v}$  = particle velocity,  $\vec{v}_r$  = relative velocity of particle



$C_D$  = drag coefficient for a particle based on frontal area

Figure 1.11 - Drag coefficient of a sphere versus Re (29), with separation into 5 commonly divided flow regimes

$$Re = \frac{\rho D_p |\vec{v} - \vec{U}|}{\mu} = \frac{\rho D_p |\vec{v}_r|}{\mu} = \frac{D_p |\vec{v}_r|}{\nu} = \frac{D_p v_r}{\nu} \quad (1.16)$$

Where  $\mu$  is the dynamic viscosity, and  $\nu = \mu/\rho$  is the kinematic viscosity. The dynamic viscosity is highly affected by temperature changes and has a very small influence from pressure changes, so for air, it can be found using Sutherland's Law equation:

$$\mu = \mu_0 \left(\frac{T}{T_0}\right)^{1.5} \left(\frac{T_0 + S}{T + S}\right) \quad (1.17)$$

Where  $\mu_0 = 1.71 \cdot 10^{-5}$  (kg/m s),  $T_0 = 273.15$  K,  $S = 110.4$  K

The relations of the drag coefficient for different flow regimes can be expressed with the following equations.

$$\text{for } Re < 10^{-1}: \quad C_d = \frac{24}{Re} \text{ for } Re < 10^{-1} \quad (1.18)$$

$$\text{for } 10^{-1} < Re < 5: \quad C_d = \frac{24}{Re} (1 + 0.0916 Re) \quad (1.19)$$

$$\text{for } 5 < Re < 10^3: \quad C_d = \frac{24}{Re} (1 + 0.158 Re^{2/3}) \quad (1.20)$$

$$\text{for } 10^3 < Re < 10^5: \quad C_d = 0.4 + \frac{24}{Re} + \frac{6}{(1 + \sqrt{Re})} \quad (1.21)$$

$$\text{for } 10^5 < Re < 10^6: \quad C_d = \text{Variable as on figure 1.17} \quad (1.22)$$

$$\text{for } Re > 10^6: \quad C_d \approx 0.2 \quad (1.23)$$

Depending on the velocity of the flow and particles that will be received in future analysis and simulations, one of those values will be used for calculations.

The equation for the mean free path  $\lambda$  is also required to find the motion of particles in a fluid.

$$\lambda(T, P) = \lambda_{STP} \left(\frac{\mu}{\mu_{STP}}\right) \left(\frac{P_{STP}}{P}\right) \sqrt{\frac{T}{T_{STP}}} \quad (1.24)$$

Where for air  $\lambda_{STP} = 0.06635 \mu m$ ,  $P_{STP} = 101.325$  KPa,  $T_{STP} = 273.15$  K

$$Kn = \frac{\lambda}{D_p} \quad (1.25)$$

for  $Kn < 0.1$ : Continuum Regime

for  $0.1 < Kn < 10$ : Transitional Flow Regime

for  $Kn > 10$ : Free Molecular Flow

Cunningham Slip Factor (C)

$$C = 1 + Kn[2.514 + 0.8\exp(-\frac{0.55}{Kn})] \quad (1.26)$$

Using variables received from the previous equation, it is possible to complete the equation for the particle drag force for any given particle.

$$\vec{F}_{drag} = -C_d \frac{\rho}{2C} \frac{\pi D_p^2}{4} (\vec{v} - \vec{U}) |\vec{v} - \vec{U}| = -C_d \frac{\rho}{2C} \frac{\pi D_p^2}{4} \vec{v}_r |\vec{v}_r| \quad (1.27)$$

#### 1.5.6.3.3. Effect of Particle Shape on Drag Force

Since particles are not perfect spheres, their trajectory can be affected by their shape. Their drag will be different depending on how greatly they differ from the perfect spherical shape. Those particles can be treated as particles with equivalent volume, however, the equation to calculate their drag will have two more variables  $D_{e.p.}$ ,  $X$ , which  $D_{e.p.}$  is equivalent volume diameter defined in terms of the actual particle volume ( $V_p$ ), and  $X$  is the dynamic shape factor.

$$D_{e.p.} = \sqrt[3]{\frac{6V_p}{\pi}} \quad (1.28)$$

$$X = (0.33 + 0.67 \frac{D_{s.p.}}{D_{p.p.}}) \frac{D_{e.p.}}{D_{p.p.}} \quad (1.29)$$

Where  $D_{p.p.}$  is the diameter of a sphere with the same projected area as the actual particle, where the projected area is the cross-sectional area of the particle normal to the direction of flow, and  $D_{s.p.}$  is the diameter of a sphere with the same surface area as the actual particle. For most of the shapes, the dynamic shape factor  $X$  has already been calculated, as can be seen in Table 1.3.

Table 1.3 - Dynamic shape factors, averaged over all orientations(29)

shape		X
sphere		1.00
cube		1.08
cylinder (L/D = 4):		
	axis horizontal	1.32
	axis vertical	1.07
ellipsoid, across polar axis, with ratio of major to minor diameters = 4		1.20
parallelepiped with square base, with various values of height to base:		
	0.25	1.15
	0.50	1.07
	2.00	1.16
	3.00	1.22
	4.00	1.31
clusters of spheres		
	chain of 2	1.12
	chain of 3	1.27
	3 compact	1.15
	chain of 4	1.32
	4 compact	1.17

By using two new variables in the equation for drag force, a new equation, universal for all shapes, can be obtained.

$$F_{drag}^{\rightarrow} = -XC_d \frac{\rho}{2C} \frac{\pi D_{ep}^2}{4} (\vec{v} - \vec{U}) \left| \vec{v} - \vec{U} \right| = -XC_d \frac{\rho}{2C} \frac{\pi D_{ep}^2}{4} \vec{v}_r \left| \vec{v}_r \right| \quad (1.30)$$

This equation is sufficient to simulate the behavior and calculate the particle dynamics in a moving fluid for the collector design.

#### 1.5.6.4. Inertial Separation Collectors

The collection of particles is used in many other fields, mostly to clean the air from harmful particles or aerosols. Most of the collectors work by letting the particle-containing air go through the collector, whereas by applying certain methods, particles get separated from the air that leaves the collector. Many devices that remove particles from a gas stream rely on the fact that solid or liquid particles have densities approximately one thousand times larger than that of the carrier gas. Thus, particles experience gravitational and inertial forces larger than the forces experienced by the carrier gas. Such devices are often called inertial separation collectors. Some examples of such collectors are cyclone collectors, which use the energy of large particles to redirect them while letting the flow escape through the outlet.

Often, cyclone collectors require a powerful pump from one of the sides to accelerate the flow and increase the amount of gas that is going through the collection chamber, which also

needs to have enough space to separate particles from the air and not take particles in a clean air outlet.

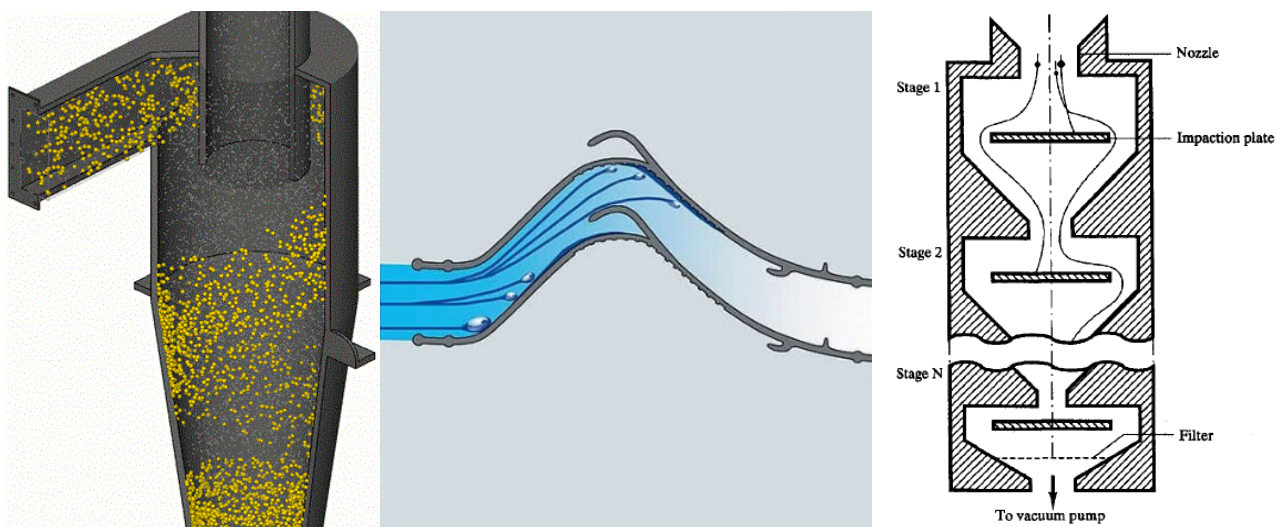


Figure 1.12 - On the left, cyclone collector particle separation. In the middle, a mist eliminator with one curve and two collection openings. On the right, cascade impactor: schematic diagram, showing trajectories of particles of three different diameters (29)

Another method of collection is mist eliminators. Mist eliminators use the density difference to separate liquids from the airflow going through the curved path, with larger droplets collected at the first curve and smaller droplets at the second curve. Since the motion of particles in the air is similar for liquids and solid particles, a similar principle can be used to separate solid particles of different sizes. The liquid can be removed from the collector using gravity or collection methods, while it is harder to do with solid particles, and thereby, that method is mostly used for mist removal from the air.

The third method of inertial collection is cascade impactors. Using a similar idea of different densities, the cascade impactors let the air with particles through the nozzles decrease with every next plate impactor's radius. Due to the inertia of the particles accelerated at the nozzle, they lack the time to change their trajectory enough to avoid the impactation plate. The impactation plate can use different methods to grab and contain particles on its surface until they are removed. Cascade impactors may use many layers, with no limitation to their number; however, the efficiency of every next layer is decreasing, and the pressure difference required to move air through the collector may limit the radius of the smallest nozzle in the impactor.

### 1.5.7. Interest in Extraterrestrial Particles

The main subjects discussed before missions were particles of cosmic origin. But why exactly would we be interested in collecting such particles? This question could be answered if

there is a need for new ways to collect extraterrestrial particles and, thereby, a need to develop a new system. The answer to this question can be divided into several parts.

#### 1.5.7.1. Solar System Formation

The theory of the origin of the solar system is still under development. By analyzing the composition of meteorites, scientists can reconstruct the conditions present during the formation of our solar system. Research of meteorites in general and interplanetary particles, in particular, has the potential to extend further understanding of solar system formation and refine existing theories. While there exist ways to observe and analyze the chemistry of such bodies at a distance or during atmospheric entry, obtaining extraterrestrial particles for research that cannot be done in such ways is still crucial. [30]

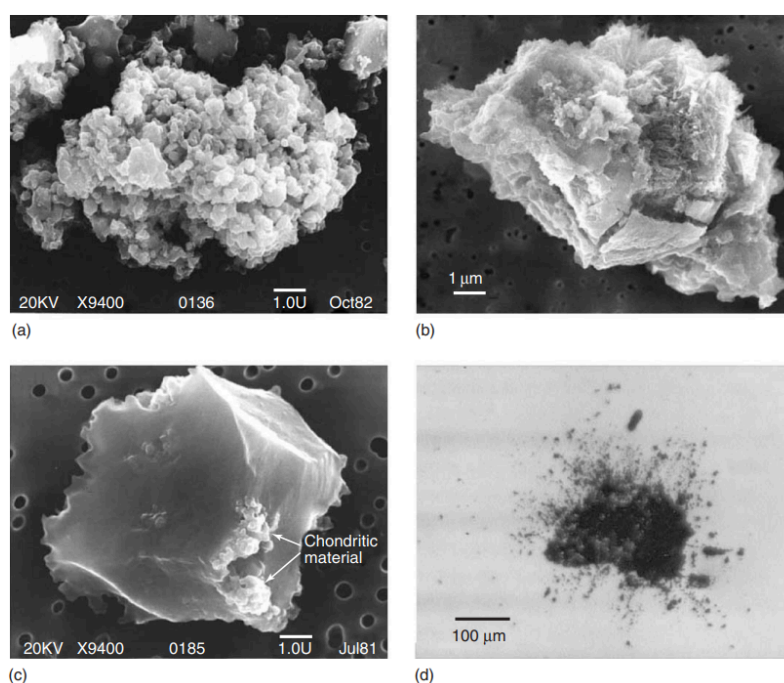


Figure 1.13 - Secondary electron images. (a) Anhydrous CP IDP. (b) Hydrated CS IDP. (c) Single-mineral forsterite grain with adhering chondritic material. (d) Optical micrograph of giant cluster IDP in silicone oil on ER2 collection flag [30]

#### 1.5.7.2. Chemistry of Cosmic Bodies

As part of the study of the solar system's origin, the study of extraterrestrial particles can give insights into the chemistry of cosmic bodies if the source of the particles can be known or approximated. As was mentioned in previous research, the extraterrestrial particle concentration during major meteor showers can increase several times, implying that the amount of material from specific meteor showers can be significant or even prevailing during certain times, to

approximate the origin of particles collected during that time [9]. It creates an opportunity to research the chemistry of bodies unreachable without big and costly missions otherwise. [32]

### 1.5.7.3. Search for Life

One of the main questions for researchers nowadays is how life originated on Earth. The research on extraterrestrial particles can partially answer this question, or at least support research in this direction. While it is impossible to say if life originated on Earth or was brought from somewhere else, the research of chemical components in extraterrestrial material can give more information on organic compounds found in them and how those compounds could influence the history of life on Earth. [33]

### 1.5.8. System Engineering Principles

The system engineering interconnects many different fields in one large process of system development. It is used everywhere in the engineering field and beyond to organize and optimize the development and work on complex systems. While there are a few different ways to organize processes and many different applications to main system engineering delivery steps, the one that is commonly used for aerospace and other applications is a V-shaped delivery process, shown in Figure 1.20

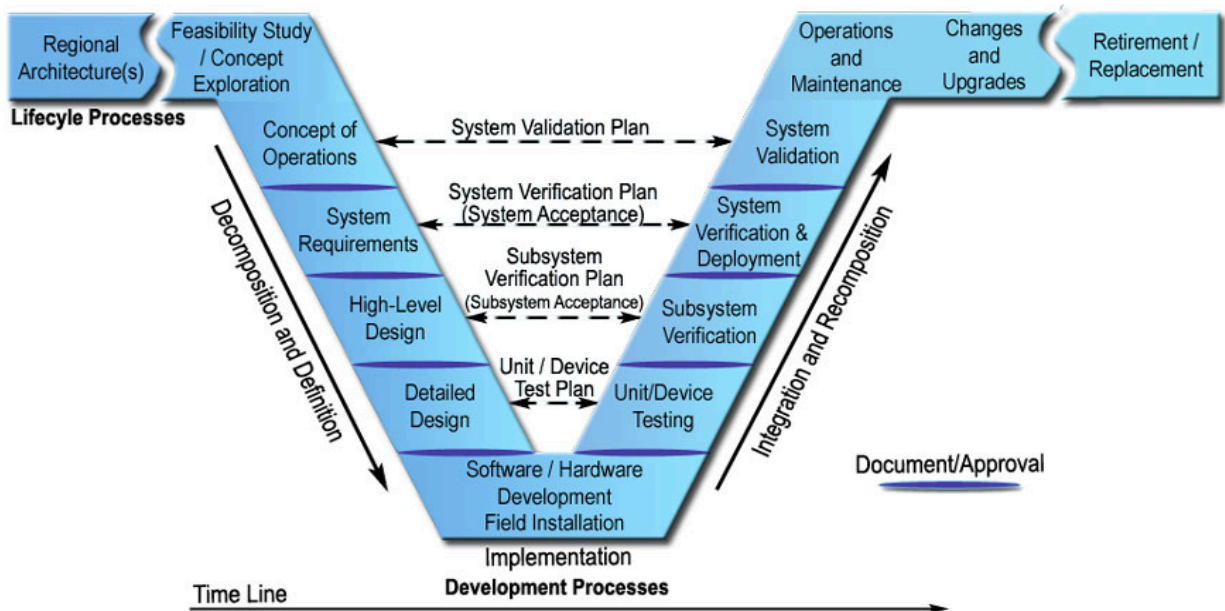


Figure 1.14 - V-shaped delivery process diagram for system engineering

The V-shaped delivery process is done by describing the entire system mission objective and concept according to stakeholder needs and developing main system requirements before partitioning it into smaller subsystems, which in turn will be partitioned into subsystem units and components. When the entire system is designed, manufacturing and assembly begin, starting with units and components. Units and components are tested and verified they complete tasks before being assembled into subsystems, which also get tested and verified before being integrated into the full system. If, after this process, the system passes validation and proves to correspond to the task set to it, the design process is considered done, transferring the system to the stakeholder for operation and maintenance. While the terminology may differ from place to place, the entire V-shaped process looks the same, no matter what words are used.

Details of the process described above are getting very complex and well structured and written down in the Space Mission Analysis and Design by Wiley J. Larson and James R. Wertz, which is going to be the main source of steps for this project [34].

The decomposition and definition process of system engineering is an iterative process that aims to deliver all required engineering data to create a system that will be ready to be assembled and tested. It starts with the development of the broad goals of the missions and results in a specific system. Before the full system can be developed, the definition of the system must occur, resulting in a good idea of how exactly the system will work and what the requirements are for all the subsystems and their elements. Using those requirements, the development of subsystems starts, going from the top level down through the levels of assemblies, components, and down to every single piece part.

Table 1.4 - Hardware nomenclature in the system development [34] from the top to the bottom level, where 1 is the top level and 5 is the bottom level

<b>1 System</b>	Complete probe
<b>2 Subsystem</b>	All of the components and assemblies that comprise a probe subsystem
<b>3 Assembly</b>	A functional group of parts, such as a hinge assembly, an antenna feed, or a deployment boom
<b>4 Component</b>	Complete functional units such as a control electronics assembly, an antenna, a battery, or a power control unit.
<b>5 Part</b>	Individual parts such as a resistor, integrated circuit, bearing, circuit board, or housing.

Implementation happens when system components are developed into every piece parts. While some components can be developed earlier than others or take more time to be

manufactured than other components, they might be started earlier. In general, the implementation stage covers all the processes that require hardware and software development. It is possible to start testing before this stage is complete or return to it if tests of certain components show the need for redesign and remanufacturing. As tests go from the lowest level to the highest, there is less room for redesign, and the manufacturing stage is mostly over by the time of higher-level verification and validation.

#### 1.5.8.1. Decomposition and Definition

The development of the system starts with the mission statement. The mission statement is the definition of what the mission needs to accomplish. It usually states the qualitative goals of the mission and tries to answer why those goals need to be achieved. During the development, it is important to come back to the mission statement to make sure that the system is completing the mission statement as stated.

The next step is to define quantitative mission needs and requirements. In this step of the system development process, it can be decided what the limits of the mission are, such as the minimum required to achieve the mission statement, limits of technology, or maximum funds that can be allocated to the project.

During the mission development, it is important to look into alternative mission concepts that can achieve the mission statement, with their mission architectures. A mission concept is a broad statement of how the mission will work in practice. It includes issues such as how the mission statement will be achieved and delivered to the end user, how the mission will be controlled, and the overall mission timeline. Alternative mission concepts may have distinct ways to resolve the problem, sometimes drastically different in their concepts, areas of activity, use, or cost. For EPC, such alternatives can be various collection methods discussed in the previous review, and each might have its pros and cons, or different ways of collecting using probe architectures. Since this project is aiming to deliver a probe, conceptually different approaches will be discarded, and this step will be focused on different architectures that can be used in the probe.

In further development of this document, the Implementation, Integration, and Recomposition sections will be covered, with the progression of the project development. Implementation is going to cover the manufacturing process and specific decisions changing the design, which possibly can be made to correspond to manufacturing capabilities. Integration and Recomposition are going to cover the process of system assembly, starting with the components level and going up stage by stage until subsystem and system levels are tested.

### 1.5.9. Air Management

A feature of the probe that can use already existing designs and technologies is the air intake. The air collector's function is to let through as much air as possible with a limited area, which is similar to the function of most air intakes for air-breathing propulsion of different kinds. As with the other intakes, the probe would require a design that can accommodate its requirements, such as length, mass, volume, or strength, maximize the air that goes in, and minimize the loss in pressure. In addition to those considerations, it is important to look into solutions for the high total pressure problem from the previous design.

The probe is expected to work in two regimes, switching from one to another, starting with subsonic at the deployment, and quickly going into supersonic flight as the probe accelerates, due to gravity and low aerodynamic drag at high altitudes. After reaching the terminal velocity in supersonic conditions, the probe will gradually reduce its velocity as it descends into dense atmospheric layers.

The problem with total pressure can be expected at any of two regimes, however, it is more crucial at the supersonic regime as the spillage as shown on the right inlet in Figure 1.23 created by high pressure can reduce the volume of air that is going through the collector, and thereby reduce the collection rate of the probe. Some active systems, such as compressors, decrease the total pressure in front of the collector and could decrease pressure or even let more air in than would be possible without such a system, as on the left inlet in the figure below.

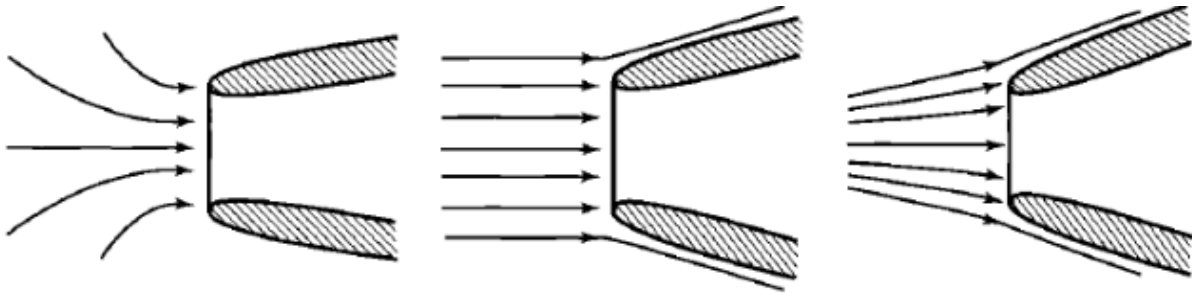


Figure 1.15 - Inlets with different spillage [35]

#### 1.5.9.1. Subsonic Management

The main objective of the subsonic inlet in aircraft is to let more air through while decreasing drag. Often, it also serves protective and geometry change functions to accommodate the specific needs of certain aircraft. In the case of the EPC probe, the main function of the inlet in the subsonic regime will be to keep the collector safe during deceleration and keep a nominal velocity for a quick descent and optimal velocity for recovery system deployment. Since no airflow is expected at the subsonic regime, the geometry will not serve as an inlet but will perform as a nosecone. Due to the need for collection in the supersonic regime, it will have

features of the inlet designed for the supersonic regime, but might accommodate some features to make the subsonic flight optimal for the performance described above.

### 1.5.9.2. Supersonic Management

As was mentioned before, the collection is expected to happen in a supersonic regime, and thereby, the collector needs a supersonic intake that will allow the highest volume of air. One of the parameters important for calculating the efficiency of supersonic management is the area ratio of the inlet to the critical area for this inlet. Assuming isentropic flow, it can be expressed with the following equation.

$$\frac{A}{A^*} = \frac{1}{M} \left[ \frac{2}{\gamma+1} \left( 1 + \frac{\gamma-1}{2} M^2 \right) \right]^{(\gamma+1)/[2(\gamma-1)]} \quad (1.31)$$

Where  $A$  the area of the inlet  $A^*$  is the critical area,  $M$  is the Mach number  $\gamma$ , and is the specific heat ratio of the gas.

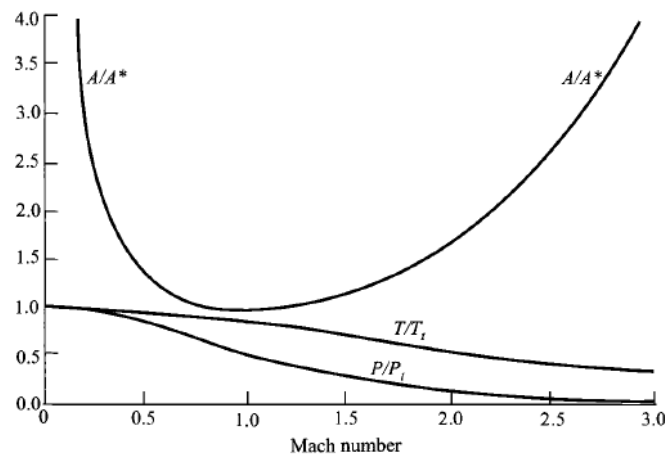


Figure 1.16 - Compressible flow functions vs Mach number[35]

Since the area ratio  $A/A^*$  represents the change in the area to achieve critical flow conditions, it is equal to 1 when the Mach is equal to 1, assuming isentropic flow. Due to shock waves expected at the entrance into the inlet, the flow will be subsonic at the entrance. The subsonic flow accelerates as the available area decreases until it reaches critical conditions at Mach 1. Since it cannot accelerate further, decreasing it further will result in less air flowing through the inlet. Therefore, it is important to calculate the optimal critical area in changing flight velocity to design it and allow the most efficient airflow.

### 1.5.9.3. Inlet Flow Distortion

Due to the shockwave pressure difference, the inlet will have spillage in supersonic conditions, and it does not matter how well the inlet geometry is designed. The fraction spilled at the inlet can be calculated using the following equation.

$$\text{Fraction Spilled} = \frac{(\rho V)_0 A_c - (\rho V)_0 A_0}{(\rho V)_0 A_c} = \frac{A_c - A_0}{A_c} \quad (1.32)$$

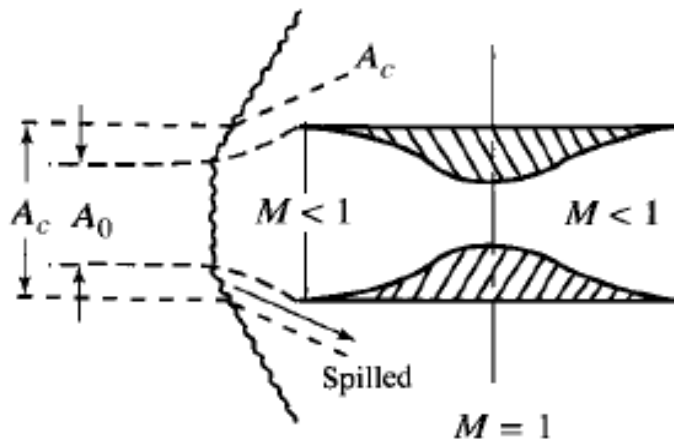


Figure 1.17 - Intlet spillage [35]

### 1.5.9.4. Active-flow Control System

The way to further decrease the spillage, when the geometry is optimised, would be active control, such as a compressor at the inlet, which will be able to increase the pressure difference between the inlet and its exit, thereby increasing the total mass flow capable of going through the restricted space. If driven quickly enough, the compressor theoretically can balance the pressure in front of the inlet with the pressure of the flow, or even make it smaller than the pressure of the flow.

### 1.5.10. Basics of Amateur Rocketry

Amateur rocketry is the practice of building and launching rockets for hobby or educational purposes. The size of the rocket may vary from the tiny rockets driven by air to large two- to three-stage rockets capable of reaching the Karman line and further.

As a rule, amateur rockets utilize

- Airframe (Body Tube)

- Main structure of the rocket; usually lightweight (plastic, carbon fiber, or fiberglass).
- Nose Cone
  - Streamlined to reduce drag; often made of plastic or fiberglass.
- Fins
  - Provide stability during flight; typically 3 or 4 fins, symmetrically placed.
  - Provide a stability margin required, depending on the flight requirements, usually varying between 1.5 and 4.
- Propulsion (Motor)
  - Solid rocket motors are most common in amateur rocketry.
    - Sold as propellant kits made for the specific size of a reusable motor container with attached nozzle.
  - Sometimes, hybrid or liquid propellant systems are used for large amateur rockets
    - Commercially available motors are labeled A through O (each step = double the impulse).
- Recovery System
  - Most often, a parachute or streamer is ejected after apogee to slow descent and allow reuse.
  - For high-altitude launches, dual-deployment methods or delayed deployment methods are used
  - Usually, gunpowder is used to increase pressure inside the airframe and separate it into designed pieces to release the recovery system
  - Alternatively, the gas release systems can be used to increase internal pressure and allow deployment
    - At high altitudes where there is limited efficiency of CO<sub>2</sub>, the gunpowder and CO<sub>2</sub> canisters can be replaced with NO<sub>2</sub>.
- Avionics
  - Usually, flight computers are used to control the deployment of recovery systems and record the
- Tracking Systems
  - Usually, GPS systems are used for each piece of the rocket that is expected to come down separately
  - Have specific material requirements to not reduce efficiency

#### 1.5.11. Stability of Falling Objects

Main two parameters for stability of any object falling through the atmosphere are location of center of mass and location of center of pressure. For the vertical stability of the

system with its nose pointing down, the location of the center of mass should be closer to the nose, while the location of the center of pressure should be as close to the rear as possible.

In addition to this, it is helpful to balance the aerodynamic forces by using the symmetrical shapes, and also sometimes spin stabilisation if applicable.

Most of the manmade object designed to fall through the atmosphere such as reentry modules such as on Figure 1.26, atmospheric probes or bombs utilise Cg and Cp locations with mostly symmetrical features of the outer geometry.

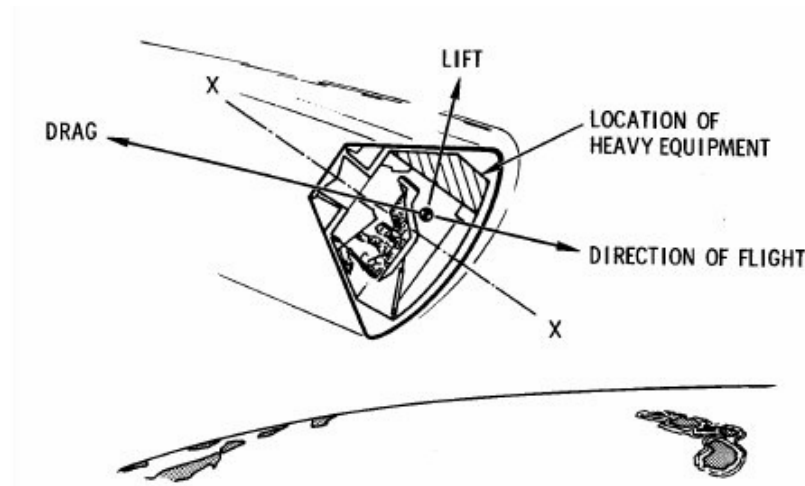


Figure 1.18 - Command module aerodynamics

#### 1.5.12. Power Cells

Not all power cells are safe and can be used in aerospace applications. Some might perform better than others in specific conditions. This section will cover research on power cell chemistry and size that can be used for EPC projects.

For aerospace applications, power cell chemistry prioritizes reliability, safety, energy density, and performance in extreme environments. An additional requirement for small-size projects in power cell chemistry is commercial accessibility.

Only several power cell chemistries meet those requirements, such as:

- Lithium Iron Phosphate ( $\text{LiFePO}_4$ )
  - High thermal stability
  - Low fire risk
  - Long cycle life
  - Lower energy density than some Li-ion chemistries
  
- Lithium Titanate (LTO)

- Best temperature performance (-30°C to 60°C)
- Very safe and durable under mechanical stress
- Can handle high charge/discharge rates
- Lower energy density than traditional Li-ion
- Advanced Nickel-Metal Hydride (NiMH)
  - Safer than Li-ion
  - Tolerates cold temperatures
  - Lower energy density than Li-ion

### 1.5.13. Bearings

Rotational components might be used for some possible features in probe development. For such components, the best base and connection to the main structural frame will be some kind of bearing.

- Ball Bearings
  - **Pros:** Low friction, good for both radial and axial loads.
  - **Cons:** Requires lubrication; can wear out over time in dusty or extreme conditions.
- Thrust Bearings
  - **Pros:** Designed to handle axial loads (important if the propeller exerts force along the axis of rotation).
  - **Cons:** Poor at handling radial loads; might need additional radial support.
- Magnetic Bearing
  - **Pros:** No physical contact, nearly zero friction, excellent for long-duration use.
  - **Cons:** Requires power (active magnetic bearings) or careful design (passive magnetic bearings); complex implementation.
- Air Bearing
  - **Pros:** Extremely low friction, high-speed capability, and no wear.
  - **Cons:** Requires a source of compressed air or gas, which might not be feasible in all applications.

The ball and thrust bearings are also possible in two configurations. The first one uses spheres, and the second one uses rollers compressed between bearing surfaces.

#### 1.5.14. Gears and Gearboxes

In the case of using rotational energy for some components of the projects, this energy might need to be transferred using gears and gearboxes. For different applications, the design of the gears might differ, starting from their tooth configuration to their relative size and position. Currently known

- **Spur Gears** – The simplest type of gear with straight teeth, used for transmitting motion between parallel shafts with high efficiency, but can be noisy at high speeds.
- **Helical Gears** – Similar to spur gears but with angled teeth, providing smoother operation, greater load capacity, and reduced noise, commonly used in automotive transmissions.
- **Bevel Gears** – Cone-shaped gears used to transfer power between intersecting shafts at an angle, often found in differential drives and power tools.
- **Worm Gears** – A gear set consisting of a worm (screw-like) and a worm wheel, offering high torque reduction and self-locking properties, commonly used in elevators and conveyors.
- **Rack and Pinion** – A combination of a linear gear (rack) and a rotary gear (pinion) that converts rotational motion into linear motion, widely used in steering systems and CNC machines.
- **Planetary Gears** – A compact gear system with a central sun gear, orbiting planet gears, and an outer ring gear used in automatic transmissions and precision machinery for high torque and smooth operation.
- **Herringbone Gears** – A double-helical gear with opposing angled teeth that cancel out axial thrust, making them ideal for heavy-duty applications like marine drives and turbines.
- **Hypoid Gears** – A variation of bevel gears with offset shafts, allowing for smoother and quieter operation, commonly used in automobile differentials.
- **Crown Gears** – A type of bevel gear with teeth perpendicular to the gear face, used for transmitting motion at 90-degree angles, often found in clock mechanisms.

- **Internal Gears** – Gears with teeth cut on the inside of a cylinder are frequently used in planetary gear systems for compact and high-torque applications like automatic transmissions.

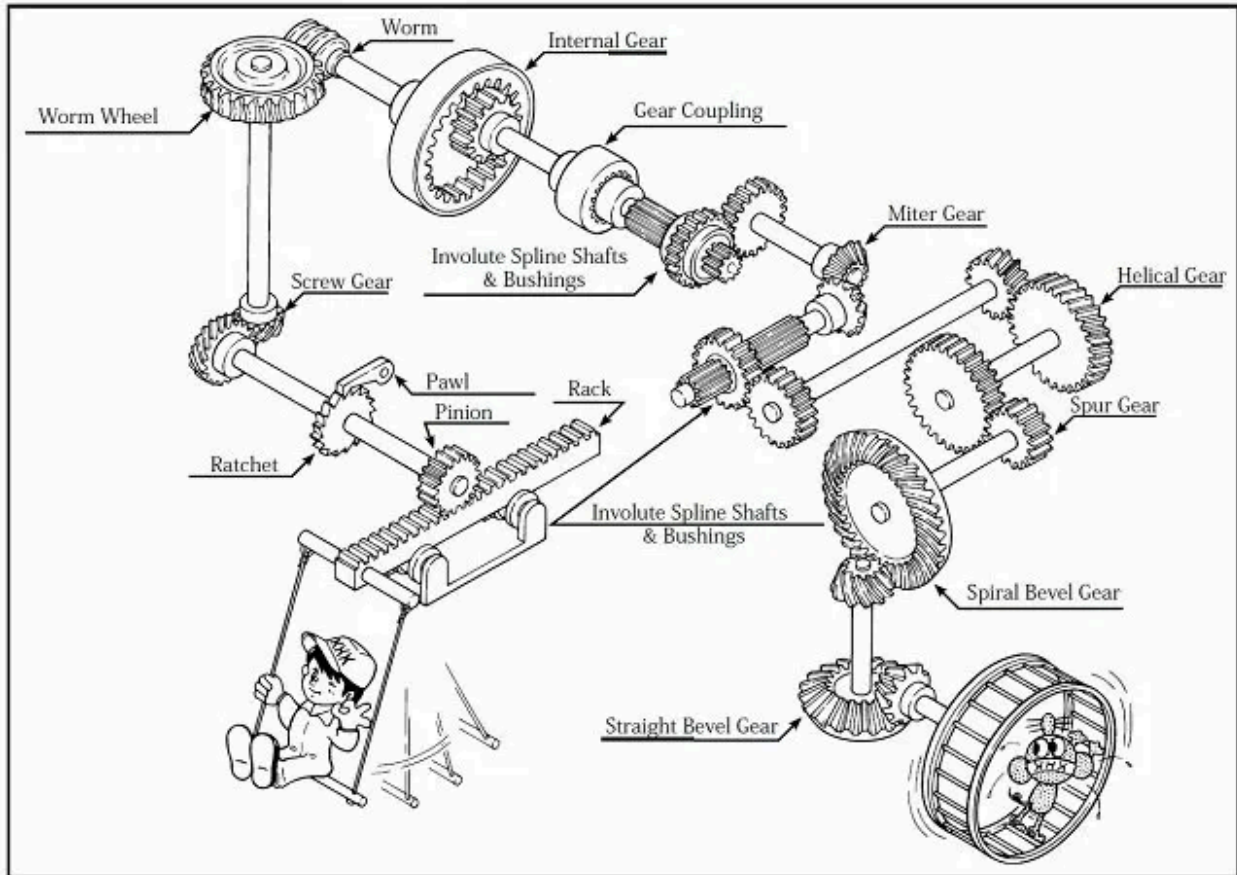


Figure 1.19 - An example of the existing types of gears used in one system

Certain system elements that might be used in the project require a change of rotation speed in exchange for torque. The standard way to change the gear ratio is simply by putting two gears of different radii together. The smaller gear, when driven, will result in slower rotation of the bigger gear with more torque, and when the bigger gear is driven, it will result in faster rotation of the smaller gear with less torque. The gears can be united in gear systems called gearboxes to achieve specific results required by the mechanical system. One such gearbox that found a wide application in aerospace engineering is the epicyclic or planetary gearbox. This is a system of gears consisting of three components: the Ring gear (Internal gear), Planet gears connected with a carrier, and the Sun gear. In the planetary gearbox, one of the components needs to stay still relative to the structure of the probe, engine, or vehicle, and the other two will be transferring torque and rotational speed between each other. The usual configuration of planetary gear is where the sun gear is a smaller gear in the middle; planet gears are bigger gears surrounding the sun gear, and the Ring gear holds all of them and is kept relatively still to the structure. In such a configuration, when the ring gear is kept still, the planetary gears and the sun gear have a high

ratio between them. If the sun gear is driven, it results in a slower rotation but higher torque for the planetary gear carrier. When the planetary gear carrier is driven, it results in a faster speed but lower torque for the sun gear. Even though the planetary gears rotate in the opposite direction to the sun gear, the carrier rotation occurs in the same direction as the sun gear does. The epicyclic gearboxes are convenient because they can be connected in series using the same direction of rotation and ring gear to allow even higher ratio changes between the input and output rotation.

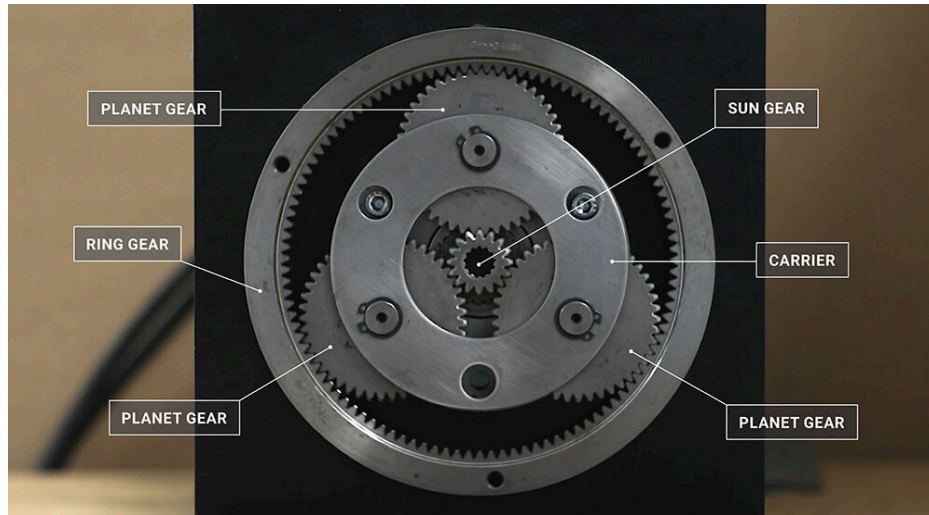


Figure 1.20 - An example of a planetary gear with a smaller sun gear

To design a new epicyclic gear, it is necessary to establish specific parameters of the gears and the ratio of sun to planetary gear requirements. When the requirements are known, we can use the following formulas to calculate the radius for other gears.

$$i = \frac{\omega_s}{\omega_c} = \frac{2r_s + r_R - r_S}{r_s} = 1 + \frac{r_R}{r_s} = 1 + \frac{z_R}{z_s} \quad (1.33)$$

Where  $i$  is a gear ratio  $\omega_s$  and  $\omega_r$  the angular velocity of the sun gear and planetary gear connector,  $r_s$ ,  $r_R$  are the radii of the sun gear and outer ring, and  $z_s$ ,  $z_R$  are the number of teeth of the sun gear and outer ring. Another condition for a properly working planetary gear is that the diametral pitch must be equal for all the gears used. The value of diametral pitch can be decided depending on how small teeth can be manufactured and how strong they need to be, with larger teeth being stronger.

### 1.5.15. Manufacturing Using 3D Printing

One of the project's goals is to make it accessible to a wide range of researchers who might use it; one of the biggest concerns is making manufacturing cheap. As commercially available 3D printers improve their capabilities, material range, and print detail, they become a favorable choice for manufacturing compared to the CNC machinery used for manufacturing the previous generation, as long as the materials used can provide the required durability, especially if the probe will be used as expendable. As with any other manufacturing method, 3D printing has specific limitations and requirements for the proper manufacturing of separate parts. The part needs to be printed from the bottom to the top, where the bottom needs to have enough surface to ensure adhesion of the part until the printing is over and the printing plate has cooled down. Certain settings of the print can help to increase the durability or speed of manufacturing, such as the layer height, vertical perimeter shells, fill density and fill pattern, layer combination, and the presence and type of the support material. Many secondary settings can influence the print of the part, but it usually depends on the specific requirements of the part and can be manually adjusted. The general setting listed above is the main factor and will allow the change of part characteristics in a specific range to improve the strength of the parts, print quality, or print speed.

The 3D printing manufacturing process put some more limiting factors on parts, such as the minimum size of details that can be printed using the smallest layer thickness for a particular printer model, the minimal surface area at the printing plate, and the need to add support, increasing roughness of the surface and need to point parts as a rule with the most of the material closer to the printing plate to improve quality, and the orientation of the printing, especially for creation of round shapes.

### 1.5.16. Materials

Materials used in this project are limited mainly by accessibility, cost of material, cost of manufacturing, and structural characteristics. Different pieces of the probe will require different structural requirements, while the less mass the probe has, the higher it can be launched, or the less it will cost to reach the desired altitude. Optimizing the probe's durability and weight will require research into materials for the EPC probe. Most of the materials selected for this research are usable for 3D printing in commercial off-the-shelf 3D printers. The strength of 3D printable materials usually depends on geometry, material, and layer thickness, where the layer thickness is primarily important for axial (out of the plane of printing direction). The list of materials below includes primary characteristics of the material provided by manufacturers. Some of the numbers are taken as averages due to small differences in composition from different manufacturers. It can be seen that while filaments for 3D printing have much less strength, they are also much lighter and cheaper, and the manufacturing method does not cost much. The glass transition temperature for some of them is high enough not to cause a problem during flow

compression, which is the temperature at which the material that is solid under normal conditions starts to behave as if it had a soft, rubbery state. The preferred materials can also be chosen based on the manufacturability and print quality of the specific part, as long as they provide enough strength and a high enough glass transition temperature.

Table 1.5 - The material characteristics and cost estimation for the materials available for the project

Material	Density g/cm <sup>3</sup>	Young Modulus (MPa)	Tensile Strength (X-Y) (MPa)	Tensile Strength (Z) (MPa)	Glass Transition Temperature (°C)	Melting Temperature (C)	Cost per kilogram, including manufacturing	Manufacturing Method
PLA	1.21	2700	47.1	38.9	65	148	10-40\$	3D-Printing
PETG	1.25	2000	44.3	38.9	85	220	20-50\$	3D-Printing
PETG CF	1.32	5000	49	40.5	85	220	26-60\$	3D-Printing
PETG GF	1.28	4300	50	41.3	85	220	27-60\$	3D-Printing
PC	1.20	2400	70	44.5	115	220	40-70\$	3D-Printing
Carbon Fiber	1.8	350000	250	NA	NA	3700	220-250\$	Custom Layering/ Molding
Fiberglass	2.5	76000	600	NA	NA	1120	110-150\$	Custom Layering/ Molding
Aluminum 6061	2.7	69000	310	NA	NA	700	200+ \$	CNC machinery

### 1.5.17. The Axial Pressure Compressor

An axial compressor is a type of compressor that uses rotating blades (rotor) and stationary blades (stator) to compress a fluid by accelerating it and then diffusing it, increasing pressure along the axis of rotation. Usually, it is stages with each stage increasing pressure by 1.1 to 1.4 times, resulting in a total increase of up to 40 times. An example of such a compressor can be seen in Figure 1.30, where the low-pressure and high-pressure compressors are shown. The design of the stator and rotor blades is a very important part of the compressor and varies depending on the characteristics of the airflow where it is used. The design of an airfoil for a specific case of application can be worth an entire paper of research itself, so instead of designing it from zero, it is possible to choose one of the airfoils from the NACA database. Specifically, the NACA 65-series which were intended for application for rotation in axial airflow. [41]

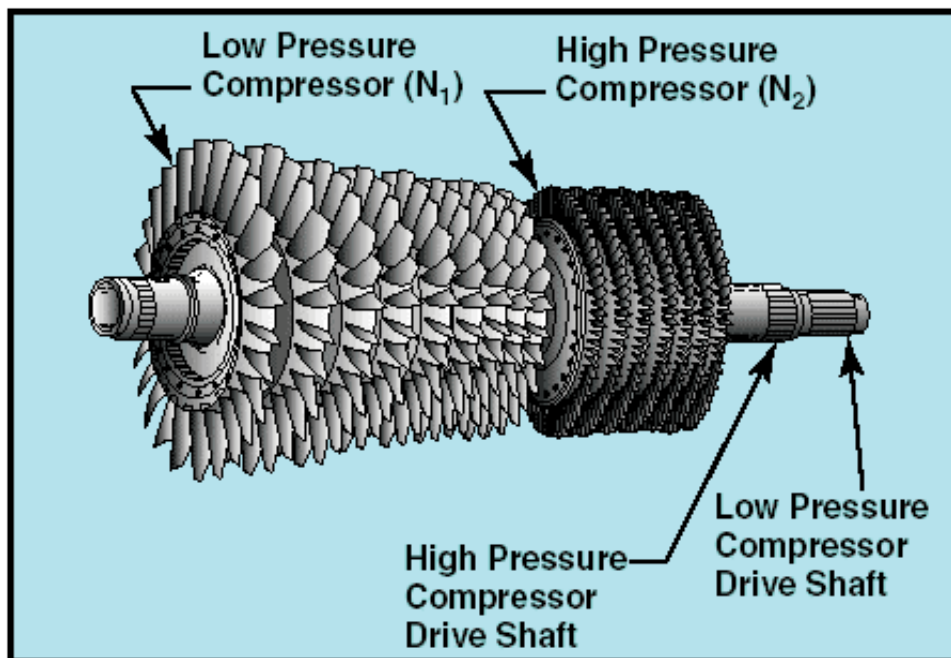


Figure 1.21- The diagram of the axial compressor used in turbojet engines

## **2. Project Objective and Methodology**

### **2.1. Project Objective**

The main goal of this project is to design a second-generation extraterrestrial particle collector (from now on EPC), using the experience obtained during the design, assembly, testing, and operation of the MMC, as well as system engineering design principles. The new probe should avoid mistakes made in the previous generation. It requires revision and redesign of every subsystem according to the requirements and constraints of the mission and environment of operation. The new probe design should analyze and correct known drawbacks from the previous design while implementing new features from existing legacy systems.

The design of the new subsystems should introduce better reliability and more convenient use, while the collection method needs to be reviewed using the calculation of particle dynamics to ensure better particle collection of the most abundant size. The choice of materials should also be investigated in favor of more lightweight and accessible materials, durable enough for freefall through the different layers of the atmosphere, and against drag upon entering the dense layers at high velocity. A new category of measuring tools, sensors, and data recording devices should be added for analysis of probe behavior during tests and after recovery. The new generation of design should have higher areas of collection to increase the chances of collection, which will be developed for a 6-inch diameter of commercially available fiberglass rocket bodies for the second stage. In addition to the probe, the deployment method will also be discussed to ensure possible implementation into any amateur rocket of defined diameter with slight design changes.

The secondary goal of this project is to develop a feasible extraterrestrial collection system that could compete with other existing systems discussed in the literature review, with its pros and cons.

### **2.2. Methodology**

The methodology of the EPC Project will differ from that used in the previous model. Further research into the topic was required before the project was developed, and special emphasis was placed on the proven systems of collection used by other missions and designs.

The problem of extraterrestrial dust collection will be analyzed using previous research about the genesis of extraterrestrial material, its concentration in the atmosphere, and particle behavior. To come up with more specific requirements and constraints for the probe. The

requirements and constraints will define the system design and collection method. After the initial analysis was completed, the concept design and concept of operations were developed. At this stage, it was possible to obtain most of the system requirements and constraints and to start developing the subsystem design. Each subsystem required its own set of tools and applications to be developed, analyzed, and tested. While some of the components of the subsystems will be impossible to define until the concept of operations is developed, it is possible to list general systems and tools that will be used for their development. Since the idea behind EPC is similar to some other spacecraft missions, it will mostly use the same set of subsystems, however, some of the subsystems might be united under one group, due to their relative simplicity for this project mission. The difference from many other similar projects will be the usage of a recoverable sounding rocket, which will require the EPC to use some unique features to make it compatible with the launch vehicle.

### 2.2.1. Structure Subsystem

In this project, the structure subsystem is going to include aerodynamics, structure, mechanical, and thermal subsystems. The frame will be designed to incorporate the required subsystems in safe and designated places using Solidworks CAD, CFD, and FEA software. A collection mechanism will be implemented in the probe while keeping the aerodynamics for the highest collection rate. The collection rate can be achieved by using certain geometrical and mechanical features to decrease total pressure and increase the volume of processed air by a unit of altitude. Material choice for structure components will be known when the concept of operations is developed with known requirements and constraints for the frame. The simulation of the geometry dynamic behavior will be done using MATLAB-Simulink, in addition to hand calculations and estimations. Some parts of the prototypes will be manufactured and tested. Certain tests will be performed as well to verify the proper function of the analyzed systems.

### 2.2.2. Payload Subsystem

The payload subsystem will include all components required for the proper operation of the particle collection system, which contains, but is not limited to, certain electrical components, controllers, and mechanical systems. While all components will be known further into the project development, the payload subsystem will require such tools as SolidWorks CAD and CFD. It is not expected that the structural components of this subsystem will encounter significant forces; therefore, a simple structural analysis will be used for testing. For electrical parts and controllers, hand analysis will be used with the support of SolidWorks electrical simulation software. Exact coding applications will be known when the exact hardware is known, however, preference will be given to hardware using MATLAB and Arduino IDE coding languages.

### 2.2.3. Recovery Subsystem

The main objective of the recovery subsystem is to slow down the probe at the end of the flight so that it is safe to land at a velocity. While certain velocities will be known after the requirements and constraints have been determined, to improve the redundancy of this system, some additional sensors should be added, which will require hand circuit development, with possible usage of Solidworks electrical simulation.

### 2.2.4. Communication Subsystem

The communication subsystem is mostly represented by the GPS and will serve as the primary way to find the probe at long distances. In addition to geolocation, it is likely to be used for certain flight events, as one of the sources of information. Additional data transmission might be added, however, it will greatly depend on the significance of such transmission for the mission, compared to its weight, power consumption, cost, and the additional complexity of the subsystem. For the development and testing of this subsystem, mostly control applications from GPS manufacturers will be used, which may vary depending on the specific commercial GPS systems that will be used. GPS will need analysis according to its position and surroundings, while some land tests can be performed to verify the analysis. Additional data transmission might require some electrical analysis.

### 2.2.5. Electrical Subsystem

The electrical subsystem is going to be the main source of power for all other systems that might require it at any moment of mission operation. The choice of specific power cell composition and chemistry will require additional research. Wiring and connections are also part of the system and will be done by hand and using electrical simulation software, with testing verification.

### 2.2.6. Data Handling

The last subsystem is data handling. It is a new subsystem for EPC and is going to serve the function of data collection for better test and flight analysis. While the system is likely not going to provide much usage to other systems, it might be crucial for other systems' improvement afterward. While the sizing of the system is yet to be determined, it should not be large or negatively influence any other subsystem more than marginally.

Every step of the project development will be described with an explanation of the reasoning behind it, and media materials created during the development will be provided to

achieve a better understanding of the development process at different stages. Most of the components for the payload will be commercial-off-the-shelf, and some manufacturing will be done with accessible tools or orders. Assembly of certain components will be done in the equipped workshop, where most of the EPC assembly will take place as well.

### **3. Mission Statement, Stakeholders, and Concept Exploration**

#### **3.1. Mission Statement**

Mission development at any level requires stating the objectives and announcing what it aims to achieve. Mission objectives stating desirable goals can be broad and not quantitative, while they can serve as a reference to desirable results and evaluate how well those results are achieved. While the mission statement for the EPC is going to be similar to MMC, it needs to be stated to serve the described above function.

#### **3.2. The Extraterrestrial Material Collector Mission Statement**

Every day, Earth is bombarded by tons of extraterrestrial material. Some of this arrives as meteors, burning and breaking apart in the atmosphere, while the majority is small enough to slow down and avoid high temperatures, allowing it to reach the ground over the following days and blend with terrestrial materials. Given the scientific interest in these extraterrestrial particles, there is a pressing need for an accessible system capable of capturing them in midair before they become significantly contaminated by terrestrial matter. Additionally, the collection method should aim to maintain the structural integrity of the particles as much as possible.

#### **3.3. Stakeholders**

While the idea of a new system for a certain goal might be enough to start development, it is crucial to understand how and by whom the system will be used. In other words, it is required to know who the system stakeholders are. In the case of EPC, the stakeholders are external and primarily going to be people who will be using the system. The primary people who are in need of extraterrestrial materials and are planning to use EPC. This means that, in this case, stakeholders are going to be the scientific community whose research depends on airborne particles, particularly extraterrestrial particles falling on Earth. In some cases, the system might be used for broader atmospheric probing at different altitudes. It is worth keeping in mind that most researchers in the scientific community, as a rule, do not have access to big funds, and it will be preferable for the system to keep its assembly and operating costs low to increase accessibility for stakeholders.

### 3.4. General Concept

The general idea of the EPC mission is to use a recoverable amateur rocket to deliver a probe to a certain altitude at which it will be released into free fall and make its way to the surface, collecting extraterrestrial materials. To address the drawbacks of the old probe, as mentioned before, the new probe will be equipped with sensors that record and store flight data both for analysis during tests and after-flight analysis. The new design will use a partially modular structure to correct problems caused by internal system location and accessibility. The design will allocate unique space for wiring and will have connectors at several points to provide reliable connections between modules. The collection rates of a new probe compared to the old one will be increased by extending the diameter. New features will be used, such as propelled air acceleration to decrease pressure at intake and increase collection volumes further. The materials used in the new probe will be reviewed in favor of lighter and more accessible materials, strong enough to sustain free-fall forces at the designed velocities. Using different materials will also allow the geometry of the probe to be less cylindrical and enable surface features behind the 6-inch diameter collection surface. The power supply system will be entirely redesigned. It will use long-lasting power cells and reliable connections with the wireless power switch to maintain power charge during preparation, launch sequences, flight, and recovery. GPS will be designed to increase tracking ability at the distances the probe might fly and avoid interference with probe structure materials. The recovery system will be designed to have a redundant input signal on when to eject. It intends to use lightweight, durable materials while decreasing damage risk due to energetics by adding more safety features between the energetics and the recovery system. The payload structure requires the shock cord trench to allow nominal deployment and recoverability of the rocket components.

### 3.5. Trade Studies

The mission concept allows several variables to be changed later during development. The ability or inability to change certain main variables and convert them into parameters early is described in the table below, with reasoning provided.

Table 4.1 - Table of trade studies of the EPC project

Element of system architecture	Can be traded?	Reason	Alternatives
Mission concept	No	The collection method is stated to be a rocket/probe collection, and the main concept cannot change	N/A
Ground Infrastructure	Yes	Alternative infrastructure can be used as long as the mission can be accomplished	Changes in launch rails, launch sites, tracking stations, and safety measurements
Launch vehicle	Yes	It can be changed as long as the desired altitude can be reached and deployment can be done safely, with a preference for recoverability	Rocket design does not matter as long as it can deploy the payload at the required altitude and recover after
Collection methods	Yes	The different collection methods discussed in the literature review can be used as long as particles can be collected safely	Inertial collection, aerogel collection, aerosol filters, or a combination
GPS	Yes	Alternative manufacturers are available	Multitronix, AltusMetrum, Featherweight, BigRedBee.
Avionic	Yes	Alternative manufacturers are available	Multitronix, AltusMetrum
Shock-cord Trench	No	Required for the recovery of the rocket.	N/A
Materials	Yes	Materials may be wary, while the preference will be given to accessible, cheap, and durable materials	Aluminum, Fiberglass, PETG, PETG+, PC, or others. Combinations are possible.
Contamination prevention	No	The absence of contamination prevention will jeopardize the samples in dense atmosphere layers and at touchdown	N/A
Accessibility and modularity	Yes	The degree of accessibility and modularity may differ. Should allow good accessibility	Full modularity, Partial modularity, Cluster modularity, Accessibility hatches
Additional pressure control	Yes	It will help to process higher volumes of air, but it can be removed if there is a decrease in redundancy	No additional, Compressor, Pump, or combination
Data recording	No	Data recording is required for post-flight analysis and cannot be removed. Simple data recording will suffice	N/A

### 3.6. Alternative Subsystem Concepts

For every tradable element, there are two or more alternatives. To design a better system, it is vital to investigate the positive and negative sides of alternative subsystem concepts. A short description of the alternative subsystem will be provided in this section.

#### 3.6.1. Ground Infrastructure Alternatives

The alternatives for the ground infrastructure are represented by various launch rails, tracking stations, safety measurements, and recovery equipment. Usually, all of it is available at specialized locations, such as FAR, which will be described in detail in the Concept of Operation section. Depending on the various factors, such as the length of launch rails available, surrounding terrain, power, range of tracking stations, and other parameters, the launch trajectory and recovery can be affected, making the launch more or less accurate and recovery more complex and demanding. While it is possible to complete the task with the minimum requirements for ground infrastructure, better equipment will significantly simplify the task.

#### 3.6.2. Launch Vehicle Alternatives

The launch vehicle for the project can vary as long as it allows safe deployment at the required altitude. If needed, it can be launched as a one-stage or two-stage rocket or even from another vehicle. The preference will be given to the cheapest and the most reliable way to complete the task, which, at the moment, seems to be the two-stage rocket configuration, with the second stage inner diameter being precisely 6 inches.

#### 3.6.3. Collection Method Alternatives

Inertial collection methods have a significant benefit over others for a moving probe in an airflow because collection can be achieved without additional power intake and by using the probe's energy in the freefall. The inertial collection can harm the integrity of large particles, which can be reduced by using additives, such as covering collection surfaces in viscous silicon oil.

Aerogel collection was the method used at ISS, and it had a very low collection rate. With the proper chemistry of aerogel, it might be strong enough to sustain direct aerodynamic forces acting upon it during descent. Utilizing an aerogel collection in the low-density atmosphere might be also possible as a secondary collection method.

Aerosol filters will work well for the delicate separation of large quantities of air while

creating a problem of high flow obstruction. The collection rate might be reduced unless special pressure control features are introduced in the design.

#### 3.6.4. GPS Alternatives

GPS alternatives are decided mainly by various brands of commercially available GPS transmitters and receivers. There are many options for commercial GPS transmitters. The ones tested for high-altitude rockets can be selected, such as brands like Multitronix, AltusMetrum, Featherweight, and BigRedBee, all of which have GPS systems reaching ranges of over 100 km. The cheapest options are Featherweight and AltusMetrum, and the most reliable are from BigRedBee and Multitronix. The size of systems and their antennas vary, and the final decision will depend on the position of the system on the probe, GPS, and electrical power requirements, as well as the size of the system.

### 4. Concept of Operations

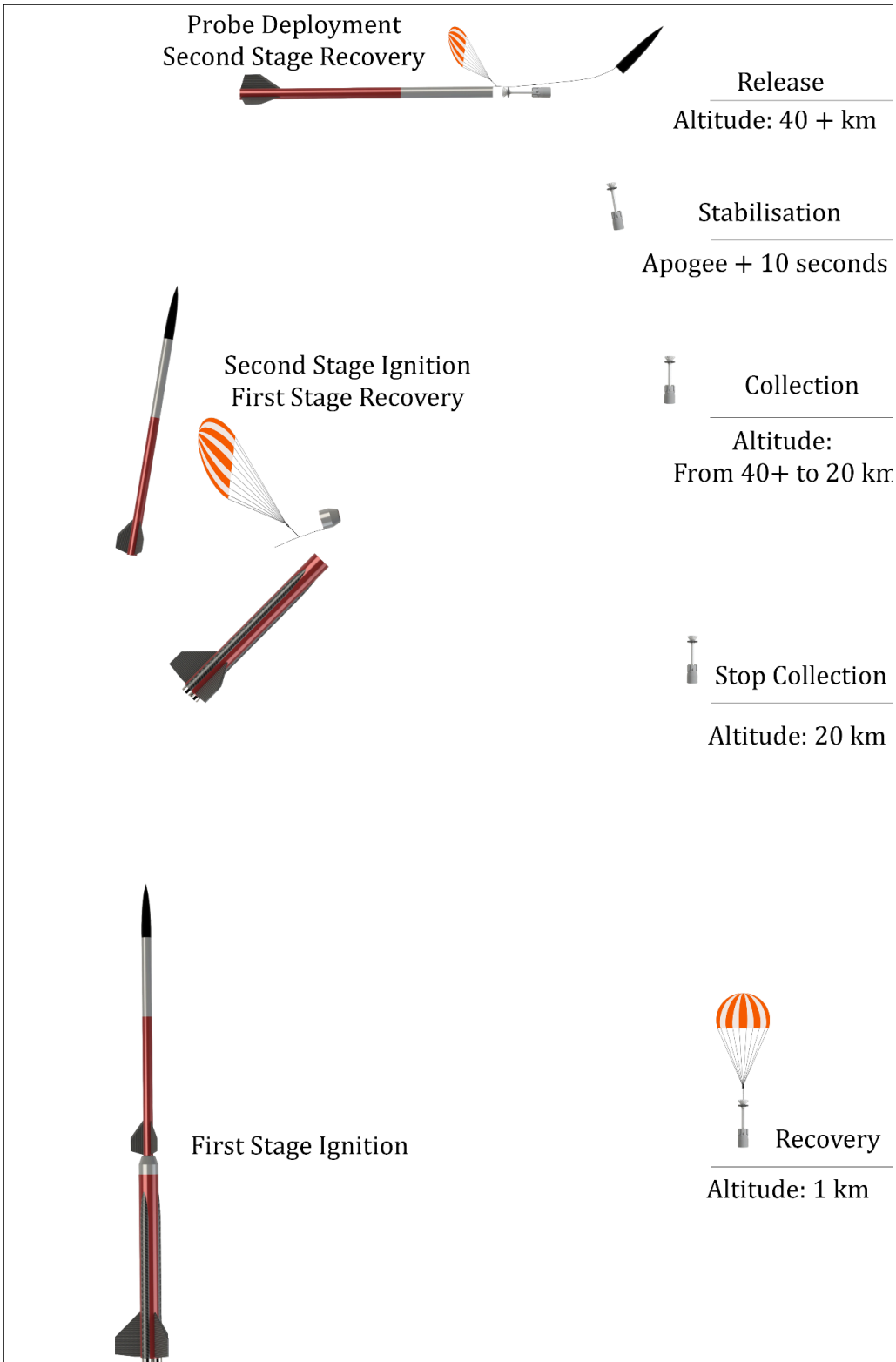


Figure 4.1 - Concept of operation

## 4.1. Ground Infrastructure

Some level of ground infrastructure is required for any rocket launch. The ground infrastructure of amateur rocketry consists of launch rails, ignition transmitters, and safety measures, while more complex projects usually require tracking equipment, recovery equipment, and sometimes control stations. Projects using liquid fuels, active control systems, or other equipment may require additional ground infrastructure.

The only place in California open for testing and launching high-altitude rockets is the Friends of Amateur Rocketry (FAR) launch site in southern California. This launch site was used for the previous attempt in the MMC project. Due to requirements from the FAA for launching altitude, it is only possible to launch rockets to altitudes high enough to allow uncontaminated collection in a short list of spots in the United States. While the EPC project is designed to be operable at any point on Earth, its actual use will be restricted by rules and regulations in each country. It will be done to simplify things and go over the necessary infrastructure using the example of the FAR launch site as the place where the first test would be planned.

The FAR launch site has infrastructure such as power sources for electronics and tracking stations, launching rails of different lengths for stable launches, and protective bunkers from where observation and tracking can occur. The area around the launch site is primarily barren with small amounts of flora, mainly consisting of bushes, dry plants, and fauna of creatures common to deserts. Weather conditions in the Mojave Desert almost guarantee the launch at the chosen time, and there is an established procedure to receive a waiver for launch.

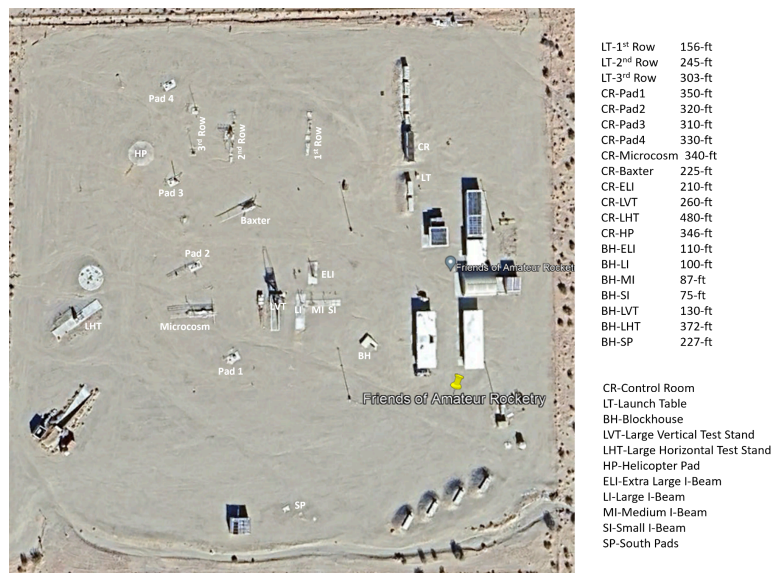


Figure 4.2 - The map of the FAA launch site [40]

#### 4.1.1. Launching Rails

The FAA launch site allows one to choose between several launch rails for a wide range of diameters used in amateur rocketry. Despite most of the flight happening when the rocket leaves the rail, the very beginning of the rocket trajectory is crucial for uncontrolled flight due to the lower velocity and, thereby, stabilization effect of aerodynamic forces and the higher effect of any possible disturbances on the final trajectory. An extended rail will let the rocket achieve higher release velocity with a proper trajectory, increasing the chances of a successful launch. While the rocket often spends less than a second on a launch rail, a change of launch rail length from a 10-foot-long one, regularly used for high-power rocketry, to 60 a 60-foot-long one, available on the FAA launch site, can result in more than twice the increase in release velocity.

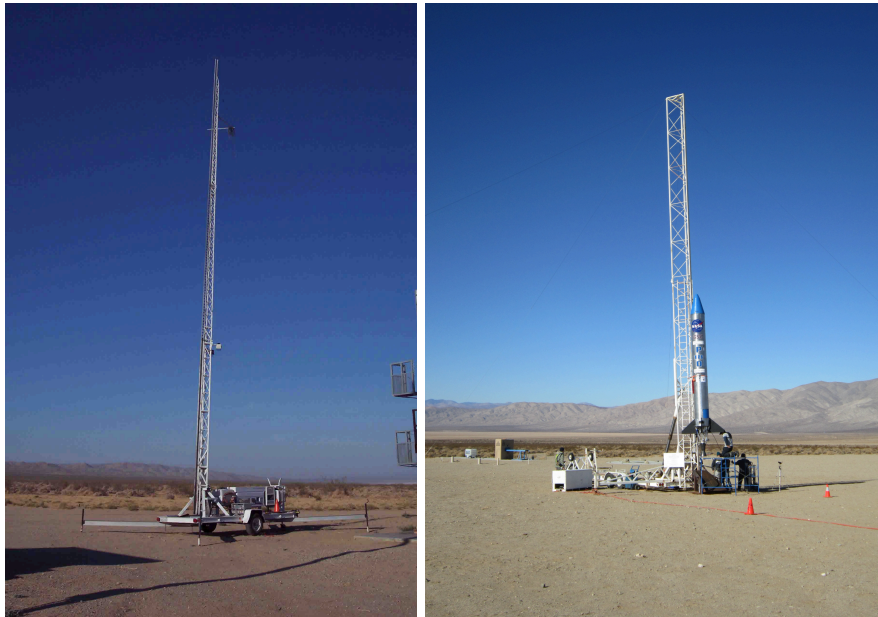


Figure 4.3 - Launching rails at the FAR launch site in the Mojave Desert. Baxter 60-Foot T-Rail at the left and Microcosm 60-Foot T-Rail at the right

#### 4.1.2. Safety Measurements

The FAA launch site is equipped with several bunkers for safe observation and tracking of the launch. While safety measurements are necessary for any launch, it is even more important at the very beginning of the rocket testing phase due to possible unforeseen problems with the newly manufactured rocket's safety. Before the first real launch tests for a large rocket are done, having a bunker around the launch rail can help maintain limbs' and bodies' structural integrity.



Figure 4.4 - Buried in the ground bunker at the FAA launch site

#### 4.1.3. Tracking Stations

The tracking station for the EPC project is expected to be able to track several objects at a distance as long as the apogee of the rocket and payload, and even further, for some degree of safety. The GPS signal is most commonly used for positioning the separately descending components. The tracking station is also required to follow the rules of use for the RF frequencies available for civil use and amateur rocketry. Most commonly, it is frequencies on 70cm and 33cm bands, with frequencies around 430-440 MHz and 900-920 MHz, with some frequencies to be avoided in that range. As a rule, lower frequencies tend to work better at longer distances and penetrate objects (Such as probes and rocket structures) more easily; however, they require additional certification to be used.

#### 4.1.4. Recovery

Recovery of the rocket and payload is usually the longest stage of rocket launch. Independent of the outcome of the launch, finding every single piece of the rocket and payload is important for the analysis and verification of subsystem work. If tracking work is good and the position of the parts and payload is known, this task is relatively easy. Otherwise, the search for the part can be a complex and time-consuming task. The recovery can also be significantly more complex depending on the terrain, flora, and fauna around the landing points. Usually, rockets of the size expected to be used for EPC can be recovered with several people and any car that can reach close enough to the landing point.

## 4.2. The Rocket

A two-stage solid motor rocket is expected to achieve an altitude of collection of 25 kilometers or higher. The rocket for the EPC will be similar in its design and work principles to the rocket used for MMC, with a few differences.

- The first stage
  - Structure
    - Fin set
      - Three fins
      - Stability margin of 1.5-2.5
    - Internal sections
      - Motor tubes
      - Avionics section
      - Recovery tube
    - Adapter
      - Connected to the body and the parachute
      - Ejected after separation
  - Cluster of motors
    - Three O-class solid motors in a compact assembly
      - Thermite ignition for simultaneous work
  - Recovery system
    - CO2 ejection charge
    - Large diameter parachute
    - Flat shock-cord connecting adapter and main parachute
  - Avionics
    - Flight computer
      - Apogee detection for parachute ejection
      - Second-stage ignition using a separation cord
    - GPS transmitter
    - Power source

The connection between the stages will be done using the adapter from the first stage diameter to the diameter of the motor used in the second stage, where the metal case used for the motor will serve as the plug, keeping the second stage stable. Ignition is done using the separation method, where the motor gets ignited as continuity to the first stage disappears.

- The second stage
  - Structure
    - 6-inch diameter body tube

- Low friction with payload
- Motor
  - One O-Class solid motor
  - Ignited as the first stage separates
- Recovery system
  - Dual deployment system
  - Drogue deployed with payload
  - Separate main parachute deployment at low altitude
  - A round shock cord connecting the body tube and the nosecone
    - Should have additional protection from cutting
- Avionics
  - GPS&Flight computer
    - Apogee detection for payload ejection
    - Readings for the main parachute ejection
    - Serves both GPS and flight computer functions
    - Has an internal power source
- Payload Ejection
  - Ejected together with a nosecone
  - Piston to push the payload
    - Moved using nitrogen gas
    - Prevents gas leakage until the body tube is out of the body.
  - Shock cord through the payload
    - The piston is attached to the shock cord
    - As an attachment point for the drogue parachute
    - To keep the nosecone connected

The concept of such a rocket was proven during the MMC test launch. However, some changes in detail were required to maintain the stability and trajectory during the lift-off and ascent.

### 4.3. Flight Plan

The flight plan for the rocket states the stages of the rocket and payload and their expected actions and behavior during the flight. This flight plan is described using the two-stage rockets described in the previous section.

- Rail
  - On the rail, all internal systems should be turned on, and feedback about optimal work should be given while tracking stations should be able to track all transmitters in rocket parts and payload. The angle of the rail should be verified to

be the same as simulations after the rail is put back into the vertical position and all systems work nominally.

- In the best scenario, the rail should be pointing with a small angle opposite to the wind direction.

- Liftoff
  - At liftoff, the rocket is expected to reach an escape velocity high enough to achieve aerodynamic stability and decrease the possible effect of side wind at the launch site.
- Ascent
  - At the ascent, the rocket should maintain a vertical or mostly vertical orientation.
  - The drag stage separation with a short delay to ignite the second stage motor
  - The CO<sub>2</sub> parachute ejection charges of the first stage activate shortly after the second stage is released, deploying the main parachute and slowing down the stage.
  - The ascent of the second stage continues mostly vertically until it reaches the apogee.
  - After a certain altitude
- Apogee
  - At the apogee of the second stage, the EPC is deployed using the nitrogen ejection charge. The drogue parachute for the second stage is deployed at the same time.
  - Right after the deployment, the EPC is open and ready to collect particles
- Descent
  - The EPC probe collects particles until they pass through most of the collection altitudes, after which it stops collecting to prevent contamination.
  - The second stage is descending on the drogue chute until it reaches the predefined altitude at which the main parachute is ejected to slow down the stage before touchdown.
  - The recovery system of the probe is activated when it reaches a predefined altitude, deploying the main parachute with the gunpowder charge.
  - Both stages and payload are expected to land in different locations at a safe velocity.
- Recovery
  - The recovery of the stages and payload will start when it is known that the stages and payload have landed.
  - The tracking system should provide the position of all parts
    - If the tracking system fails at a particular stage, the approximated direction of recovery and additional equipment can be used to attempt to recover the part

- The car will be used to recover the first stage landed closer to the launch site, while other groups will attempt to recover the second stage and payload using cars or, if terrain does not allow, by walking to the expected landing positions

## 5. System Requirements

Functional requirements define what a system must do, outlining its features and capabilities. In contrast, non-functional requirements describe how well a system performs its functions, focusing on performance, usability, security, and reliability.

The system requirements must be defined to base the subsystems, components, and parts on them. It might be hard or even impossible to design a system that fits all needs if it is not done unless the system is simple and the requirements for all components are not defined.

### 5.1. Functional Requirements

For the EPC project, functional requirements attempt to specify the main points for system and subsystem design, ensuring that the system corresponds to them after all parts, components, and assemblies are completed.

Table 5.1 - Functional Requirements

#	Requirement Name	Numerical/Specific Requirement	Rationale
1	<b>Sample Collection Requirements</b>		
1.1	Contamination prevention ascent	Keep the collection space isolated until the probe reaches apogee and is fully deployed. (T apogee + 3 s)	The collection space needs to be protected to ensure the collection occurs at a chosen range of altitudes
1.2	Contamination prevention, descent, and recovery	Close the collection space from the surroundings when entering possibly contaminated altitudes (Altitude < 60000 ft)	The collection space needs to be protected to ensure the collection occurs at a chosen range of altitudes
2	<b>Power Management Requirements</b>		
2.1	Power storage	Enough power to maintain systems for 2 hours and GPS for a day	Enough energy for preflight preparation once the probe is on, and locate the probe for enough time to commence recovery operations.
2.2	Power cell chemistry	LiFePO <sub>4</sub> , NiMH, Alkaline, Li-Ion	Power cell chemistry should be able to sustain high loads and be considered safe for application in rocketry
3	<b>Structural Requirements</b>		

3.1	Stability	The aerodynamic stability during freefall should maintain the probe in the range of <10 degrees from the vertical	In case of high divergence from the vertical position, the collection rate will significantly decrease
3.2	Intake Area	The intake area should be as close as possible to the maximum area of a 6-inch diameter circle	The maximum collection rates can be achieved only by utilizing the maximum available area
3.3	Durability	Surfaces should maintain maximum possible aerodynamic forces with a margin of safety of at least 2. The structure should also be able to endure high-G forces at launch and recovery	The safety margin should be higher until more data is available to prevent deformation due to known and unknown forces.
3.4	Shock cord trench	Opening at the side should be at least ¼ inch wide and ⅛ inch high to let shock cords through	The shock cord opening is required for a recoverable rocket to be used. After deployment, the opening lets the shock cord keep the nosecone attached to the rocket.
4	<b>GPS Requirement</b>		
4.1	GPS range	GPS should reach a range of at least 50 kilometers	The GPS should be able to track the probe on its way up until maximum altitude and down, with possible horizontal displacement
5	<b>Data Acquisition Requirements</b>		
5.1	Data collection	Basic sensors can measure static and dynamic pressure, temperature, density, position, and orientation of the probe, throughout the flight duration	The data needs to be collected to allow post-flight analysis of the dynamics and surroundings of the probe
5.2	Data storage	Store all collected data	Data storage of the obtained flight data.

## 5.2. Non-Functional Requirements

For the EPC probe, the non-functional requirements are mostly “quality of life” features that should be present to make the probe easier to operate and more accessible to stakeholders, in this case, researchers who will be using it.

Table 5.2 - Non-Functional Requirements

#	Requirement Name	Numerical/Specific Requirement	Rationale
1	<b>Reliability Requirements</b>		
1.1	Reliability of components	Rely on tested electronics and systems	Increase the chance of success by decreasing the number of new systems

			and new electronics
2	<b>Usability Requirements</b>		
2.1	Probe Systems Accessibility	Easy accessible avionics and collector unit	Decrease preparation time and the chance of negative involvement during pre-flight procedures.
3	<b>Manufacturing</b>		
3.1	Manufacturing Cost	Use inexpensive materials for most of the design	The probe needs to be cheap enough to be produced for researchers with minimal funding
3.2	Manufacturing Accessibility	Design parts and components for accessible manufacturing methods, such as 3D printing	Should be available for manufacturing to most researchers

## 6. Component Design

After requirements are established, the high-level design can begin, narrowing down the possible look of EPC subsystems. Several iterations of the high-level design might be needed to properly understand all underlying design challenges and interactions between subsystems. In this section, the high-level design will be separated into subsections describing the design process of each subsystem, starting with the first iterations and explaining the thinking process during their development.

### 6.1. Structure

The structure development process started with creating a preliminary design model of the EPC, similar to the geometry of the MMC. During its creation, it became clear that with a larger diameter and usage of more accessible materials, it is possible to make geometry less cylindrical and create more surface features, creating more flexible designs while keeping similar durability qualities. It also allows the creation of an internal frame structure that will serve as an attachment point and support for other structures inside and outside the probe, such as internal holders for subsystems or outer walls. It allows easy access to any point inside the probe. Theoretically, such walls can be modified into modular subsystems, where each wall will contain specific systems, connecting with the rest of the probe when inserted into place.

As one of the requirements for the probe is the largest possible intake area, the nosecone of the probe extends to 6 inches in diameter. As was mentioned in the previous probe overview, the nosecone had a problem with high total pressure, which caused spillage to occur, making it easier

for particles to miss the collection area and reducing the efficiency of the probe. Another structure-related requirement is stability, which depends entirely on airflow and has no active stabilization systems. As the probe might have unpredictable dynamics at the beginning of its flight after deployment, the stabilization system needs to be able to return it to a vertical position, or one in the range of 10 degrees deviation from a vertical position, as it gains velocity in that direction. In simple words, the stabilization system will need a structure generating enough drag in the tail to keep the payload mostly vertical while keeping the center of mass as far as possible from it and having enough durability to resist aerodynamic forces at maximum velocity. Both components will need an analysis to find shapes that will lower the pressure without adding too much weight for the nosecone, and where the around-vertical position can be maintained with a reasonable additional structure for stabilization.

### 6.1.1. Nosecone Design

A probe's nosecone is a component that collects the particles and converges the air containing those particles to the collection unit. As was mentioned before, the nose cone design is required to have the following:

- 6-inch entrance diameter
- Reduce particle deflection caused by air spillage by reducing pressure
- Converge the flow to be fed into the collector unit

A nosecone design has several variables, such as length, exit area, and wall geometry, which result in different flow parameters. The best combination of such parameters will be the one that provides the pathway that captures particles for the wide range of particle diameters, with more attention to small particles, as the ones that are more influenced by flow parameters at given velocities. Some additional design variables that are not directly related to the efficiency of the nose but influence the system design as a whole are the thickness of walls to maintain the structural integrity of the nose and the location of internal systems in walls to bring the center of mass closer to the nosecone tip. With more pressure in the nosecone, the thicker walls will be required to keep the structure intact, and internal systems will have to move further from the tip, moving the center of mass closer to the stabilizer and requiring the stabilizer to be moved further away to maintain the same stabilization efficiency. A similar applies to the wall geometry; if it leaves more space for the internal components, the mass accumulates closer to the tip. With the additional design variables in mind, the nose cone design will need an analysis of possible shape variable changes and combinations for the approximated conditions of the maximum operational velocity (For this payload, maximum operational velocity is not the same as maximum velocity, and means the maximum velocity it is predicted to have after deployment and not the maximum velocity it can experience without damage). Using knowledge from the previous design and experimental data, the maximum velocity payload obtained after release depends on the release altitude, which is around 310 m/s for an altitude of 30 kilometers above sea level and 380 m/s for

an altitude of 40 km. Such data allows us to assume that with the change of materials and higher area, the new probe design can maintain maximum velocity in subsonic conditions with a maximum velocity of around 300 m/s or less, approaching but not crossing Mach 1. Due to the aerodynamics, the outer walls of the probe can experience transonic or supersonic conditions that will happen behind the nose tip and not influence the flow inside the nosecone. The flow inside the probe nosecone will experience only subsonic conditions, simplifying the task of analyzing it. Using the estimations of the previous probe, such a velocity can be achieved after around 30-40 seconds, equal to an altitude 5 to 6 kilometers lower than the deployment altitude. For analysis, the case somewhere between those conditions will be taken, with the altitude of maximum velocity being around 30 kilometers above sea level, relative air velocity of 300 m/s in the vertical direction. Using equations 1.6 and 1.7, the temperature and density of air for an altitude of 30 kilometers are -41.51 degrees Celsius (231.64 degrees Kelvin) and 1158.3 Pa, respectively. It will be the main case for analysis, as it has the most significant relative pressure change and might influence the particle trajectory the most.

To simulate the micrometeorite particles' motion in interaction with the nosecone, the spherical with a diameter of 5 and 200 micrometers and density of  $2.7 \text{ g/cm}^3$  similar particles with rocky origin, according to section 1.5.6 will be added in the airflow in front of the component at an equal horizontal distance on both sides from its center. This data will be used to analyze nosecone design using the SolidWorks Flow Simulation add-in to find which parameter results in better component efficiency. Due to the simplicity of the component, better component efficiency on its own will result in better efficiency when integrated into the system, and thereby, each nosecone will be analyzed separately from the rest of the system. The analysis of different nosecone designs was used to generate the table below, showing the results of changing variables on airflow parameters in the component. The few designs with possibly the best optimization for the payload needs were taken as a design with two consequent curves after a short linear slope at the tip of the wall, made for manufacturing purposes, and is almost parallel to the end of the top curve, as depicted in Figure 6.2. The design of two consecutive curves with a smaller central nosecone for different flow diversions is shown in picture 6.4, and the design with a more minor central nosecone feature. The additional length was added at the bottom of each nosecone design, further moving the internal flow point of interaction with the external flow to help with flow analysis. The surface roughness is assumed to be around the maximum for a 0.05 mm layer 3d printing and is equal to  $15 \text{ }\mu\text{m}$ . For all shapes, several parameters will be analyzed, such as maximum pressure, which influences the particle path, deflecting it away; the maximum temperature to be used for manufacturing purposes; the pressure, temperature, and velocity of the flow to be used in performance analysis of the geometry and future study of the following components.

For the first design, the radius of the curve will differ from one extreme point to another to cover most of the possible configurations to find the best fitting. The small steps in radius change will allow us to see changes in the flow parameters as the geometry of the internal walls changes. See Figure 6.2 for reference.

The second design will modify the two curvature walls with a minor nosecone feature some distance from the exit. This will help vary the area change at different stages of the flow convergence. The small steps in the radius change of the wall and central feature, as well as the location of the central feature, will be used to determine the influence on flow parameters. See Figure 6.3 for reference.

The third design will consist of two curved walls and a central nosecone. It attempts to make more changes closer to the center of the nosecone, possibly increasing the airspeed in near-wall areas at the entrance of the nosecone. See Figure 6.4 for reference.

The entrance and exit areas in all three cases are the same, which means the total area change will be the same for all cases. The length of the nosecone for all cases is the same and equals 4 inches. When the best case for a 4-inch nosecone is found, additional analysis for other lengths of nosecone will be conducted to find the optimal length. The main difference will be in the rate of area change at different lengths of the nosecone. The additional features may help to change the pressure and velocity of the air, especially at the entrance, letting more particles be captured in the airflow trapped inside the nosecone and helping there with air that keeps pressing from outside with constantly increasing total pressure as the payload descends. The flow results for the best nosecone analysis will be used as limiting flow parameters for analysis of the following component along the flow in the following sections - the collector unit.

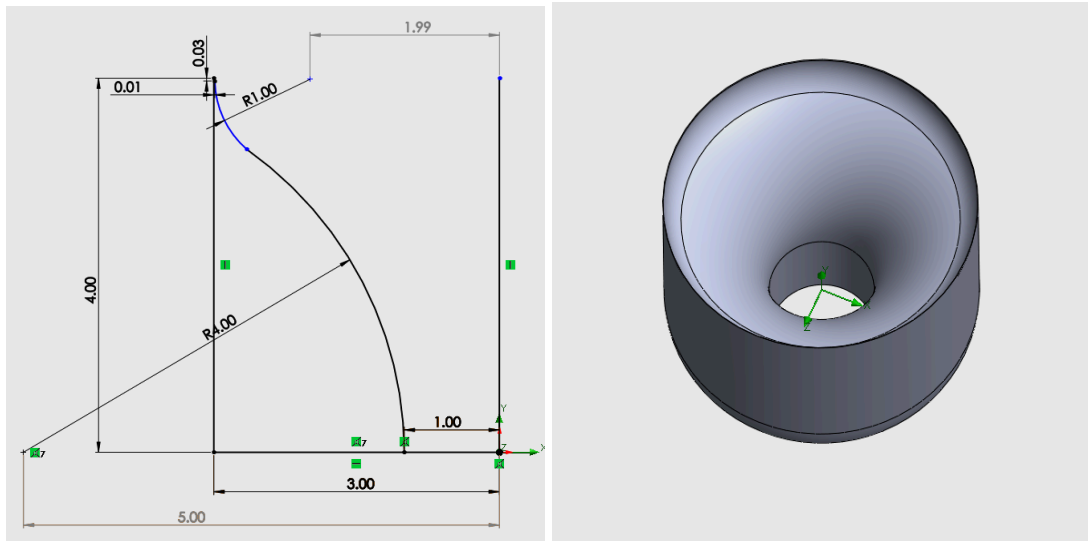


Figure 6.1 (At the left is the sketch; At the right is the geometry of the first design)

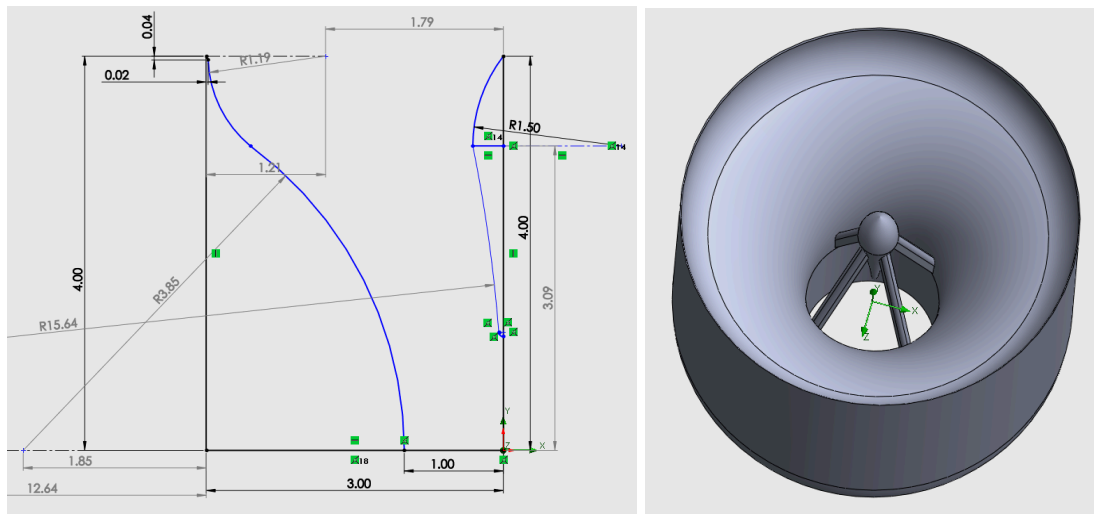


Figure 6.2 - At left is the sketch; At the right is the geometry of the second design.

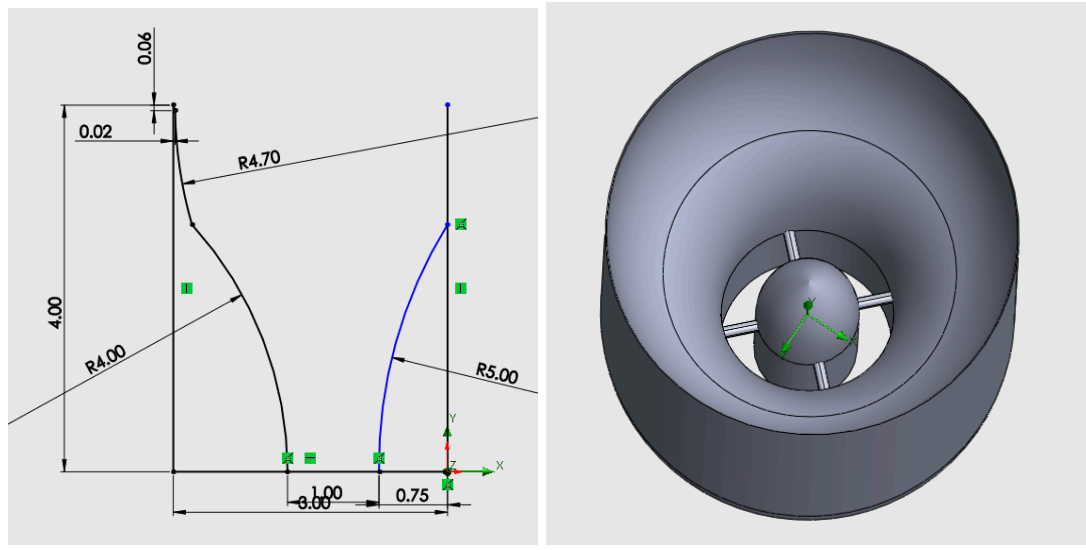


Figure 6.3 - At the left is the sketch; At the right is the geometry of the third design.

Table 6.1 - The analysis of 4-inch long nosecone configurations with variable curvature radius

Nose cone case #	Top curve radius (in)	Bottom curve radius (in)	Maximum pressure in the nosecone (Pa)	Maximum airflow temperature in the nosecone (Kelvin)	The pressure of the flow at the convergent exit (Pa)	Temperature of the flow at the convergent exit (Kelvin)	The velocity of the flow at the convergent exit (m/s)
1	0.5	4.5	2168.04	283.18	1392.72	247.71	255.93
2	1	4	2146.26	285.29	1401.94	247.83	254.45
3	1.25	4	2145.23	285.20	1401.31	247.80	254.54
4	1.5	3.5	2160.59	282.33	1418.22	248.50	252.24
5	2	3.5	2158.56	282.25	1417.91	248.49	252.30

6	2	3	2164.71	284.26	1427.01	248.93	250.18
7	2.5	3	2161.87	283.97	1427.35	248.92	250.1
8	3	3	2160.04	283.77	1428.12	248.94	249.95
9	2.5	2.5	2167.19	284.49	1432.69	250.50	245.80
10	3	2.5	2165.07	284.32	1433.75	250.57	245.63
11	3.5	2.5	2162.97	284.07	1434.16	250.58	245.56
12	3	2	2167.83	284.58	1429.52	251.81	244.85
13	3.5	2	2166.38	283.25	1429.45	251.83	244.92
14	4	2	2165.13	284.11	1429.48	251.85	244.97
15	4	1.5	2168.48	283.84	1471.92	252.92	237.69
16	5	1.5	2167.62	284.42	1491.42	253.47	234.51
17	6	1.5	2165.33	284.39	1491.12	253.44	234.59
18	4	1	2167.99	284.06	1505.35	254.65	234.23
19	5	1	2169.57	283.85	1507.20	254.68	233.78
20	6	1	2168.87	283.91	1517.56	255.11	231.973

From the analysis and table, it can be seen that with an increase in the radius of the top curvature and a decrease in the radius of the bottom curvature, the maximum pressure decreases but stays around 2200 pascals for most cases. The pressure and temperature at the exit increase while the velocity of the flow decreases. It means that the shape where the area decreases faster is closer to the entrance, which happens when the bottom curvature occupies most of the shape in the sketch in Figure 6.2. For all shapes, the temperature at any point of the geometry was around 285+-2.5 degrees. One of the best-performing geometries was nosecone case number 3, with relatively low maximum pressure and high flow velocity at the exit. All geometries had a similar problem: high-pressure zones at the sides close to the entrance and low flow velocity in those areas. It harms the total collection rate of the small particles because they are being heavily deflected and miss the collector's wall, as seen in Figure 6.5.

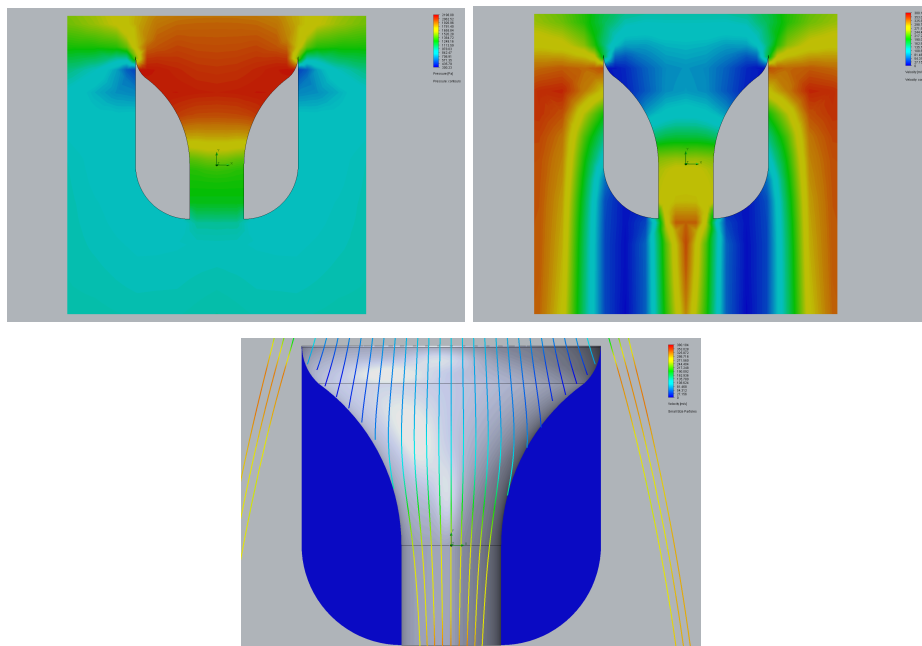


Figure 6.4 - CFD analysis of the nosecone

In Figure 6.4, the top image shows the pressure distribution in the nosecone, the middle image shows the velocity distribution in the nosecone, and the third image shows the path of the particles of a 5-micrometer diameter with an initial velocity of 300 m/s. Images with the original resolution are available in Appendix A.

The analysis of the first design showed a slight change in the flow parameters with the geometry change; the following two analyses will use fewer geometries for analysis to let more focus on improving the best-performing geometry when found, and analysis of nosecone length change on flow parameters.

Table 6.2 - The analysis of 4-inch long nosecone configurations with variable curvature radius and central nosecone feature at the distance from the exit

Nose cone #	Top curve radius (in)	Bottom curve radius (in)	Central nosecone distance from the entrance (in)	Central nosecone radius (in)	Central nosecone tail length (in)	Maximum pressure in the nosecone (Pa)	Maximum airflow temperature in the nosecone (Kelvin)	The pressure of the flow at the convergent exit (Pa)	Temperature of the flow at the convergent exit (Kelvin)	The velocity of the flow at the convergent exit (m/s)
1	0.5	4.53	0	1	0.7	2176.33	282.30	1403.86	247.55	251.92
2	0.5	4.53	1	1	0.7	2180.58	282.71	1393.10	248.87	245.96
3	0.5	4.53	2	1	0.7	2173.01	283.15	1378.47	248.59	245.48
4	1	4.13	0	1	0.7	2169.60	282.75	1411.72	247.86	250.60

5	1.5	3.56	0	1	0.7	2177.95	282.75	1421.48	248.41	249.08
6	1	4.13	0	1	1.5	2170.06	282.77	1411.70	247.81	250.78
7	1.5	3.58	0	1.5	1	2175.14	282.35	1408.6	250.81	243.471
8	3	2.03	0	1	0.7	2188.19	284.01	1468.33	251.30	241.30
9	1	4.13	0	0.75	0.7	2165.99	282.72	1409.46	247.93	250.40
10	1	4.13	0	removed	removed	2147.14	285.92	1396.65	247.86	255.251

In the first three cases, analysis quickly showed that the central nosecone feature has a worse effect when it is located closer to the middle and provides better velocity of the flow on the sides when it is located at the level of the top curvature. Adding a central nosecone resulted in cases where the maximum pressure point was not next to the wall but between the wall and the central nosecone. By trying different cases, it was found that adding any feature in front will result in increased pressure and does not help with the problem of low velocity at the walls near the entrance. In general, the second design was less effective than the first one.

Table 6.3 - The analysis of 4-inch long nosecone configurations with variable curvature radius and central nosecone feature at the distance from the exit

case #	Top curve radius (in)	Bottom curve radius (in)	Central nosecone radius (in)	Maximum pressure in the nosecone (Pa)	Maximum airflow temperature in the nosecone (Kelvin)	The pressure of the flow at the convergent exit (Pa)	Temperature of the flow at the convergent exit (Kelvin)	The velocity of the flow at the convergent exit (m/s)
1	0.8	6.5	1	2151.09	288.35	1415.15	249.91	245.91
2	0.8	6.5	0.75	2150.49	290.64	1416.31	250.86	244.005
3	0.8	6.5	1*	2155.77	287.44	1505.55	255.20	224.546
4	0.8	6.5	2	2148.93	288.74	1393.30	248.60	251.06
5	0.8	6.5	3	2149.77	288.99	1388.49	247.50	252.79
6	0.8	6.5	5	2151.14	288.93	1387.63	247.50	254.75
7	0.8	6.5	8	2155.35	288.31	1386.22	247.20	254.44
8	0.8	6.5	11	2153.55	288.59	1384.91	247.10	255.03
9	2.14	5	2	2156.65	289.94	1401.23	249.09	249.92
10	4.12	3	2	2161.61	292.08	1419.86	250.33	246.42
11	0	7.03	2	2149.29	285.07	1390.77	248.23	251.515

\* The star specifies the radius with the center moved in the vertical instead of the horizontal direction

The analysis of the third design showed some practical cases when the central nosecone is moderate in size and the wall has a primarily consistent curve, as can be seen in nosecone number 4. The third design performed better than the other two for small particle collection. It theoretically makes adding a fan powered by the wind behind the nosecone exit possible. However, it adds a lot of structure and leaves less space for internal systems, which can negatively influence stability and add too much weight to the system without significant output.

The nosecone design analysis included more than three designs, but only three were worth mentioning. It showed that the first design, nosecone three, could be the best fit if no fan was used, while the third design, nosecone four, could be the best fit for a design that utilizes a fan powered by electricity or wind. Further analysis of the nosecone will focus on improving the design in combination with the other components of the probe, testing cases with variable nosecone length to improve nosecone performance, and making space for internal components behind it, which will be discussed in the following sections.

### 6.1.2. The Collection Unit Design

From the literature review of the collection methods, the most applicable method for the payload purpose is an inertial collection method, where the particle's mass helps to separate it from the airflow. This is similar to how the nosecone, designed from the previous section, collected particles from the airflow that was passing by it without being collected because particles couldn't change their trajectory as fast as air did. The main idea behind the collector is to create geometries that accelerate and deflect the flow with many stages (or cascades) of acceleration and deflection. The flow is accelerated by decreasing the total area of the openings compared to the total area of openings in the previous stage and the distance between the stage and the collection plate. Ideally, as a particle gets into the accelerated flow, it obtains energy, and by having a higher mass than the flow particles, it takes a longer path to deflect and touches the surface of the collector plate, usually covered with viscous fluid. The stages have to decrease the area gradually to maintain the flow accelerated at each stage, despite the pressure losses.

Two types of cascade inertial collectors can be used for this project. The first one is the cascade collector with a single opening per stage, which decreases the area at every stage. In subsonic flow, a decrease in area increases the flow speed, giving all kinds of particles more energy and making it harder to deflect with every stage while not obstructing the flow too much. Another type of inertial collector is where, with every stage, the number of openings increases. At the same time, their diameter significantly decreases, so every subsequent stage has more openings but less total opening area. In both cases, after every stage, there is a collection plate designed to catch particles with inertia and direct airflow to the next stage, and the height of each subsequent stage decreases to make less space for particles to deflect and increase the collection rate. Collection plates are usually covered with silicon oil or similar substances, so particles will stick and get absorbed by the oil to be protected from the surroundings during and after

collection. Sometimes, a filter is placed after the last stage to collect the smaller particles or prevent particles from leaving the exit. Both types of cascade collectors can be assembled in cylindrical shapes, adding as many stages as needed. Still, the second type of collector can be shaped as an extruded washer, allowing other probe features or systems to be located inside it. From the review of different tests on cascade impactors, the usual area change ratio between stages lies between 2 and 3 times. It provides the pressure difference necessary to push the flow further at each stage.

The data obtained in nosecone analysis for cylindrical or washer-shaped exits will be used to simulate and analyze respective collector designs for both types of cascade collectors. The first type of collector and the first option of the second type will use the flow parameters obtained for the first design, nosecone number three, with the diameter of exit equal to 2 inches and flow parameters as follows:  $p = 1401.31$  Pa,  $T = 247.80$  K,  $v = 254.54$  m/s, and the second option of the second type of collector will use the washer-shaped opening from the third design, nosecone number four with an inner diameter of the exit being 0.75 in an outer diameter 1.75 in and following flow parameters:  $p = 1393.30$  Pa,  $T = 248.60$  K,  $v = 251.06$  m/s. The particle velocity for the two nosecones is very close to the actual flow velocity, and for this simulation, it will be set equal to the flow velocity. The collector itself will be designed by applying the physical properties of particles and air described above and analyzed with the jets of particles of 5 micrometers and 200 micrometers in diameter and a density of  $2.7 \text{ g/cm}^3$ . One of the significant dictating conditions for each part of the collector unit is to be 3D-printable, restrict the design to specific geometries, and not allow features under flat surfaces.

#### 6.1.2.1. Cylindrical Cascade Collector with a Single Opening

The first type of collector is the cylindrical cascade collector with only one opening per stage. The initial testing collector unit had five stages, with radius openings of 0.7, 0.5, 0.35, 0.2, and 0.1 at respective stages from stage 1 to stage 5, where stage 5 is the last in geometry, as seen in Figure 6.6. From particle trajectory analysis, it became apparent that larger particles tend to get into the collection plates by stage number three, while smaller particles keep flowing further. One of the issues with the tested geometry was low-pressure and high-pressure zones in various parts of the stage surface, particularly close to the openings and behind the structural beams holding collector plates. The solution to this problem can be a better airflow direction past the stage and before the next one. The subsequent iterations of the collector unit design will attempt to resolve those problems and result in a geometry that works better for both values of particle diameter.

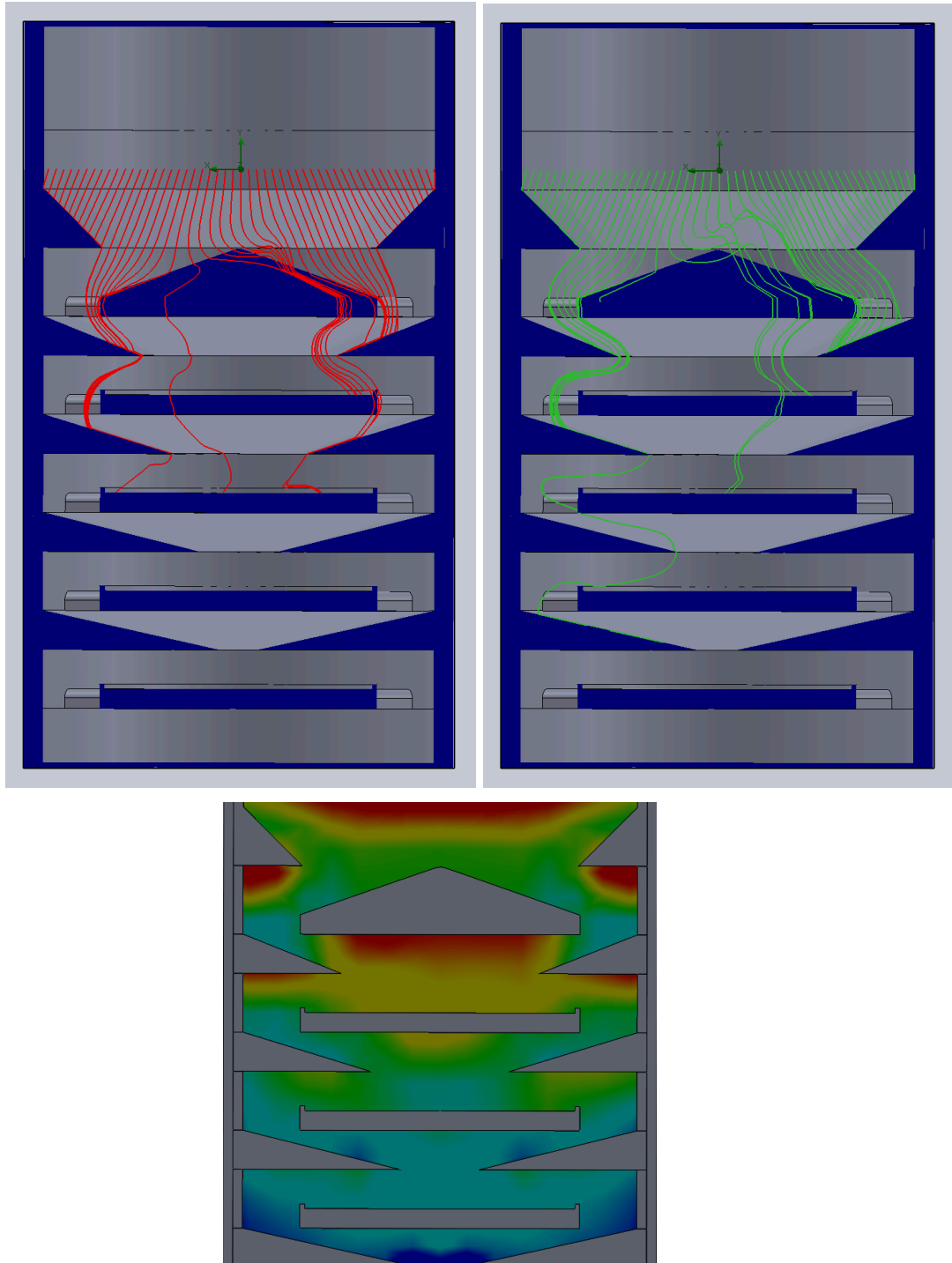


Figure 6.5 - CFD analysis of the collector unit

On figure 6.5 the top images, the trajectories of particles in the first iteration of the cylindrical cascade collector design with a single opening per stage. The red lines represent spherical particles of 200 micrometers in size, and the green lines represent spherical particles of 5 micrometers in size. The density of particles used is  $2.7 \text{ g/cm}^3$  for both cases. On the bottom,

the relative pressure distribution inside the collector unit shows low-pressure and high-pressure zones.

After several more iterations, the geometry reached the point where the particle trajectory simulation showed that out of 100 equally spaced particles 5 micrometers in diameter created at the flow inlet, the majority did not pass through stage 3; some got stuck between stage 3 and 4, none were captured at stage 4 and 5, and only two passed through stage 5. This was achieved by decreasing the area available for the flow at each collection plate and adding a chamfer behind the stages. Iteration 5 had some changes, including smoothing edges and reducing the distance between the opening and collection plate for stages 4 and 5, resulting in no particles passing beyond stage 4. However, it still had problems with low-pressure zones at some surfaces, and some particles were stuck in them. Iteration 6 had some changes in the curvature of stages and collection plate corners that resulted in less abundant low-pressure zones, and out of 100 particles, four got stuck in a low-pressure zone between stages 3 and 4, and five particles reached level 5, where all of them were directed at the collection plate. The following iterations did not resolve the problem of particles getting stuck. This resulted in a worse collection rate, so it was decided to keep iteration 6 as the final iteration for this component development until further tests in combination with the nosecone are performed.

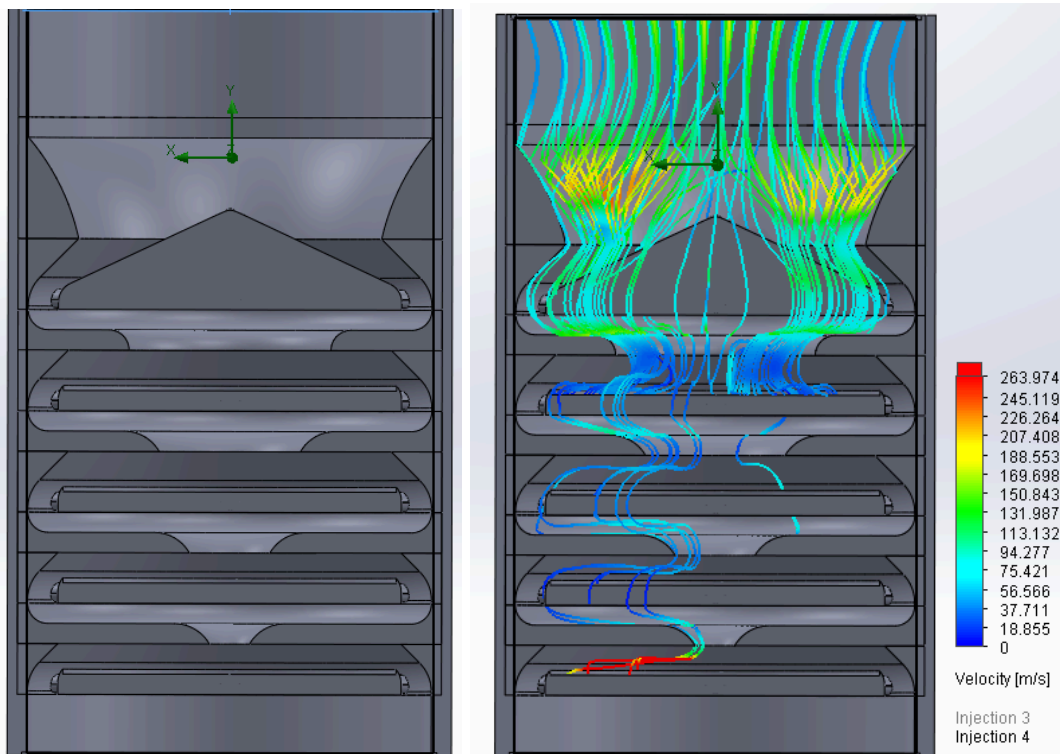


Figure 6.6 - Iteration 6 of cylindrical single opening per stage collector design geometry and with one hundred 5-micrometer diameter particles injection

### 6.1.2.2. Cylindrical Cascade Collector with Multiple Openings

The second type of cylindrical collector is the cascade collector with multiple openings per stage. The initial design uses five stages, proving reliable for collecting all particles in the chosen diameter range. Due to the lack of powerful pumps usually used in connection with cascade impactors, it was decided to keep the area ratios between stages between 1 and 2 and see if it would be enough to maintain pressure and accelerate particles between layers. The first stage uses six 0.44-inch openings, the second stage has twelve openings 0.2 inches in diameter, the third stage has seventy-two openings 0.1 inches in diameter, the fourth has seventy-two openings 0.08 inches in diameter, and the fifth has seventy-two openings 0.06 inches in diameter.

The flow simulation and particle injection showed very high pressure in front of the collector, which can significantly decrease the nosecone's collection rates. However, all particles in injections of 200-micrometer and 5-micrometer diameter particles were collected in the first two stages. To reduce pressure in front of the collector, the opening area at each stage will be increased while maintaining similar area ratios between stages.

An increase in area at each stage, smothering the edges of the collector plates and nosecone for flow direction at the first stage, resulted in decreased pressure in front of the collector. At the same time, all of the particles were collected. There were almost no low-pressure zones where particles got stuck. By stage 4, all particles of the chosen diameter were captured by collection plates, which proves that the current geometry of the cylindrical cascade collector with multiple openings is suitable for testing in combination with the nosecone. The results of iteration three can be seen in Figure 6.8.

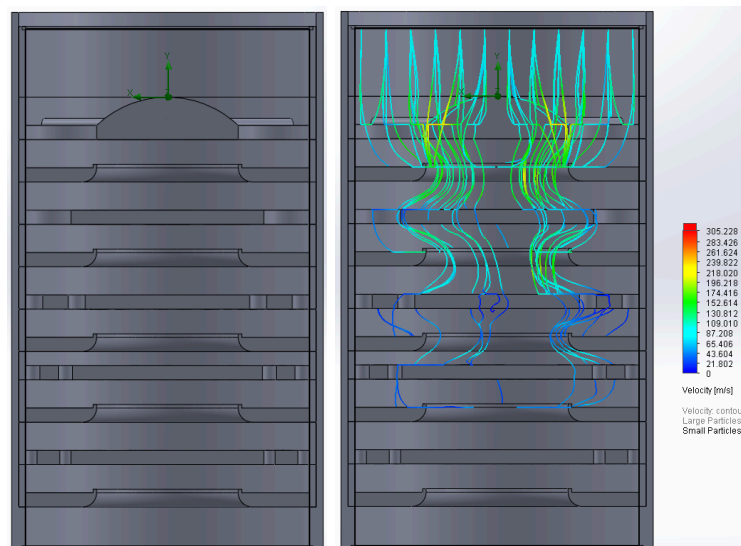


Figure 6.7 - Iteration 6 of cylindrical multiple opening per stage collector design geometry and with one hundred 5-micrometer diameter particles injection

### 6.1.2.3. Extruded-Washer-Shaped Cascade Collector with Multiple Openings

The last configuration of the cascade collector to be tested is the washer-shaped extruded collector. Such a shape might be needed if the payload design requires a wind-powered or electrical-powered fan in front of the collector, with a shaft or an electrical motor inside the inner collector walls or nosecone, with other configurations than the two previous collectors used. Depending on the inner diameter of the collector, other electronic parts or components may be located inside. The internal features of this configuration will be very similar to the internal features of the cylindrical multiple-opening cascade collector. The first iteration design will maintain similar area ratios to the cylindrical one, with the following diameter of openings per stage: 0.5 at stage 1, 0.32 at stage 2, 0.18 at stage 3, 0.12 at stage 4, and 0.1 at stage 5. The results of the first iteration were satisfactory, as all 5-micrometer diameter particles were collected at the first two stages. The following stages could be removed if required by the design.

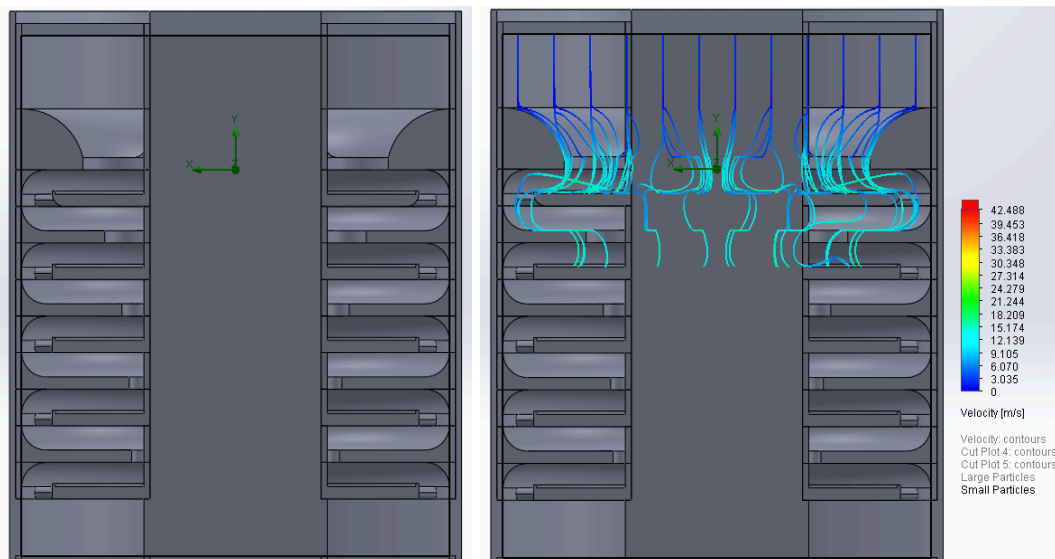


Figure 6.8 - Iteration 1 of extruded-washer shaped with multiple openings per stage collector geometry and with one hundred 5-micrometer diameter particles injection

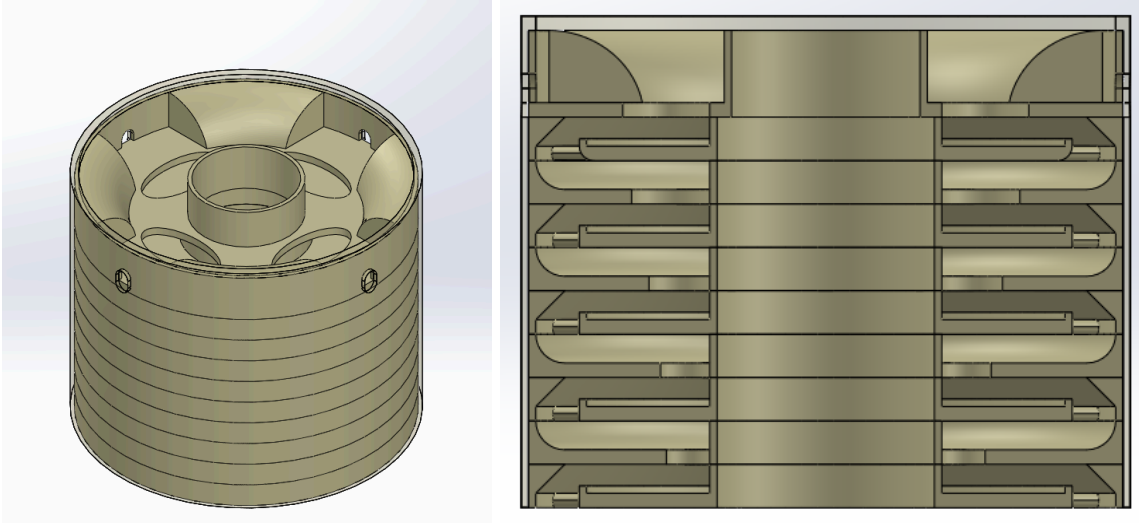


Figure 6.9 - The final iteration of the collector unit adapted for the rest of the probe assembly

#### 6.1.2.4. Nosecone-Collector Assembly Analysis

As the collectors' designs on their own were analyzed and showed good performance for given conditions, they were tested in combination with the respective nosecone. The results showed a major problem with pressure in the nose cone, resulting in a big air spillage and particles of the entire diameter range. It was caused by the significant area decrease when the collector was attached to the nosecone, and while they work well separately, together, they needed some additional redesign. The problem with high frontal pressure could be partially resolved by introducing the new component to assist with airflow compression. The compressor will be positioned between the nosecone and the collector to decrease pressure at the nosecone exit and increase pressure at the collector entrance, which should result in better assembly performance. The following section will describe the compressor design.

#### 6.1.3. The Compressor Design

The idea of a compressor for the probe comes directly from low-pressure compressors used in aircraft engines. In these, the flow from a larger intake area gets compressed before entering the following smaller-area high-pressure compressor, which then feeds it into the combustion chamber. The compressor will require a rotor and stator airfoil design, a shaft, a shaft gearbox, and a torque source.

The airfoil design can be very time-consuming and complex since each profile must be tested for different parameters under different conditions to show how well it completes its task. To simplify the design process and save a significant amount of time, the airfoil design for the rotor and stator will use one of the existing designs available in the NACA airfoil database. As was mentioned in several sources describing the design of compressor systems for engines and

turbines, the NACA 65 - series airfoils are a generally great fit for such applications. Additionally, the airfoil design usable for the current project will significantly depend on the part's durability when it is manufactured using the available materials. The airfoil has to be not more than 2 inches in chamber length and not more than 3 inches in extruded airfoil length. When manufactured with 3D printing techniques, additional attention needs to be paid to the total width of the part, as too thin parts can have issues with printing and axial strength of the created part, as it might experience high axial loads, which usually means lower layer height and longer printing times.

Usually, compressors for turbines and engines have many stages to ensure proper air pressurization when it gets to the combustion stage or to get as much energy as possible from the flow. This is different for this project application because the main goal is not to pressurize air but to reduce spillage and take as many particles from the incoming flow as possible. In contrast, the actual airflow rate doesn't matter as long as there is a pressure difference between the entrance and exit of the collector unit. The stability and dimension requirements of the probe will not allow too many stages for the rotor to be present inside the nosecone, and since each rotor stage needs a stator stage, depending on the size, realistically, the payload can have 2 or 4 stages of rotors and stators inside the compressor. It should be enough to help reduce the pressure in front of the nosecone to let more particles in the airflow go through the collector unit. The number of blades to be used in the rotor will depend on factors such as intake velocity, exit velocity, angle of attack of blades at the stage, and chord length, and it will also be influenced by the radius of the holding structure. The structure itself will be a part of the nosecone, likely similar to the third design of the nosecone tested previously, where both converging walls and the central nosecone were used.

To utilize the previously obtained data and results, the compressor design will attempt to combine the nosecone design with the central nosecone before and the compressor design of a turbojet engine, where the central nosecone will be used for both the converging of the flow and as the end of the shaft for the rotor blades.

#### 6.1.3.1. The Rotor and Stator Airfoil Design

The Von Karman-shaped nosecone should provide a relatively small amount of drag when used as the shape of the central nosecone on the rotor. The entire nosecone can work as a drag reduction for the converging shape and as a carrier for the rotor blades at the end of the shaft. The rotor's blades will be attached to the rotor to make it secure so that the rotor can rotate at a maximum approximate rotational velocity.

The NACA 65 series airfoils have a wide variety of designs created for use in the axial-flow compressor and many of which are a good fit for the blade design, as they provide good lift coefficient and optimized for high deflection angles. As for the EPC project, the NACA 65-221, 65-410, and 65-618 were the airfoils first chosen to estimate how well they could fit the

performance and manufacturing requirements for the project because they represent the airfoils with different thicknesses to chord ratio and chord curvature.

Out of the three airfoil profiles, only the 65-410 could satisfy both the performance and manufacturing requirements for the estimated size of the blade as it offers a high maximum-thickness-to-chord ratio, which ensures the strength of the blade when manufacturing with the 3D-printing method and allows a higher maximum deflection angle, up to 20 degrees before airfoil stalls.

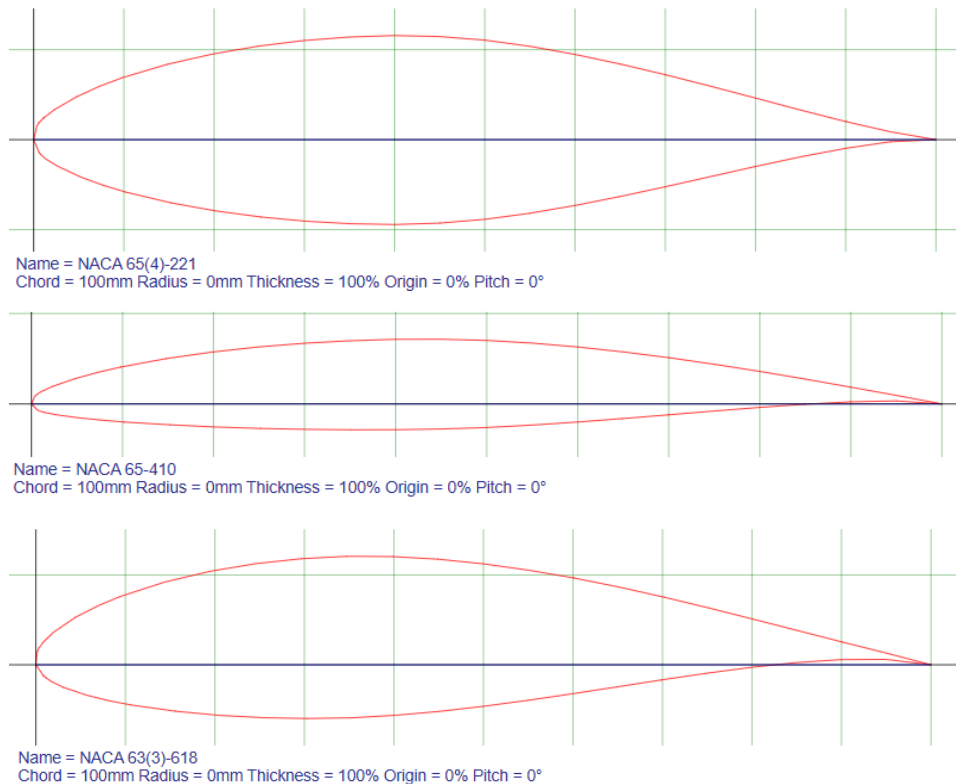


Figure 6.10 - The NACA 65-series airfoils analyzed for the compressor

Combining airfoils with the nosecone is enough to calculate the airfoil's vertical distance at a specific deflection angle and add some spaces between the rotor and stator for both safe rotation and flow diffusion. The nosecone will have radial airfoil-shaped openings at each layer of the rotor and stators. In contrast, blades for rotors and stators will be manufactured separately, accounting for the distance inserted into the nosecone.

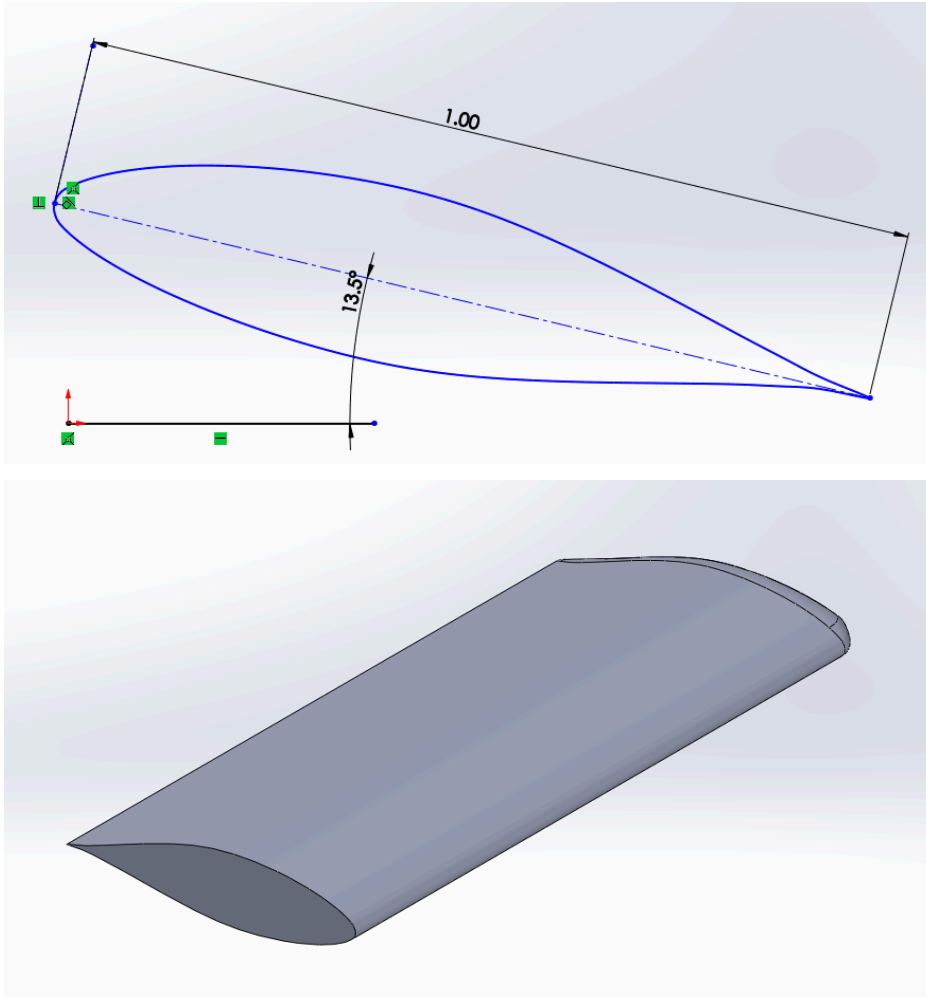


Fig 6.11 - The NACA airfoil sketch with a one-unit length and extruded shape with one rounded edge

#### 6.1.3.2. The Shaft Gearbox

The shaft gearbox for the rotor serves two purposes: It transfers rotational energy to the rotor and changes the gear ratio between the input shaft and the rotor. The epicyclic gearbox commonly used in aerospace engineering gearboxes is due to its compact size and radial symmetry, and its ability to be combined with other epicyclic gearboxes in series. The gearbox for this project will have to be designed to fit the specific characteristics, such as to fit behind the nosecone of a diameter of 2 inches and provide a high drive ratio of around 5:1 while staying relatively short. Limiting parameters for the gearbox will be the maximum outside diameter of

the outer ring and its structure, as well as the required gear ratio of the gearbox system, which depends on the rotor and driver designs. To simplify the design, specific parameters of existing gears will be used, such as a particular diametral pitch for the size of gears and predefined pressure angles for teeth.

The gear ratio should be around one planetary carrier rotation to five sun gear rotations. A planetary spur gear drive ratio of 5:1 means the sun gear must make five revolutions for each revolution of the planetary carrier. For such a scale, the optimal diametral pitch would be at least 24 or more, and the pressure angle would be fixed to 20 degrees. Using equation 1.33, it is possible to find the number of the sun gear. Knowing the required drive ratio is 5:1, we can find out that the number of teeth on the sun gear should be four times smaller than the number of teeth on the outer ring.

$$5 = 1 + \frac{z_R}{z_s} \quad (6.1)$$

$$z_s = \frac{z_R}{4} \quad (6.2)$$

Due to the component's dimension restriction, the choice of database gear designs is limited, and only several configurations of the outer ring fitting in the required dimensions work to maintain both ratio and structure. The number of teeth for the outer ring is chosen to be 56 as it provides large enough gears while allowing the maintenance of the good ratio and diametral pitch of 32 for the chosen radius of gear. It means the sun gear will have only 14 teeth to provide a ratio of 5 to 1. The sun gear with 14 teeth and  $PM = 32$  has a radius to the roots of 0.17925 inches, and the radius of the outer ring to the root is 0.9145 inches. It leaves a diameter of planetary gears from the teeth edge at 0.73525 or slightly less with  $PM = 32$ . As long as it can fit in between and the teeth can reach both the outer ring and sun gear as designed, any number of teeth can be chosen. After several attempts, the planetary gear with 21 teeth was the best fit. The test models manufactured for demonstration showed planetary gears with 21 teeth performing better than planetary gears with 20 and 19 teeth, as they provide a larger interaction area between the gears and rotate smoothly when lubricant is added. The teeth tip radius of the planetary gear is 0.359375 inch, which fits in a 0.73525 diameter, while the root radius of the planetary gear is 0.288625. The one-stage assembly can be seen in Figure 6.12.

The increased ratios even more, additional stages will be added, where the sun gear of the previous stage will be directly connected to the planetary connector of the next stage, providing a ratio of 25:1 with two stages and 125:1 with three stages that can fit in around 1 inch long 2 inches in diameter gearbox system, with some redesign.

After initial tests were done, the first stage with the most torque was reinforced with larger connections and a large connector to the shaft, while the last stage sun gear was reinforced with longer and wider connection to the compressor nosecone.



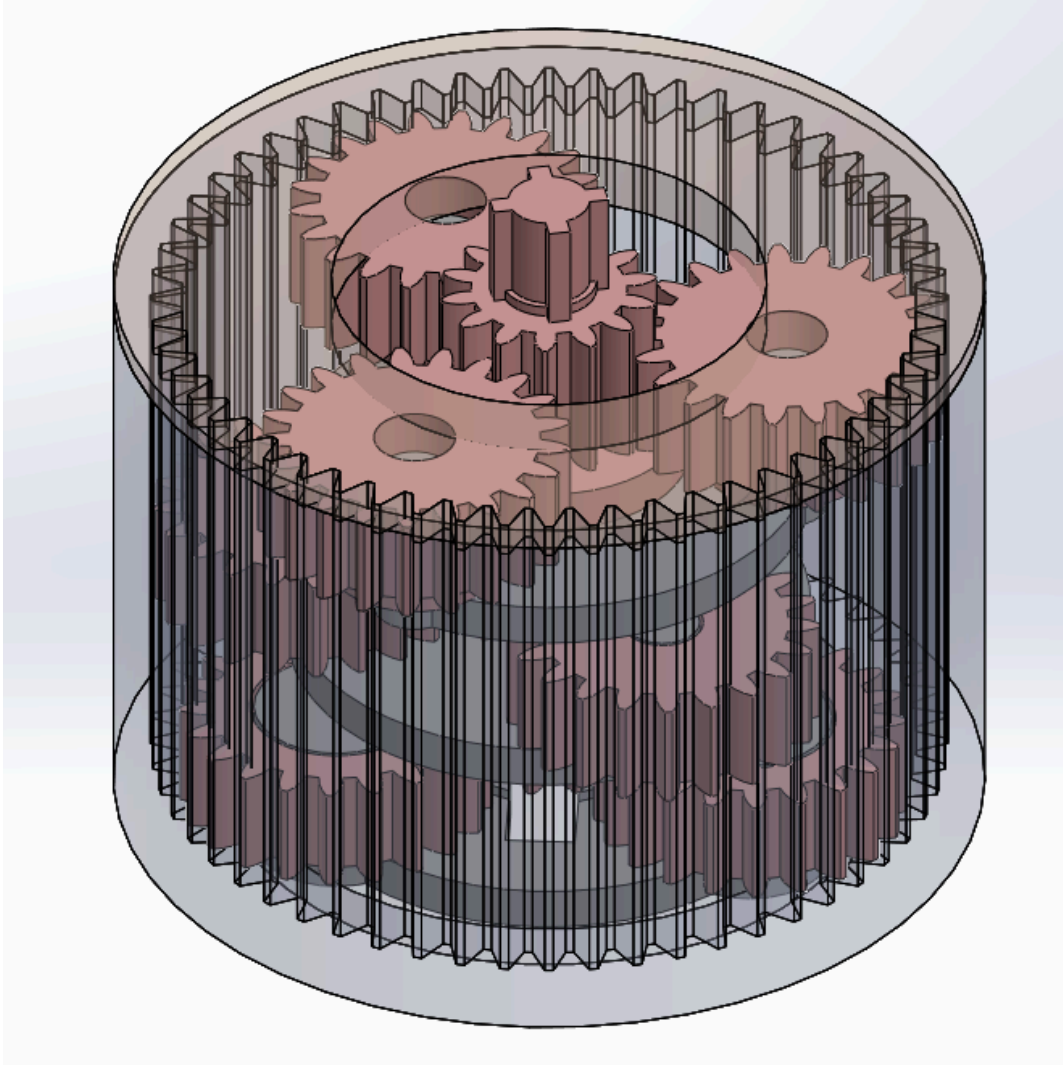


Figure 6.13 - The assembly of three three-stage planetary gearbox after several iterations of physical model testing

#### 6.1.3.3. Compressor Assembly

When manufactured, all previously described parts of the compressor will be assembled together. Methods of connection include epoxy, special imprinted connectors, and natural friction of the parts' surfaces. The figure below shows what the final compressor assembly will look like.

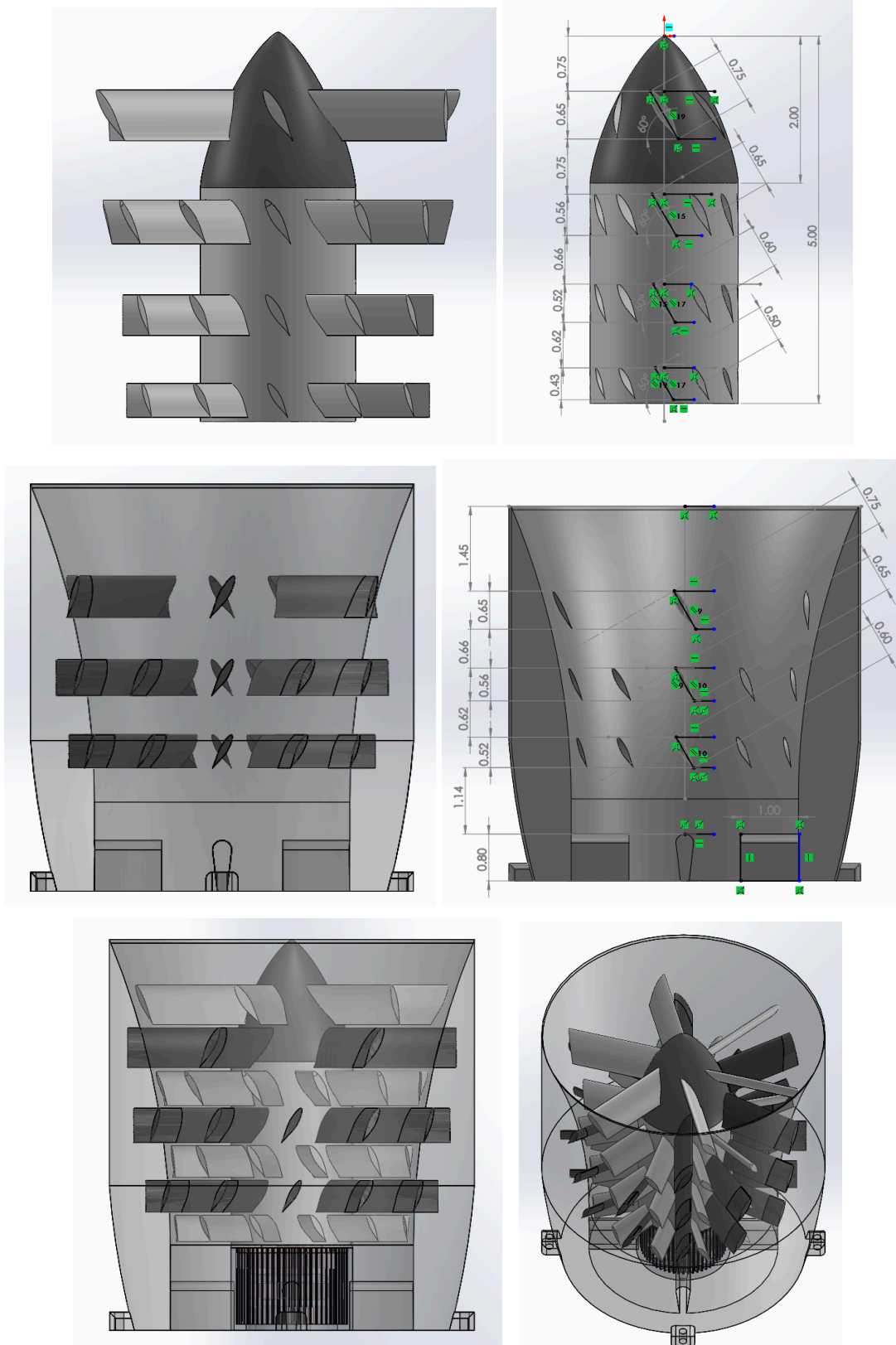


Figure 6.14 - Nosecone subsystem components separately and in assembly

#### 6.1.4. The Torque Source

The compressor requires the torque input to produce a pressure difference in front of the nosecone. There are two prominent ways to produce torque: The electric torque source and the aerodynamic torque source. The electric torque source is a simple electric motor that is capable of providing enough torque to rotate the compressor and additional battery capacity to power the motor. The aerodynamic torque source is a larger propeller from behind the probe that can collect the energy of the flow and convert it to rotation, transferred by the shaft to the smaller compressor propeller in the nosecone. Technically, they are different in the way they obtain energy to move the flow in front; if the electric one is used, the probe will have to carry energy in the form of batteries with it and find space for a powerful motor inside, increasing the weight of the probe. If the aerodynamic torque source is used, it could reduce the weight by removing the need for the rotor and additional batteries, and airbrake partially or entirely, if the stability can be achieved by using just the propeller from behind. However, it adds a problem with the propeller design, bearings, and long shaft.

##### 6.1.4.1. Electronic Torque Source

One of the possible sources of torque can be the electric motor, powerful enough to rotate the compressor. In combination with the epicyclic gearbox, the motor will be able to accelerate the compressor to high velocities, as long as it has power.

The drawbacks of this decision, however, include a lot of additional mass, such as the motor itself, the additional battery capacity, wiring, and structure. The motor needs to be powerful enough to accelerate the compressor to high angular velocities; otherwise, it would be obsolete, which means additional mass. The mass can be reduced if the entire torque source subsystem is designed anew to provide the required torque while minimizing the mass and power consumption. However, it might not be feasible, as it drives development time, manufacturing cost, and complexity higher.

##### 6.1.4.2. Aerodynamic Torque Source

Another source of torque can be a turbine positioned behind the frame, which can be accelerated by the ongoing air that does not get inside the collection unit. The torque created by the turbine needs to be transferred by a shaft to the compressor gearbox. Since the compressor gearbox has a high ratio and requires a lot of torque, the amount of torque can be increased by introducing another epicyclic gearbox between the turbine and shaft with the needed ratio, to keep the compressor operational in a range of conditions. It means that this option will also require additional weight and some complexity. The benefit of using a turbine to generate torque is that it can combine the function of a stabiliser and reduce the required mass from the airbrake,

as described further in this section. The torque source can be more reliable since it is purely mechanical and will be tested directly with the compressor system. Thereby, the aerodynamic torque source option presents itself as more feasible.

Since it was decided to pursue this option, some more development was done on the turbine part. Similarly to compressor blades and stator, the turbine blades has to sustain high force, while being easily manufacturable, and because of this it will utilise the sama NACA 65-221 airfoil. The blade has a relatively large chord of 0.75 inch long, and extends 1.8 inches, with the tip located 3 inches away from the main axis of the probe, with a slightly curved end to fit into a 6-inch diameter restriction. The structure holding the blades is extended to provide an attachment surface for the Penguin R16 2RS C3 bearing, allowing it to rotate freely.

Part of the function of the turbine is to create drag for additional stability, and thereby, the angle of the blades is much higher than it is normally for energy collection in wind turbines. The blades are also pointed 90 degrees from the blades in the nosecone subsystem, due to the usage of the one-stage reductive epicyclic gearbox, where a ring gear of the gearbox is attached to the rotating turbine, while planetary gears are held still by the structure tail.

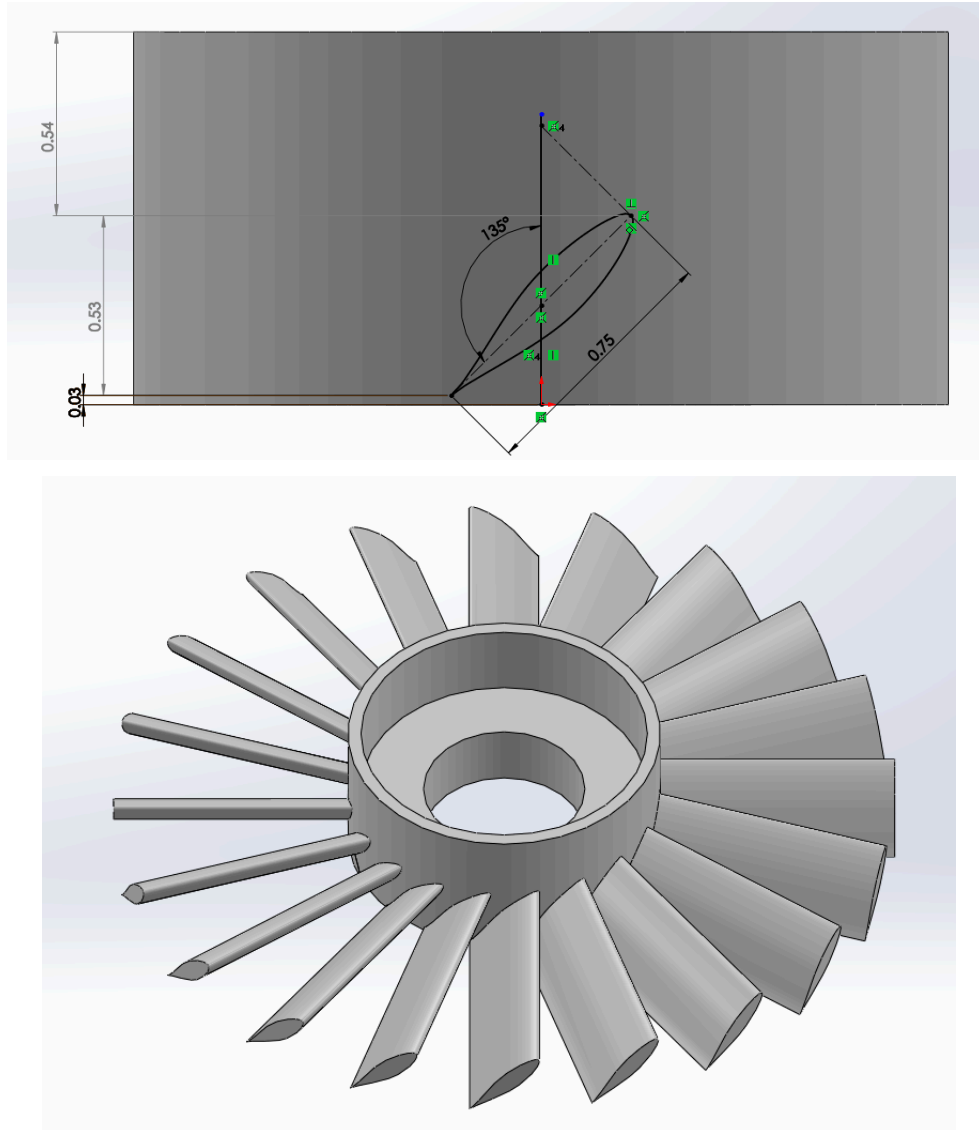


Figure 6.15 - The initial 3D model of the turbine part

### 6.1.5. The Shaft Design

The shaft should be able to transfer rotational energy over the required distance without significant torsional deformation that could damage or destroy the shaft while it is working. It might be used in combination with a torque source and transfer rotation from it directly to the compressor gearbox. There are several ways to design the shaft, such as utilizing several beam section shapes and introducing internal reinforcements. The primary condition for the shape to be good in resisting torsion is a closed cross-section shape; another important consideration is the possible slippage of the shaft when connected to the drive or rotor, and finally, the weight of the shaft should be as small as possible. The best shape for creating a shaft is the solid circular

shape, as it can sustain the highest torsion. Any other shape is generally not used as it will have issues with stress concentration and thereby lower safety margins for the same stress. Another potentially beneficial option is to use the hollow circular weight, as it can reduce the total weight of the component while leaving enough strength to perform its function.

The shaft designed for this probe is 16.7 inches long, including connectors to the gearboxes. It utilises a 0.3 in radius cylindrical shape with a 0.1 radius hole in the middle from the connector to the connector. The connector is done by introducing an extruded feature at each end of the rod. The circular part has a radius of 0.45 inch and is 0.2 inch long, with a 45-degree chamfer going from the central rod to the sides of the connector. It is connected to the epicyclic gearboxes using the three-sided feature with a circular shape in the middle, identical to the cut on the first stage of the epicyclic gearbox. It is designed to provide sufficient leverage to safely transfer torque while resisting possible torsion.

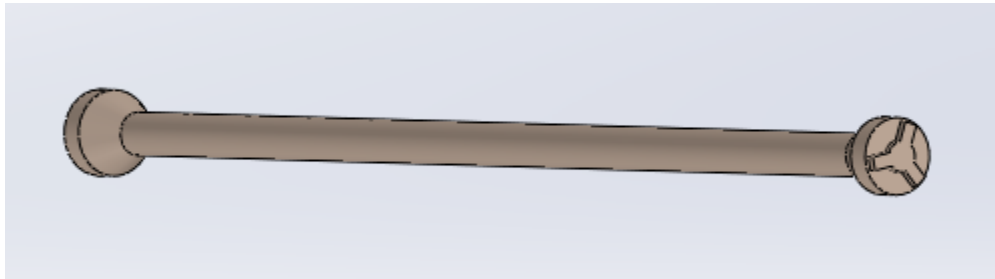


Figure 6.16 - The shaft design with connectors

#### 6.1.6. Stabiliser

For better collection rates, the probe needs to direct itself and remain as vertical as possible with its unusual nosecone shape. From a simplified dynamics perspective, the probe can be viewed as a system of point forces acting along its main axis, extending from nose to tail. The component of forces to the main axis will change the velocity of the probe in the respective direction, while the perpendicular component of those forces will provide both the change to velocity and the angular acceleration around its center of mass.

##### 6.1.6.1. Tail

The tail of the probe primarily serves structural functions and houses the airbrake, parachute capsule, and turbine, along with their respective mechanisms. Inside the tail, there is space for the shaft going from the turbine gearbox to the compressor gearbox.

For stability purposes, the required length of the tail is approximately 12.5 inches, at the end of which the additional structure holding the turbine, air brake, and parachute capsule is located. The tail has a hollow, cylindrical shape with a 1.5-inch inner diameter and 1.7-inch outer diameter, reinforced with two beams going along the surface to add more margin of safety for axial forces. The diameter of the tail is larger than required for the shaft and fits wiring that goes to the parachute capsule. However, the required diameter and thickness of the tail are mostly dictated by the amount of force it has to sustain during the slowdown and recovery.

#### 6.1.6.2. Airbrake

The airbrake is the main stability feature of the stabiliser, as it is supposed to generate the most drag. It had a diameter of 6 inches and was shaped to have the largest allowed area. The shape of the airbrake is conic with a 45-degree angle and a cut tip 2.1 inches away from the base. The surface of the airbrake is covered with holes parallel to the main axis of the probe. The beveled surface of the airbrake and the holes are both features that improve the ability of the probe to direct itself vertically, as they have increased drag when the probe is away from the vertical position, and the lowest drag when it is at the vertical position.

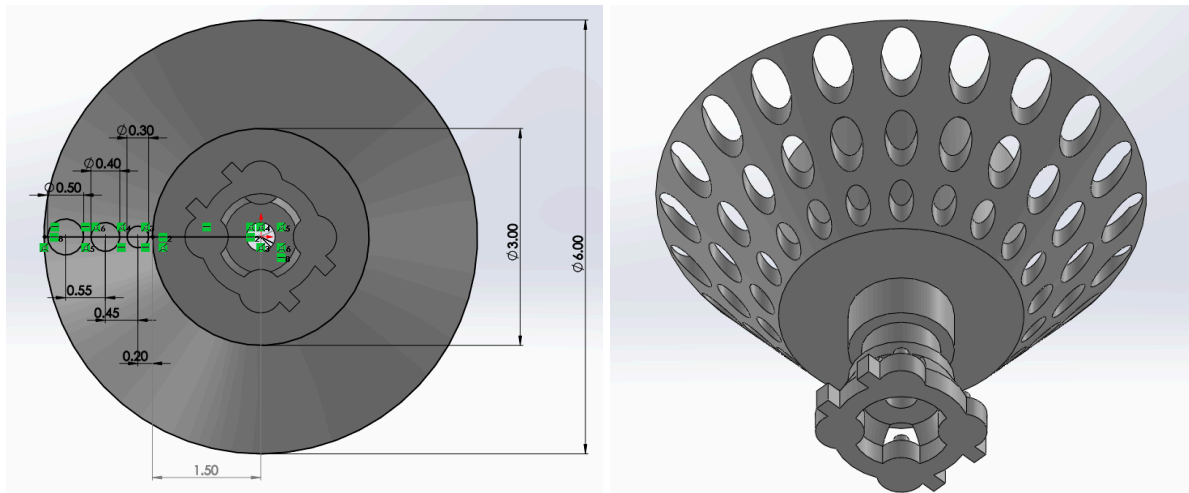


Figure 6.17 - The geometry of the airbrake with attachment to the tail and gearbox

#### 6.1.6.3. Turbine

Another feature of the stabiliser is the turbine. As was described before, it gathers the energy from the flow and transfers it through the shaft to the compressor. The turbine propeller uses the same blade geometry as the compressor, due to the same reasons; however, it is positioned at a higher angle of 45 degrees, because in addition to generating energy it is also

serving as additional stabilising feature, and it supposed to not be lift/drag efficient and should create more of the drag to increase the intake of the compressor by moving probe in more vertical position. The total number of blades is larger than the number of blades per stage at the compressor, to cover more area at each instance, and is equal to 20.

The turbine also utilises the reducing epicyclic gearbox, similar to the one designed for the compressor, to increase torque at its output. The turbine is connected to the outer ring of the epicyclic gearbox, which is attached to the structure connected to the commercially available bearing, to ensure it can experience high axial forces.

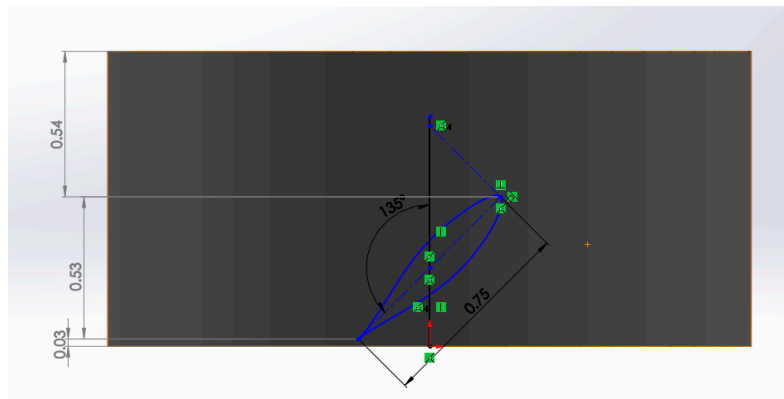


Figure 6.18 - The blade position and sizing on the turbine

#### 6.1.6.4. Parachute capsule

The last component of the stabiliser is the parachute capture, which is a volume large enough to contain a packed 30-inch elliptical parachute, attachments, and deploy charge with wiring. The capsule is covered with a thin plastic cover that is ejected with a parachute when the deployment charge activates, and stays connected to the shock cord.

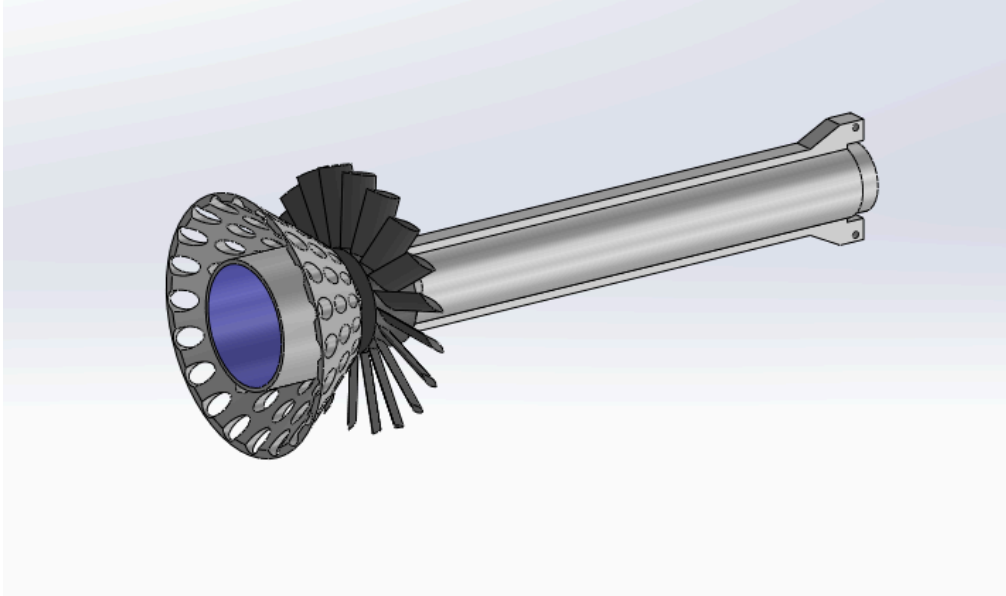


Figure 6.19 - The assembly of the stabiliser

With the absence of the rest of the shaft that enters the probe. The blue region shows where the parachute will be packed before being enclosed with a protective cover.

#### 6.1.7. Sealing Mechanism

The prevention of contamination is one of the requirements for the probe design. The collection unit should be exposed to a minimal amount of terrestrial particles from the assembly in a clear place until it reaches the lab. While the total prevention of the contamination is very hard to achieve, most of it can be prevented if the collector unit stays inside the probe with partial sealing as long as possible, and the time when it is moved to or from the probe is minimal. To allow such prevention, the probe needs an internal sealing mechanism that will be activated after the probe is ejected from the rocket, and before it enters layers of atmosphere containing terrestrial particles.

##### 6.1.7.1. Sealing Principle

The main idea for preventing contamination is to close the entrance into the collector unit with a moving part at a specific time, which will prevent a large amount of air containing terrestrial particles from going through the collection unit. Despite closing the entrance, the back of the collector is still going to be open, so the seal will not be total; however, the amount of air getting into the collector unit from behind is very limited during the descent, and mainly due to the air pressure changes as probe descends, while the flow of the air inside of the collector unit will be negligible when the probe has landed. In addition, all possible contaminants during interaction with silicon-covered plates will not have velocities similar to extraterrestrial particles

during collection, and should stay at the very top of the oil. In contrast, extraterrestrial particles will be mostly covered with it.

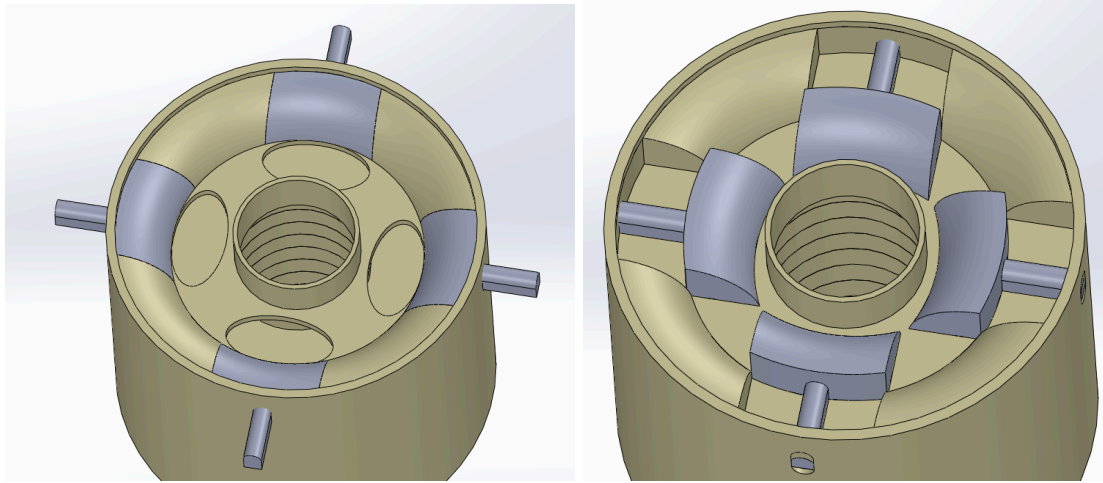


Figure 6.20 - The sealing principle when intake is open on the left, and when intake is closed on the right

#### 6.1.7.2. Sealing Servos

To allow the sealing described above, the part blocking the air passage should be moved by a servo of some kind at a specific time. The command for it can be sent by the computer with interaction with the IMU, which will be able to record the position, and when the setup conditions are met, the command can be sent to the servo. The servo itself should be small enough to fit in the electronics section allowed on the sides of the collection unit. The speed of the opening and closure does not matter as long as it can be completed within 5 to 10 seconds, but the torque of the servo must be sufficient to resist the pressure of the ongoing flow and friction with other parts. It would also be best to use commercially available servos to remove the need to design a new one.

The servo fits the description and requirements of the SG90 Micro Servo Motor, with dimensions of 0.34 x 1.29 x 1.33 in. It also offers the option to remove part of the plastic frame manually. The operating voltage of this servo is from 3 to 6 volts, which is in the range of voltage requirements for most electronics, as described later in the next subsection. It has a stall torque of 1kg/cm and turns with a speed of 600 degrees/s with a total weight of 9 grams, according to the manufacturer's data. Its size and weight mean it is possible to position four of such servos around the circumference of the collection zone to move a part blocking the collection entrance. By using a small system of transmission of torque to linear acceleration, it is also possible to adjust the force on the part and the velocity of the part when moving.

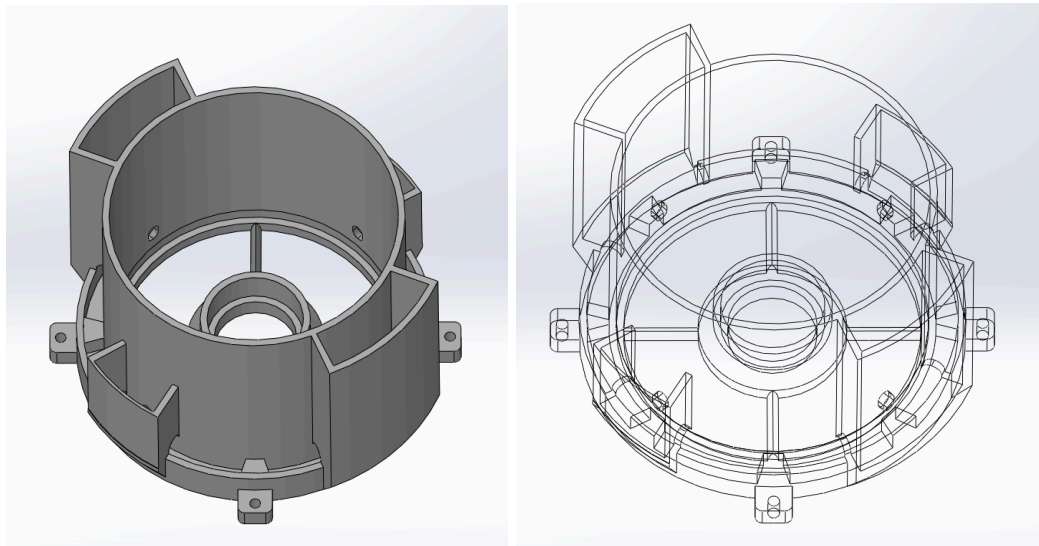


Figure 6.21 - SG90 Micro Servo Motor

#### 6.1.8. Main Body

The collector unit requires a secured space on the probe, which also will provide the required structure to hold the nosecone, compressor, and gearbox, connecting them with the stabiliser through the tail. All the electronic components, power supply, and wiring with easy access to them will also be located in this part in two large and two small sections with enough space to locate servos in designed positions and the rest of the electronics described below. The diameter of the structure will be smaller than the maximum diameter of the nosecone to decrease the possible friction during deployment.

The acceptable design of such a part is shown in Figure 2.22



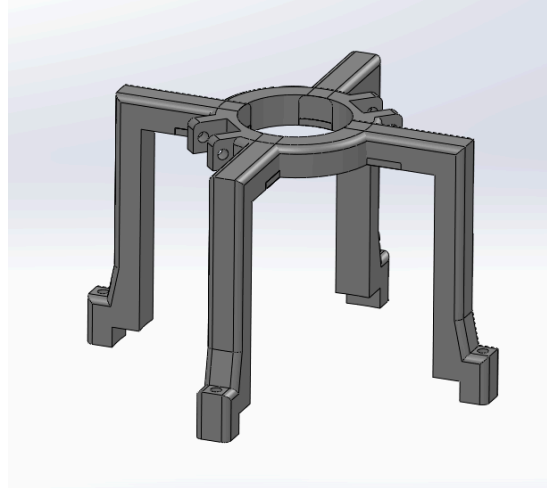


Figure 6.22 - The main body part at the top contains electronics and the collector unit, and the tail connector secures the collector unit and the stabiliser

## 6.1.9. Electronics

### 6.1.9.1. Control Computer

The control computer is mainly required to control the servos when proper conditions are met. The signal about such conditions will be inserted into the program, calculating the approximate vertical position of the probe relative to the Earth, depending on the initial launch prediction and internal calculations from the Internal Measurement Unit connected to the computer. While the position is calculated in that way, and thereby the moment when the servos open and close the air intake into the collector unit is not going to happen exactly at apogee or at 60000 feet, it gives enough accuracy to for computer to do so with acceptable error, taking into the account the fact that most of them contamination will occur if the intake is left open at lower atmosphere and close to the ground.

The computer of choice for such a function is Arduino Nano 33 BLE, depicted in Figure 6.23, due to its compact size, strict dimension requirements, cost-effectiveness, relative reliability, and ease of use and testing. In addition to its other qualities, it has a built-in 9-axial Internal Measurement Unit, which, in addition to the lateral and angular acceleration, is able to measure the Earth's magnetic field, to better estimate the altitude of the probe. The dimensions of the computer are 44.5 x 17.6 x 4.1 mm.



Figure 6.23 - Arduino Nano BLE 33

#### 6.1.9.2. Recording Device

The recording device is required to store and analyze data such as position, velocity, acceleration, temperature, and pressure from sensors inside the Controller Computer and external sensors, if they are used. The computer itself is not able to store this data for a long time, and everything is erased after the power turns off or overwritten if records are being recorded for a long period. The challenge here is that Arduino Nano BLE does not have any ports other than the Micro USB B and its pins. In addition to physical ports, it has Bluetooth capabilities. Any device used for recording will have to utilise one of the available ways.

One of the reliable ways for recording data for the long term, known to the Arduino users community, is by utilizing the external chip SparkFun OpenLog with a MicroSD socket, and is itself not much larger than the MicroSD used in it. The approximate size of the spark fun is 17 by 11 by 5 mm.

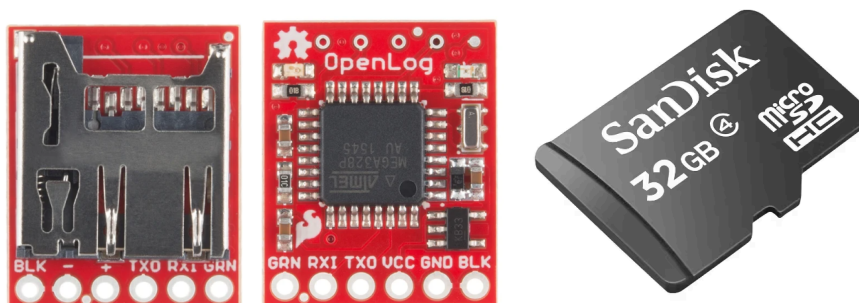


Figure 6.24 - SparkFun OpenLog and MicroSD

#### 6.1.9.3. GPS

The GPS system of the probe will be responsible for tracking its location before, during, and after flight. The GPS corresponding to the requirements of size, transmission distance, and

accessibility is Featherweight GPS. It represents the compact chip module with a short monopole antenna attachment, which can be used directly with an antenna or to send the signal through the cable to the antenna located elsewhere. The featherweight is capable of tracking the location of the GPS transmitter at altitudes up to 80 km. The receiver uses Bluetooth to connect with a user device, where it delivers all the data about the position of the transmitter.



Figure 6.25 - Featherweight GPS transmitter and receiver

#### 6.1.9.4. Power Source

All electronic components described above will require power to function. The voltage and current requirement are somewhat different for most of them, however the task is simplified since the Arduino Nano BLE has ability to power wired to it components to the required level, using its power source, and since all components but gps are going to be attached to it, so only Arduino is required to have it power requirements met by the power source used for it.

The GPS will require a separate power source due to its specific power requirements and concerns of reliability of gps system. Tracker can run 16 hours on a small, 400 mAh single LiPo cell sold with it, or can use larger capacities if needed to extend it to a day or more, which gives plenty of time to locate and find the probe, in case it is not possible to do quickly.

#### 6.1.9.5. Wiring

Most of the electronic components on the probe will require custom wiring between them. It is relatively easy to connect them; however, since the components need to be accessible,

it requires more work than usual to make sure the electronics can be removed and put back, without any additional need to connect separate wires. This can be accomplished by utilising wiring connectors and a modular structure of the frame containing electronics, where a module containing all electronics in one part of the probe can be removed entirely without disturbing the wiring. This feature will be needed to quickly test electronics during pre-flight preparations, replace or recharge the main power source and the GPS power source, and decrease the chance of disrupting the wiring.

The 22-gauge wires (0.05 in diameter) and Morex connectors were chosen to fulfill wiring requirements. The 22-gauge wires are small and can easily fit in between structures, even if connected together in wire bundles, while having a power rating several times higher than expected. Morex connectors are small, sturdy, and reliable, and can support many pins in one connector, which makes them good for connecting many wires between modules. They are widely used in different vehicles due to their good reliability when exposed to various forces.

#### 6.1.9.6. Electronics Covers

To protect electronics from undesirable aerodynamic forces, large and small electronics sections with wiring tunnels in main body will be enclosed with removable plastic covers secured by the tail connector or small screws through the plastic walls. The GPS antenna will have an opening in the cover to stay outside the body as much as possible, while everything else will be protected until opened on the ground.

## **7. Final EPC System Design**

### **7.1. EPC System Design Description**

The final system design, when all parts are designed, looks as depicted in Figure 7.1. The length of the probe from the nose to the aft is 26.65 in, with a diameter of 6 in. After minor changes, all the parts were successfully integrated into the respective components and subsystems in CAD, proving correct sizing and readiness for manufacturing.

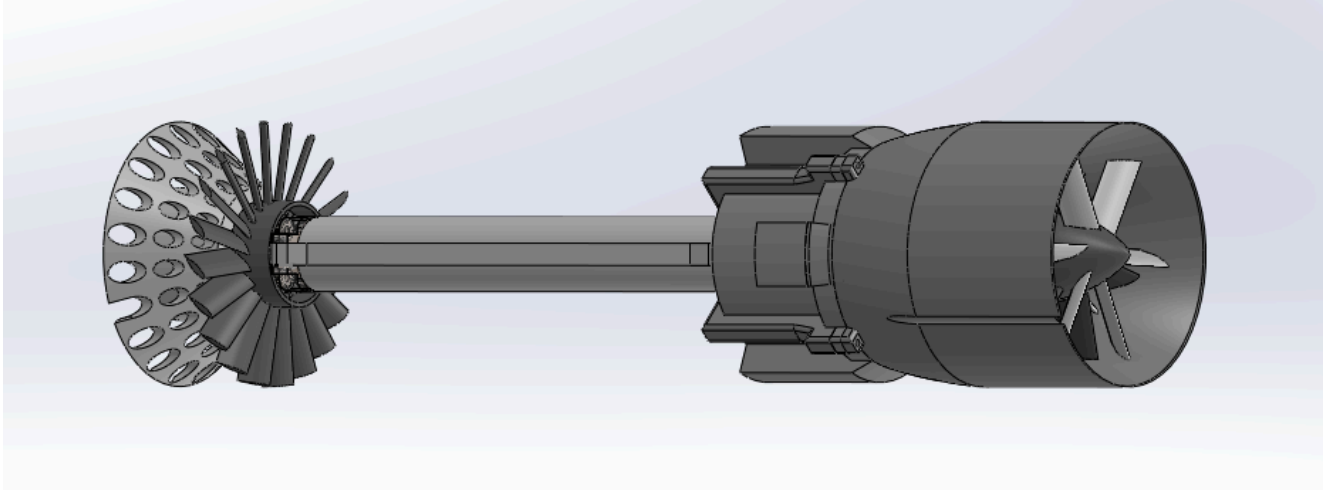


Figure 7.1 - The external geometry of the assembled EPC probe system

The probe can be divided into three subsystems by their location and functionality. In Figure 7.2, the location of the probe components can be seen. The first one is the nosecone in front with the structure in gray, the compressor nosecone and rotor blades in lighter gray, and the stator blades in black. Right behind the compressor, the gearbox is located, shown in red, with all three stages and connection to the compressor and shaft in orange. The second subsystem is the body frame, where the electronics are located in a safe space on the outer side of the frame, and the collection unit in yellow is located inside it. It provides protection for electronics and the collection unit, and transfers forces from the nosecone to the stabiliser at the back. The third subsystem is a stabiliser which consists of the structure in gray, the shaft in orange, a turbine in black, and the parachute capsule in blue.

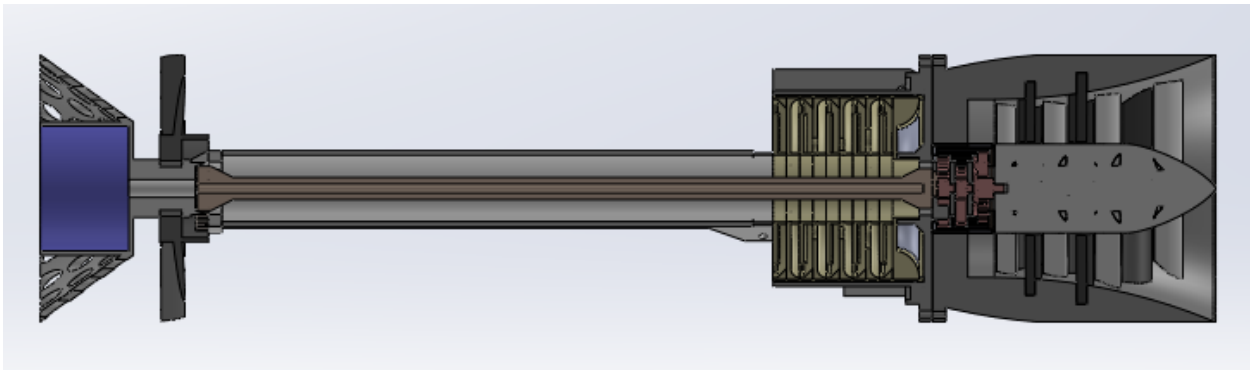


Figure 7.2 - Section view of the assembled EPC probe system

## 7.2. EPC System Operation Concept

The probe operates according to the following concept: The probe is launched on an amateur rocket to an altitude of over 40 kilometers. Near the apogee, the probe is released from the second stage of the rocket by sliding on the shock cord. As it leaves the rocket, the stabiliser

positions the probe mostly vertically within 10 seconds, as the probe accelerates, while the computer starts the servos to open the collection. The air with particles gets inside the compressor, which increases density and pressure to allow a higher flow rate and pressure difference inside the collector unit. Compressed air gets accelerated as it enters the first stage of the collector unit, where it has to deflect 90 degrees, collecting some of the particles on the silicon oil-covered collection plate. It repeats at every stage, as each next stage has less and less area, keeping the flow accelerating. After the fifth collector plate, the air filtered of particles leaves the lower pressure zone behind the probe's body frame. At the same time, the air that is not getting collected goes along the surface of the main frame and stabiliser before it reaches the turbine. The airflow pushes the turbine, slowing the probe down and providing rotational energy to the shaft, which transfers it into the gearbox and compressor. Right behind the turbine, there is a beveled airbrake that adds additional drag so the probe can remain in a vertical position.

As the probe flight, the electronics inside the body frame record its dynamic pressure and temperature. When pressure increases to the pressure normal for an altitude of 60-65 kilometers above sea level, or the IMU records that the probe should be around that altitude, the computer sends a signal to the servos to close the collection and protect the collection plates from terrestrial dust. Meanwhile, the GPS records and transmits the probe location to the team on the ground, which can start leaving for the recovery operation. As the probe approaches the surface, the electronics detect the required altitude or pressure to release the parachute at around a kilometer above the ground. It slows down the descent to safe velocities and allows the recovery team to track the probe more easily until it lands. When the probe is found and delivered back, it can be opened in clean conditions, and the collector unit and batteries can be replaced to allow another launch if needed.

## **8. Manufacturing and Assembly**

As the system design is complete, the next step of the project is to manufacture the prototype of the EPC probe that is suitable for future tests and further improvements of the design. The manufacturing process will consist mostly of 3D printing in addition to obtaining commercial off-the-shelf components. The assembly of the components will show if the designs of separate components connect easily and reliably with each other, and if certain functional components are able to fulfil their design requirements, such as the gearbox, compressor, and turbine design.

### **8.1. Parts Manufacturing**

Parts of the system design have various requirements for their roughness, which, in 3D printing, will heavily depend on the layer height of the print part. For some designed

components, the preferred layer height should be as small as possible, with the best result being 0.05 mm in height or lower. Such parts are the collector unit, rotor, and stator blades. Some after-print refining methods could help reduce the roughness of the part by using a larger layer height, in return for printing speed if needed. However, it adds a lot of manual work and might not be preferable if enough manufacturing time is available. Other parts that are not affected by the roughness of the surface can use a layer height of 0.2 mm and larger if needed, keeping in mind that the thinner layers usually result in higher shear force resistance. Another adjustable parameter for parts would be the infill, which allows for reducing the total weight of the part by reducing the material used for internal layers. The borders of any model usually have at least three layers, which provide sufficient strength for the model if no forces are applied. The reduction of weight is not directly proportional to the reduction of strength; there are certain infill options that result in optimal strength while significantly reducing the material used, thereby reducing the time and cost of manufacturing.

The total number of parts needed to be manufactured for assembly of the EPC probe prototype is 140, with two-thirds of the separate parts being the blades. Those parts can be separated into categories by the components and subsystems into which they are assembled. Those categories can be manufactured, assembled, and tested separately, one after another in any order, if needed, to streamline the building and testing process. The parts and their main parameters, such as count, size, weight, and infill, are described below to allow for better estimation of material usage and 3D printer requirements for each of them, or whether it is possible to group certain parts into one print. Due to the highest expected forces having a collinear direction with the direction of the probe's main axis, the infill is chosen to reinforce parts the most in this direction. Therefore, the general infill pattern used in parts is the grid pattern; however, with 100% infill, the rectilinear pattern is used to make it more optimised. Some manufacturing decisions for the first prototype are also described below.

Images of all parts manufactured for the prototype model of the EPC probe can be found in Appendix B.

#### 8.1.1. Nosecone Parts

The nosecone is the single largest part of the entire probe assembly. The nosecone component includes an entire nosecone part and 30 stator blades to be inserted into it. Blades, when inserted, are very hard to remove and are prone to breaking into two pieces at a section coplanar to the internal surface of the nosecone if too much force is applied. Due to its long manufacturing time and risk of breaking the blade during assembly and testing, the prototype nosecone was divided into four parts that assemble into one equal to the nosecone part. The negative side of such a split is that it means more flat printing surfaces and parts of the ceiling, unnecessarily increasing the weight of the actual part.

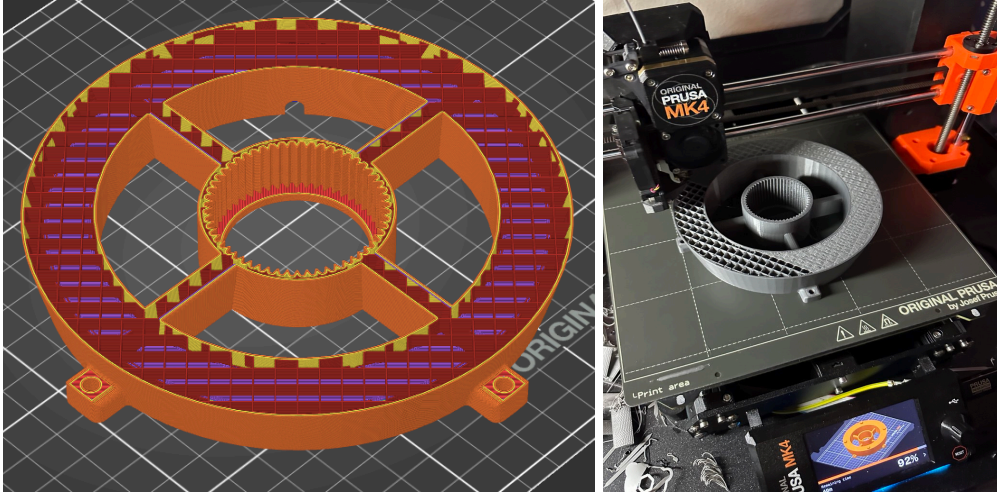


Figure 8.1 - Example of part slicing and 3D printing on Nosecone Part 1

Thereby, there are two options of assembly, one that involves prototype nosecone subparts and the other that does not. All parts, their sizes, weights, and infill settings are described in Table 8.1 below. The layer thickness used for nosecone parts is 0.2 mm, and for stator blades is 0.1 mm.

Table 8.1 - Nosecone component parts dimensions and parameters

Name	Count	Size (in)	Mass (g)	Infill (%)
Nosecone	1	6 x 6 x 6.25	426.46	20
Nosecone Subpart 1	1	6 x 6 x 1.65	115.71	15
Stator Blade (C = 0.60 in)	12	0.126 x 0.6 x 1.35	1.31	100
Nosecone Subpart 2	1	6 x 6 x 1.65	111.65	15
Stator Blade (C = 0.65 in)	12	0.137 x 0.65 x 1.55	1.76	100
Nosecone Subpart 3	1	6 x 6 x 1.25	95.14	20
Stator Blade (C = 0.75 in)	6	0.158 x 0.75 x 1.75	2.55	100
Nosecone Subpart 4	1	6 x 6 x 2.6	163.96	25

### 8.1.2. Compressor Parts

Similarly to the stator nosecone component, the compressor Von Karman nosecone includes a single nosecone and 44 rotor blades attached to it. Due to the risk of blades breaking during assembly and tests, and long manufacturing time, a prototype version comprised of 4 subparts was also made, allowing faster replacement in case of problems. The prototype compressor Von Karman nosecone part has a larger total weight, which might be slightly stronger due to the increased structure of the printing surface and the top surface of each subpart required for printing.

The blades use 100% infill to reinforce the structure, which still results in a relatively small mass of each blade.

Table 8.2 - Compressor component parts dimensions and parameters

Name	Count	Size (in)	Mass (g)	Infill (%)
Von Karman NC	1	2 x 2 x 5	137.89	50
Von Karman NC Part 1	1	2 x 2 x 1.25	36.91	50
Rotor Blade (C = 0.5 in)	14	0.105 x 0.5 x 1.45	0.98	100
Von Karman NC Part 2	1	2 x 2 x 1.25	36.54	50
Rotor Blade (C = 0.6 in)	12	0.126 x 0.6 x 1.5	1.45	100
Von Karman NC Part 3	1	2 x 2 x 1.25	36.35	50
Rotor Blade (C = 0.65 in)	12	0.137 x 0.65 x 1.75	1.92	100
Von Karman NC Part 4	1	2 x 2 x 2	35.65	50
Rotor Blade (C = 0.75 in)	6	0.158 x 0.75 x 2.2	3.16	100

### 8.1.3. Gearbox Parts

The ring gear of the gearbox is united with the stator nosecone and is printed separately. The rest of the gearbox need to be printed using unique parts for each stage of the gearbox. The design of the gears for each stage has to differ due to ratios of torque, RPMs, and need to hold compressor attached to the surface. All parts were manufactured, assembled and tested using separate ring gear of required size, to find possible problems and develop iterations as was described in the chapter 6.

The first stage of the gearbox has the highest torque and thereby requires attachments to gears that can experience higher forces. The middle stage simply transfers decreased torque and higher rpm to the next stage. The last stage has special geometry that does not let the sun gear attached to the compressor move axially when the gearbox is assembled and closed by the ring gear cover. Despite some design differences, all gears remain in the same ratios for each stage when assembled.

Table 8.3 - Gearbox component parts dimensions and parameters

Name	Count	Size (in)	Mass (g)	Infill (%)
Ring Gear Cover	1	2 x 2 x 0.1	4.06	100
Planetary Gear First Stage	3	0.716 x 0.716 x 0.25	1.03	100
Planetary Gear Middle Stage	3	0.716 x 0.716 x 0.25	1.51	100
Planetary Gear Last Stage	3	0.716 x 0.716 x 0.35	1.69	100
Planetary Gear Connector First Stage	1	1.32 x 1.32 x 0.375	4.05	100
Planetary Gear Connector	2	1.22 x 1.22 x 0.375	2.70	100
Sun Gear	2	0.498 x 0.498 x 0.375	0.83	100
Sun Gear Last Stage	1	0.65 x 0.65 x 0.7	1.8	100

#### 8.1.4. Body Frame Parts

The main body simply serves as a cover for electronics, wiring, and the collector unit, allowing easy access. Custom lids for electronics and wiring might be required in case some parts (such as antennas) exceed the designed protected space.

The tail connector is a part that transfers forces between the rest of the parts and components and securely connects the tail to the main body and nosecone. Both parts require support settings to be chosen to avoid possible manufacturing issues.

Table 8.4 - Body Frame component parts dimensions and parameters

Name	Count	Size (in)	Mass (g)	Infill (%)
Main Body	1	5.97 x 5.97 x 3.6	161.40	15
Tail Connector	1	5.97 x 5.97 x 3.75	76.23	50

#### 8.1.5. Collector Unit Parts

The collector unit component is assembled from stages of various opening areas with a collector plate behind them. As additional parts, there is an outer shell to allow easier usage of the collector unit before and after it is used to collect particles, and sealer parts that move through the designed openings in other parts to block the airflow.

Since the parts are not expected to experience significant forces, their infill settings are low, while the rest of the structure is automatically in place when manufactured using a 3D printing method. The number of bottom and top solid layers should be set at 5 and 4, respectively.

Table 8.5 - Collector Unit component parts dimensions and parameters

Name	Count	Size (in)	Mass (g)	Infill (%)
Collector Plate First Stage	1	4.1 x 4.1 x 0.3	21.36	15
Collector Plate	4	4.1 x 4.1 x 0.3	21.35	15
First Stage	1	4.1 x 4.1 x 0.6	29.43	15
Second Stage	1	4.1 x 4.1 x 0.3	19.93	15
Third Stage	1	4.1 x 4.1 x 0.3	20.64	15
Fourth Stage	1	4.1 x 4.1 x 0.3	21.56	15

Fifth Stage	1	4.1 x 4.1 x 0.3	21.42	15
Outer Shell	1	4.2 x 4.2 x 3.4	44.06	15
Sealer	4	1.2 x 1.44 x 0.5	3.38	25

#### 8.1.6. Stabilizer Parts

The last parts to manufacture are the stabilizer parts, which include the tail structure, the connector parts to the turbine, the shaft, and the turbine parts. Due to the size limitations of most 3D printers, there is an option to manufacture the tail and shaft parts using two subpart prints instead of one part print with minimal weight increase.

The turbine's gearbox requires only planetary gears to be manufactured separately, since the rest of the parts are intended to have geometry to fit in it and work without any other additions.

Table 8.6 - Stabilizer component parts dimensions and parameters

Name	Count	Size (in)	Mass (g)	Infill (%)
Tail	1	1.7 x 2.42 x 14.2	125.54	25
Tail Part 1	1	1.7 x 2.42 x 7.25	62.91	25
Tail Part 2	1	1.7 x 2.42 x 6.95	62.68	25
Shaft	1	1 x 1 x 16.70	47.57	50
Shaft Part 1	1	1 x 1 x 8.57	24.83	50
Shaft Part 2	1	0.9 x 0.9 x 8.13	22.80	50
Planetary Gear	3	0.716 x 0.716 x 0.25	1.51	100
Turbine Rotor	1	2.4 x 2.4 x 1.1	27.10	50
Turbine Blades	20	0.158 x 0.75 x 2.1	3.15	100
Airbrake	1	6 x 6 x 2.1	101.65	50
Airbrake Connector 1	1	2.35 x 2.35 x 1.1	26.98	100
Airbrake Connector 2	1	1.34 x 1.34 x 1.9	27.78	100
Airbrake Connector 3	1	0.9 x 0.9 x 0.3	1.66	50

## 8.2. Component Assembly

When all the parts of a specific component are manufactured, assembly can begin. In the following subsections, the assembly process for each element is described as being further integrated into subsystems or directly into the system.

### 8.2.1. Nosecone Assembly

Assembly for the nosecone requires a small hammer with a soft head. Depending on whether the prototype or the actual part is manufactured, the nosecone might need assembly of its subparts. The assembly of the nosecone part is done by inserting each subpart of the nosecone into predesigned connection points of the next part in numerical order according to their names. When it is done, the parts will be held together by friction, and it will be hard to disconnect them. If the prototype nosecone is not intended to be tested anymore, some plastic glue should be added between its supports by slightly opening them with a thin object and pressing when the glue has been added.

After the nosecone part is ready, insert the blades into their respective openings with the flat surface facing the opening. It is enough to insert them by hand, before pushing them further with slight hammering in a vertical motion with respect to the blade's longest axis. The smaller blades are inserted closer to the bottom of the nosecone, and the larger ones closer to the circular tip. When assembled, the nosecone should look similar to Figure 8.2, with the only difference being that stator blades have not been added at that stage for simplicity of demonstration during showcases.



Figure 8.2 - The nosecone component assembly without stators

### 8.2.2. Compressor Assembly

The compressor assembly is very similar to the nosecone, where the Von Carman compressor nosecone might require assembly of its subparts before blades can be inserted into the openings. The compressor subparts will also require some glue to be injected between them when testing is over to reinforce the component.

The blades should be inserted into the holes by hand, after which they are slightly hammered into the opening using the soft hammer. It is recommended to start with the smaller blades closer to the Von Carman compressor base, before moving to larger ones closer to the tip, as shown in Figure 8.3.

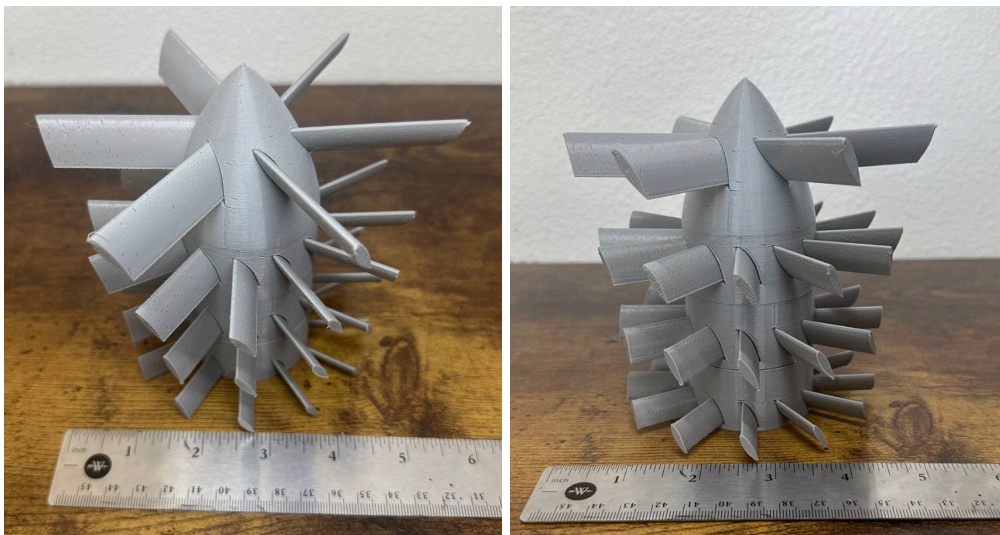


Figure 8.3 - The compressor component assembly with rotor blades

### 8.2.3. Gearbox Assembly

It is recommended to use the long and thin pair of pliers to assemble the gearbox. The assembly will also require a simple liquid lubricant to make the gears rotate more smoothly and reduce friction.

Assembly starts with the first stage planetary gears, the first stage planetary connector, and the stator nosecone. The first planetary gears should be inserted with radial symmetry into the ring gear implanted into the nosecone. The first stage planetary connector needs to be inserted inside the planetary gears before adding the sun gear. The sun gear should fit between them. If it doesn't happen, some planetary gears should be moved one or two teeth at the tangent point with the ring gear. The easiest way to see is to move planetary gears while holding the planetary gear with one side tangential to the sun gear and looking at the entire assembly from above, when it is standing on a flat surface, to see if the planetary gear can be inserted into the

planetary connector. As the first stage is done, the planetary connector of the middle stage should be inserted onto the sun gear of the first stage. Planetary gears can now be inserted into the planetary connector with their openings before adding the sun gear. The planetary connector of the last stage should be inserted onto the sun gear of the middle stage. The two last-stage planetary gears should be put on the planetary connector with the circular extrusion facing the connector. The final stage sun gear must be inserted into its position between the two present planetary gears with circular extrusion facing the same direction, before the third planetary gear can be added to fix the sun gear in place. Some lubricant should be added at this stage, on the side of the ring gear and between the planetary and sun gears. The ring gear cover should be inserted on top at this point to ensure the gears in the gearbox stay fixed.

As gearbox is assembled, it will be helpful to rotate it from one of the sides to spread the lubricant and check for any obstructions possible after manufacturing. If gearbox works as intended, and requires no more opening, the ring gear cover can be glued using plastic glue from its outer side.

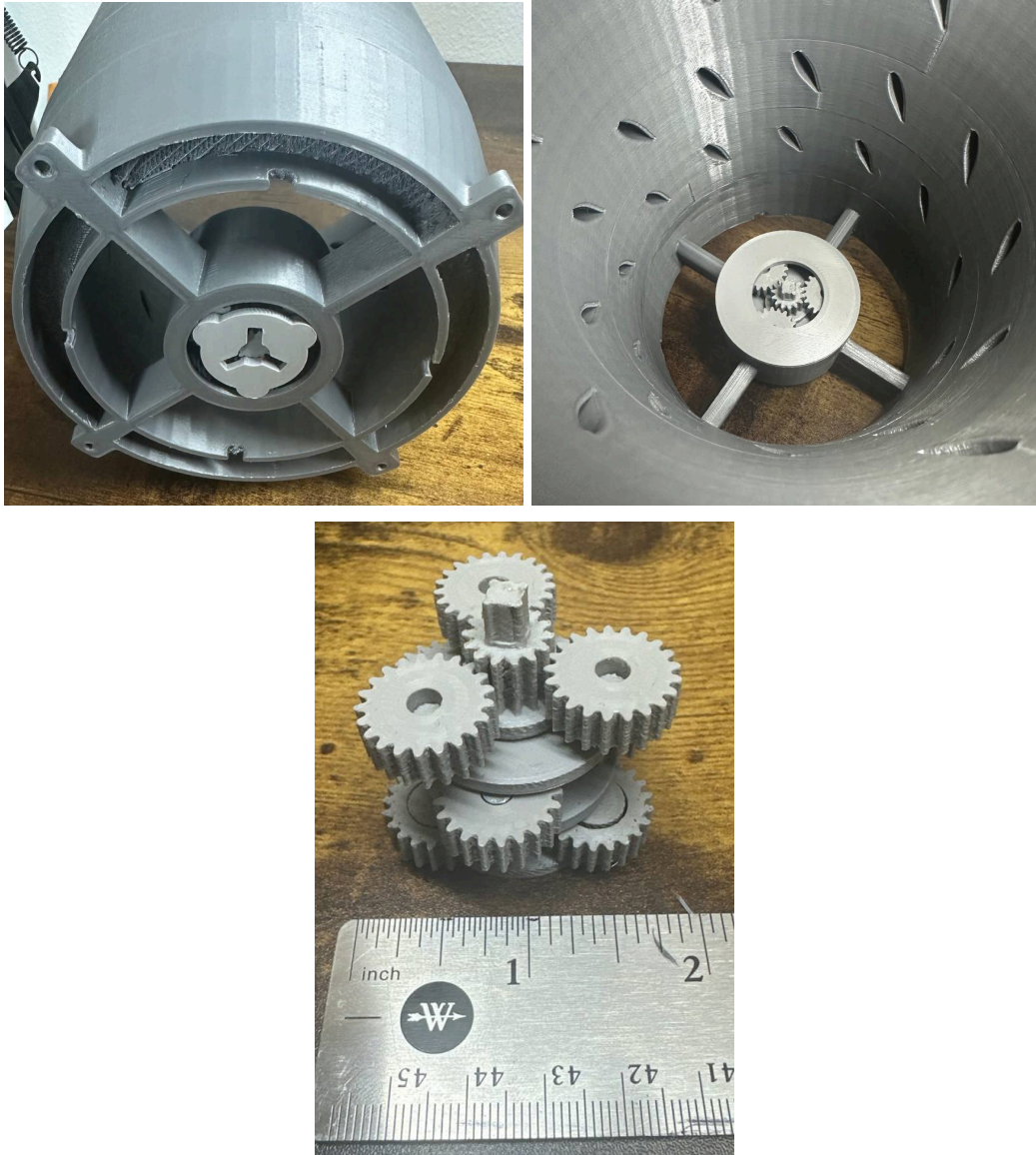


Figure 8.4 - The gearbox inside the nosecone from the top and the bottom view, and the gearbox outside of the ring gear

#### 8.2.4. Collector Unit Assembly

Collector unit components need to be assembled starting from the outer shell and the first stage. The first stage has an opening that should align with the opening on the outer shell. The curved surfaces of the first stage should face the side of the outer shell with the circular extrusion. The first stage collector should be inserted right after, with the plate collection surface facing the first stage, with the opening. All the rest of the stages and collector plates need to be

inserted one by one in a similar manner without respect to their rotation, with each stage followed by a collection plate. The final assembly will look as shown in Figure 8.5.



Figure 8.5 - The assembly of the collector unit

#### 8.2.5. Main Body Assembly

Electronics should be inserted into their places in the main body and wired through the wiring channels. It is best if the electronics are inserted into the base that fits the shape of the allowed space to make it even more accessible and ensure it can sustain expected forces. When ready, it can be covered with custom-made lids and secured with small screws. The lids for the wiring channels do not need screws as they will be fixed by the tail connector in further assembly.

#### 8.2.6. Tail and Shaft Assembly

If the tail was manufactured in two pieces instead of one, it needs to be connected using plastic glue. Prior to the connection, flat surfaces on side beams facing up and toward the center need to be slightly sanded on both parts. When connecting the parts, the side beams and the circular shape of the tail structure should align perfectly before gluing them together. The shaft should be assembled similarly, without any difference in its rotation.



Figure 8.6 - The tail structure assembly

### 8.2.7. Airbrake Assembly

Airbrake consists of several smaller parts to make it possible to insert the bearing of the turbine into it. Those parts can move vertically only in a direction opposite to the direction of the expected drag force. The airbrake and airbrake connector 2 need to be glued together with the smaller side of the connector facing down with respect to the probe assembly on Figure 7.2. The COTS bearing can be inserted into the airbrake connector in 2 parts.



Figure 8.7 - The airbrake assembly

### 8.2.8. Turbine Assembly

Similar to the nosecone and compressor components assembly, each turbine blades need to be inserted by hand into the opening, after which carefully hammered into palace. The turbine now can be put on the COTS bearing and locked on it.



Figure 8.8 - The turbine assembly

## 8.3. Subsystem Assembly

Similarly to component assembly, the subsystem assembly can start when all needed parts and components are ready. It will result in the assembly of three separate subsystems that can be quickly integrated with each other.

### 8.3.1. Nosecone Subsystem Assembly

For the assembly of the nosecone subsystem, the compressor needs to be inserted into the sun gear on the gearbox, which is located inside the nosecone. It might require some rotation to let the blades of the rotor go through the blades of the stator. Each stage between stators has slightly more space than required for the biggest blade that can reach there, and with careful movements, it should get through until it reaches the bottom, where the compressor nosecone can be inserted. If the part was tested before and it is the final assembly, it is recommended to use plastic glue on the connection between the final stage sun gear in the gearbox and the compressor nosecone. The final assembly of the nosecone subsystem is depicted in Figure 8.9 below.

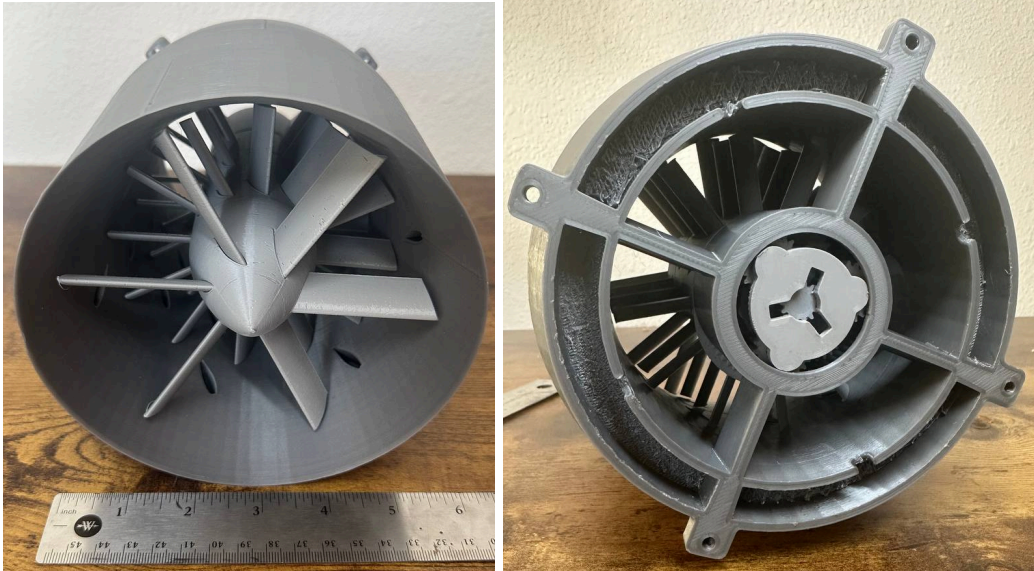


Figure 8.9 - The nosecone subsystem assembly

### 8.3.2. Body Frame Assembly

To assemble the body frame subsystem, the collector unit should be inserted into the main body with the opening on the outer shell of the collector unit aligning with the opening on the inner side of the main body. The lids on the wiring channels should be placed at this moment. The tail connector should be inserted onto the main body, with its structure aligning with the connection points on the main body. The connection points on the tail connector should be positioned next to the large electronics spaces on the side of the main body. The body frame assembly will look as shown in Figure 8.10.

After it is aligned, it takes 4 M4 bolts, at least 3.5 cm long, and M4 nuts to connect the tail connector with main body. The bolts should be inserted from the side of the tail connector, and screwed until the tip of the bolt reaches the other side of connection opening on the main frame, to be screwed further later on during system assembly.

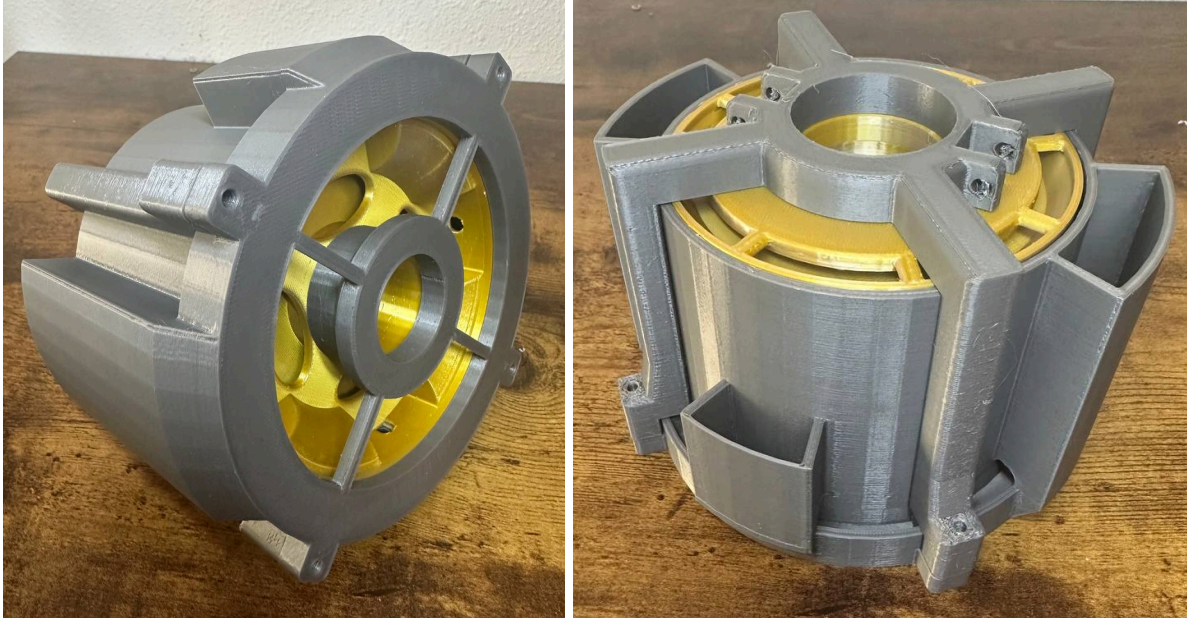


Figure 8.10 - The body frame subsystem assembly

### 8.3.3. Stabilizer Assembly

Assembly starts with the shaft being put inside the tail, with its side leaving the tail structure from the top to a distance of a few inches away from the edge. Insert the Airbrake connector 3 inside the connector 1 without fixing it. The airbrake connector 1 can be inserted into the tail, and planetary gears can be placed on. When the shaft is pulled down from the other side, it will lock on the gears and will be ready to be connected to the gearbox from the other side. The connection between the tail and the airbrake connector 1 will require 2 M4 bolts with a length of 2 cm.

The turbine components need to be placed on connector 2, locking with the bearing, after which the airbrake with the turbine and connectors can be connected with the rest of the tail. The connector part 3 inside part 1 should lock with part 2, but will need some plastic glue for higher reliability. The tail assembly is shown in Figure 8.11 below.



Figure 8.11 - The stabilizer subsystem assembly

#### 8.4. System Assembly

Separate subsystems of the system are being connected using 2 M4 bolts with a length of 1.5 cm at the tail connection, and 4 M4 bolts with a length of 3.5 cm at the tail connector - main body - nosecone connection point. All connections should have a pre-designed opening for them. When bolts are inserted and secured with nuts, the system is assembled and ready.

Figures 8.11 and 8.12 on the next two pages show the final look of the EPC system probe in assembled and open view.



Figure 8.11 - The open view of the assembled EPC probe



Figure 8.12 - Assembled EPC probe system

## 9. Verification and validation

The important part of the system engineering is to ensure that the designed system meets requirements and expectations. It is completed during the verification and validation stage for each part, component, subsystem, and finally, the system after manufacturing or assembling them. Usually, it takes a team of people and access to testing facilities to evaluate how well parts perform in reality compared to how they were designed to perform; however, due to a lack of time and resources at the current stage of the project development, only sizing, weighting, and some functionality was tested.

### 9.1. Component Verification and Validation

#### 9.1.1. Nosecone Component V&V

The designed nosecone was successfully integrated with stators, proving the sizing of the openings. The dimensions of the prototype subparts were correct to integrate with each other without a problem, and they have a good structural integrity when tested with a point force in various directions. The maximum diameter of the nosecone is slightly under 6 inches.

Figure 9.1 - Force testing for the nosecone

#### 9.1.2. Compressor Component V&V

The compressor subparts were connected without a problem, while the blade integration had some issues. Some of the smaller blades were prone to breaking when pushed into openings, requiring the replacement of one of the compressor subparts.

#### 9.1.3. Gearbox V&V

The gearbox assembly required some redesigns of the first stage due to a lack of strength in the connection points between gears. After increasing the strength, the gearbox was working as designed, providing a 1 to 125 rpm increase with manual rotation of the first stage. Some refinements were made to the surface of the gears and their connections, which decreased the friction and made rotation easier and more stable.

Figure 9.2 - The testing handle for the gearbox

#### 9.1.4. Collector Unit V&V

The collector unit sizing was proper, combining all stages and collector plates into one unit. However, no proper way was found to test a real collector unit model, so the only results are available from the CFD simulations made in chapter 6.

In later verification, it was found that the outer shell has too much friction when integrated with the Body Frame subsystem and needs a slight adjustment in outer diameter to allow better integration.

## 9.2. Subsystem Verification and Validation

#### 9.2.1. Nosecone Subsystem V&V

The combination of components into the nosecone subsystem was not without issues. While the gearbox could be well integrated, the compressor was unable to fit into the nosecone due to the presence of stators. Since the components under V&V are the prototype ones, they could be separated and added subpart by subpart to allow the assembly. However, it would pose a problem if the non-prototype components were used.

#### 9.2.2. Body Frame Subsystem V&V

The body frame is assembled from several large parts, and there is no problem with the connection between the main frame and the tail connector. The collector unit appeared to be too thick to slide easily inside the body frame, and requires small adjustments in size.

After collector unit adjustment were done, it was able to slide and safely connect with the main frame before it was locked with the tail, by screwing m4

#### 9.2.3. Stabilizer Subsystem V&V

The stabiliser system had issues with the turbine integration, as the bearing and planetary gears could not fit into the gearbox. Therefore, the shaft was not tested since there is no way to generate torque without a working turbine. To integrate them, the turbine, gearbox, and shaft must be redesigned.

The airbrake was able to fit into its connections and be securely attached to the rest of the tail. Preliminary force tests showed that the tail is able to hold the force coming from the airbrake. However, it needs to be tested again when the rest of the parts are redesigned.

### **9.3. System Verification and Validation**

Despite the stabilizer not passing through V&V, the rest of the system can be tested for sizing, weight, and some of its functionality. The nosecone and body frame subsystems could be well integrated and attached to each other with M4 bolts mentioned in section 8.3.2. The manual torque generated by directly rotating the first-stage planetary connector was able to generate airflow by rotating the compressor. The airflow amount was insufficient to estimate how well the airflow goes through the collector unit.

## **10. Project Outcome and Future Work**

### **10.1. The Outcome**

At this stage, the EPC project is not likely to be cheaper or more efficient than some other methods of collecting extraterrestrial material, but it does have some benefits over other methods. Some parts of the probe could not pass through the verification and validation and will need more work to operate as intended. When finished, it could be tested in simulated flight conditions to verify electronics and used in a real launch similar to its predecessor. The probe is 26.6 inches; it has a low Cg, just 6 inches from the tip. From assembly estimations, the probe weighs 6.2 pounds, compared to 3.96 pounds from the last generation, and is just 2 inches longer than the MMC. The EPC probe is 56% heavier than the MMC, with 2.37 times more area and significantly improved airflow, accelerated by the newly introduced turbine-compressor system, which receives energy from the flow around it.

At this point, the project has established the main elements of the probe system required to collect and recover uncontaminated particles using a rocket launched in the stratosphere, allowing attempts to change or improve the collection system. Some new engineering solutions could be applied to those elements to attempt.

### **10.2. Future Work**

#### **10.2.1. Parts Design Iterations**

To improve the overall design for future iterations of the probe, more work will be required on each part in terms of design, testing, and V&V, and more iterations for each of them. Access to test facilities will also be needed to obtain real data.

#### **10.2.2. Parts Materials**

Certain parts, such as blades and gears, could use better materials or composites for better performance and higher reliability. Making the cloud also makes those parts smaller, potentially saving weight.

The material choice for the tail makes it prone to breaking if too much side force is applied, and should be reinforced with rods in the other direction of printing or light composites.

### 10.2.3. New Applications

A similar probe configuration could be used for quick air sampling at a specific altitude in case of urgent need to know the state of the air above the dangerous zone or unreachable areas.

### 10.2.4. New Challenges

As the project is only in its second iteration, many new challenges were also found in this iteration. First and foremost, the diametral limit due to using a rocket is a significant limitation for any probe with a fixed geometry. If there were a way to increase the area of the stabilizer and intake after the deployment of the probe, it could utilise more area for stabilization and air collection. It could be done using deployable and retractable struts with lightweight but durable material covered for collecting particles, which will be hidden when collection is finished.

Another direction of development could be improving the turbine-compressor system to allow more air to enter the collector, theoretically exceeding the area of the nosecone geometry.

## References

- [1] Della Corte, V., “DUSTER (Dust in the Upper Stratosphere Tracking Experiment and Return): A Balloon-Borne Dust Particle Collector,” *Memorie della Società Astronomica Italiana Supplementi*, Vol. 16, 2011, pp. 14. URL: <https://adsabs.harvard.edu/pdf/2011MSAIS..16...14D>
- [2] Ceplecha, Z., Borovička, J., Elford, W. G., Revelle, D. O., Hawkes, R. L., Porubčan, V., and Šimek, M., “Meteor Phenomena and Bodies,” *Space Science Reviews*, Vol. 84, 1998, pp. 327–471. <https://doi.org/10.1023/A:1005069928850>
- [3] Ceplecha, Z., “Fireballs as an Atmospheric Source of Meteoritic Dust,” *Interplanetary Dust and Zodiacal Light*, edited by H. Elsässer and H. Fechtig, Lecture Notes in Physics, Vol. 48, Springer, Berlin, Heidelberg, 1976. [https://doi.org/10.1007/3-540-07615-8\\_512](https://doi.org/10.1007/3-540-07615-8_512)
- [4] Love, S. G., and Brownlee, D. E., “A Direct Measurement of the Terrestrial Mass Accretion Rate of Cosmic Dust,” *Science*, Vol. 262, Oct. 1993, pp. 550–553. <https://www.jstor.org/stable/2882575>
- [5] Jenniskens, P., “Meteor Showers in Review,” *Planetary and Space Science*, Vol. 143, Sep. 2017, pp. 116–124. <https://doi.org/10.1016/j.pss.2017.01.008>
- [6] Jopek, T. J., and Kaňuchová, Z., “IAU Meteor Data Center—The Shower Database: A Status Report,” *Planetary and Space Science*, Vol. 143, Sep. 2017, pp. 3–6. <https://doi.org/10.1016/j.pss.2016.11.003>
- [7] Mane, P. B., and Mane, D. B., “Study of Aerosol Vertical Distribution During Meteor Showers of January 2009,” *Journal of Atmospheric and Solar-Terrestrial Physics*, Vol. 213, Feb. 2021, 105511. <https://doi.org/10.1016/j.jastp.2020.105511>
- [8] “Perseids – NASA Science,” NASA, URL: <https://science.nasa.gov/solar-system/meteors-meteorites/perseids/>
- [9] “Major Meteor Showers,” American Meteor Society, URL: <https://www.amsmeteors.org/meteor-showers/major-meteor-showers/>
- [10] Junge, C. E., Chagnon, C. W., and Manson, J. E., “Stratospheric Aerosols,” *Journal of Meteorology*, Vol. 18, Feb. 1961, pp. 81–108.
- [11] Schneider, J., Weigel, R., Klimach, T., Dragoneas, A., Appel, O., Hünig, A., et al., “Aircraft-Based Observation of Meteoric Material in Lower-Stratospheric Aerosol Particles Between 15 and 68° N,” *Atmospheric Chemistry and Physics*, Vol. 21, Jan. 2021, pp. 989–1013. <https://doi.org/10.5194/acp-21-989-2021>

- [12] Brownlee, D. E., “25th Annual Lunar and Planetary Science Conference,” *Lunar and Planetary Science XXV*, Vol. 126, Mar. 1994, pp. 183–184.
- [13] Tabata, M., Yano, H., Kawai, H., Imai, E., Kawaguchi, Y., Hashimoto, H., and Yamagishi, A., “Silica Aerogel for Capturing Intact Interplanetary Dust Particles for the Tanpopo Experiment,” *Origins of Life and Evolution of Biospheres*, Vol. 45, Mar. 2015, pp. 225–229.
- [14] Yamagishi, A., Yokobori, S., Kobayashi, K., Mita, H., Yabuta, H., Tabata, M., et al., “Scientific Targets of Tanpopo: Astrobiology Exposure and Micrometeoroid Capture Experiments at the Japanese Experiment Module Exposed Facility of the International Space Station,” *Astrobiology*, Vol. 21, Dec. 2021, pp. 1451–1460.
- [15] “ACP Collection Description,” NASA, URL:  
[https://curator.jsc.nasa.gov/dust/ACP\\_Collection\\_Description.cfm](https://curator.jsc.nasa.gov/dust/ACP_Collection_Description.cfm)
- [16] “Ares,” NASA, URL:  
<https://ares.jsc.nasa.gov/astromaterials-newsletter/vol3-no1/cosmic-dust-news.cfm>
- [17] “ER-2 High-Altitude Airborne Science Aircraft,” NASA, URL:  
<https://www.nasa.gov/centers-and-facilities/armstrong/er-2-aircraft/>
- [18] Denton, E., Hord, J., Jacobs, R., and Martell, E., *Preliminary Design, ENCAR-1 Rocket-Borne Cryogenic Air Sampler*, UCAR/NCAR Library, 1966.  
<http://n2t.net/ark:/85065/d74x575q>
- [19] Hedin, J., Gumbel, J., and Rapp, M., “On the Efficiency of Rocket-Borne Particle Detection in the Mesosphere,” *Atmospheric Chemistry and Physics*, Vol. 7, Jul. 2007, pp. 3701–3711.
- [20] “Technical Papers and Presentations,” COMSOL, URL:  
<https://www.comsol.com/paper/investigation-of-the-efficiency-of-a-supersonic-rocket-aerosol-collector-122001>
- [21] Le, T.-C., and Tsai, C.-J., “Inertial Impaction Technique for the Classification of Particulate Matters and Nanoparticles: A Review,” *KONA Powder and Particle Journal*, Vol. 38, Jan. 2021, pp. 42–63.
- [22] Sioutas, C., Ferguson, S. T., Wolfson, J. M., Ozkaynak, H., and Koutrakis, P., “Inertial Collection of Fine Particles Using a High-Volume Rectangular Geometry Conventional Impactor,” *Journal of Aerosol Science*, Vol. 28, Sep. 1997, pp. 1015–1028.
- [23] Plane, J. M., “Cosmic Dust in the Earth’s Atmosphere,” *Chemical Society Reviews*, Vol. 41, 2012, pp. 6507–6518.

- [24] Hunten, D. M., Turco, R. P., and Toon, O. B., “Smoke and Dust Particles of Meteoric Origin in the Mesosphere and Stratosphere,” *Journal of the Atmospheric Sciences*, Vol. 37, Jun. 1980, pp. 1342–1357.
- [25] Mallios, S. A., Drakaki, E., and Amiridis, V., “Effects of Dust Particle Sphericity and Orientation on Their Gravitational Settling in the Earth’s Atmosphere,” *Journal of Aerosol Science*, Vol. 150, Dec. 2020, 105634. <https://doi.org/10.1016/j.jaerosci.2020.105634>
- [26] “Earth’s Atmosphere: A Multi-Layered Cake,” NASA, URL: <https://science.nasa.gov/earth/earth-atmosphere/earths-atmosphere-a-multi-layered-cake/>
- [27] “Layers of the Atmosphere,” National Oceanic and Atmospheric Administration, URL: <https://www.noaa.gov/jetstream/atmosphere/layers-of-atmosphere>
- [28] “Earth Atmosphere Model – Metric Units,” NASA, URL: <https://www.grc.nasa.gov/www/k-12/airplane/atmosmet.html>
- [29] Heinsohn, R. J., and Cimbala, J. M., *Indoor Air Quality Engineering: Environmental Health and Control of Indoor Pollutants*, CRC Press, Boca Raton, FL, 2009.
- [30] Bradley, J. P., “Interplanetary Dust Particles,” *Treatise on Geochemistry*, Vol. 1, 2007, pp. 1–24.
- [31] De Laeter, J. R., “Cosmochemical Applications Using Mass Spectrometry,” *Encyclopedia of Spectroscopy and Spectrometry*, Vol. 1, 1999, pp. 359–367.
- [32] Flynn, G. J., Consolmagno, G. J., Brown, P., and Macke, R. J., “Physical Properties of the Stone Meteorites: Implications for the Properties of Their Parent Bodies,” *Geochemistry*, Vol. 78, Sep. 2018, pp. 269–298.
- [33] Bradley, J. P., Ishii, H. A., Gillis-Davis, J. J., Ciston, J., Nielsen, M. H., Bechtel, H. A., and Martin, M. C., “Detection of Solar Wind-Produced Water in Irradiated Rims on Silicate Minerals,” *Proceedings of the National Academy of Sciences*, Vol. 111, Jan. 2014, pp. 1732–1735.
- [34] Wertz, J. R., and Larson, W. J., *Space Mission Analysis and Design*, Microcosm Press/Kluwer Academic, Torrance, CA/Dordrecht, Netherlands, 1999.
- [35] Mattingly, J. D., *Elements of Propulsion: Gas Turbines and Rockets*, Knovel, Norwich, NY, 2007.
- [36] Friends of Amateur Rocketry, Inc., URL: <https://friendsofamateurrcketry.org>

[37] Megner, L., Rapp, M., and Gumbel, J., “Distribution of Meteoric Smoke—Sensitivity to Microphysical Properties and Atmospheric Conditions,” *Atmospheric Chemistry and Physics*, Vol. 6, Oct. 2006, pp. 4415–4426.

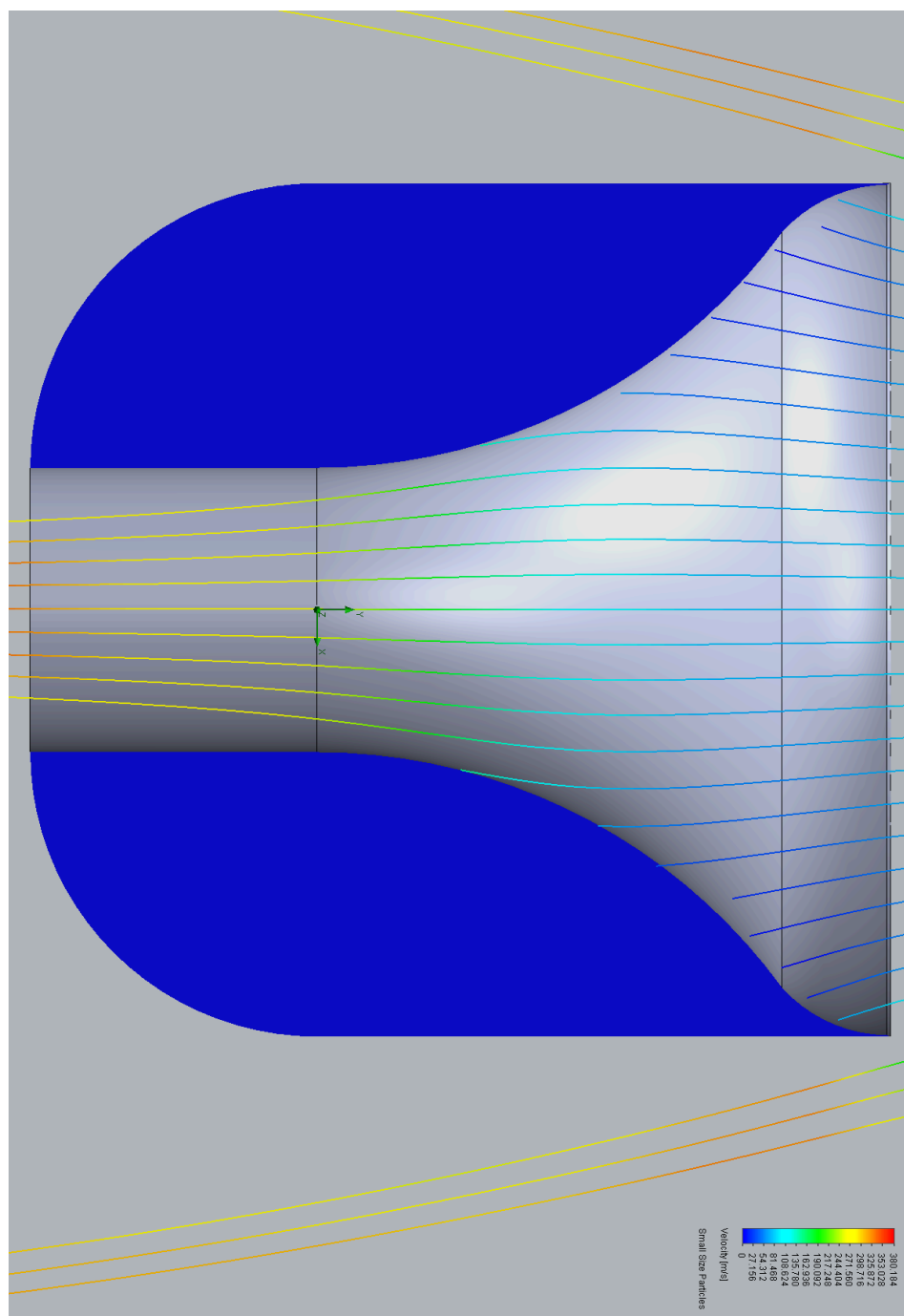
[38] Pilat, M. J., “UW Faculty Web Server,” University of Washington, URL:  
<https://faculty.washington.edu/mpilat/opman.htm>

[39] Garcia-Jares, C., Barro, R., and Llompert, M., “Indoor Air Sampling,” *Comprehensive Sampling and Sample Preparation*, Vol. 1, 2012, pp. 125–161.

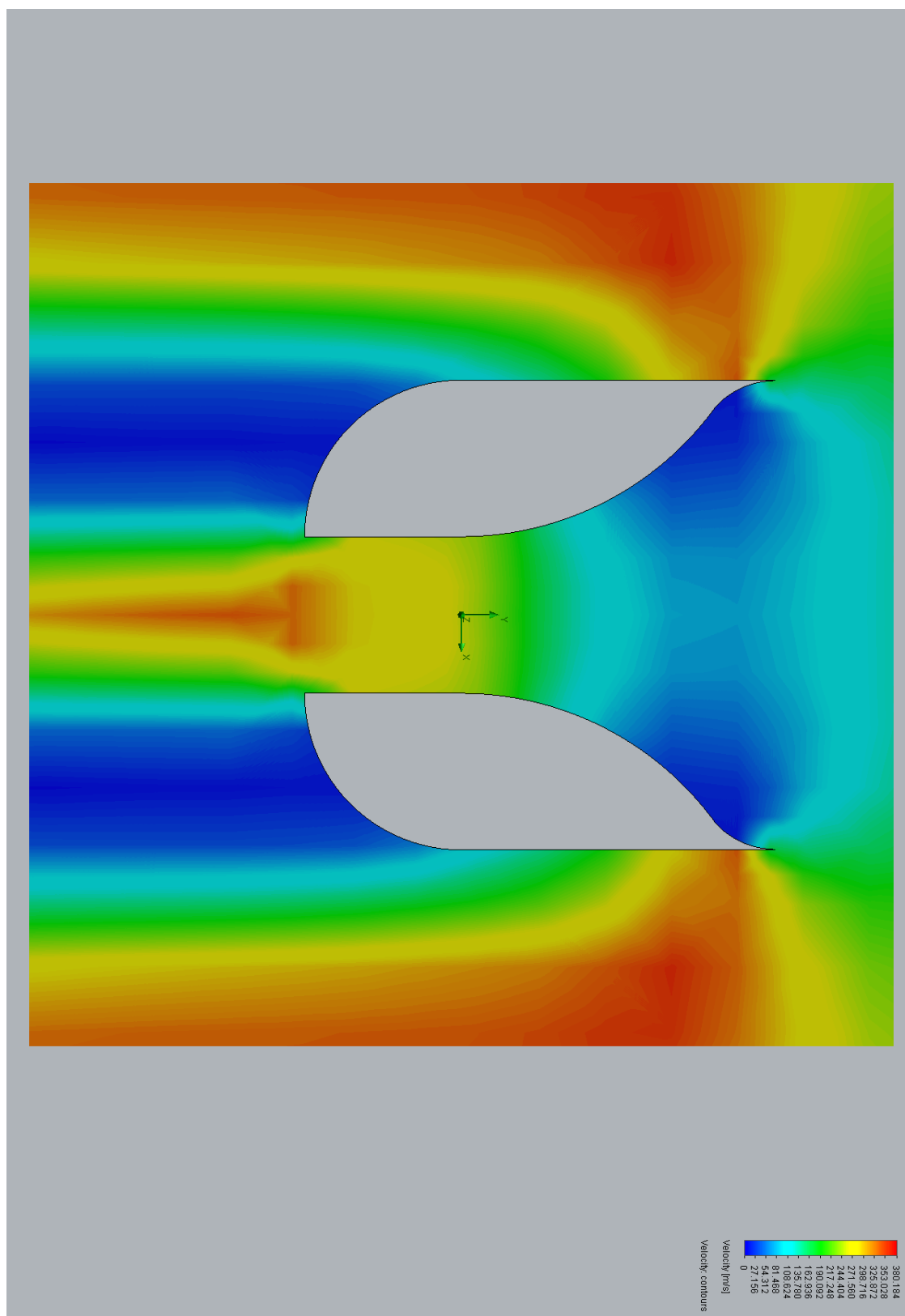
[40] Ayrilmis, N., “Effect of Layer Thickness on Surface Properties of 3D Printed Materials Produced from Wood Flour/PLA Filament,” *Polymer Testing*, Vol. 71, Oct. 2018, pp. 163–166.

[41] Boyce, M. P., *Introduction: Axial-Flow Compressors*, Gas Turbine Handbook, U.S. Department of Energy, URL:  
<https://www.netl.doe.gov/sites/default/files/gas-turbine-handbook/2-0.pdf>

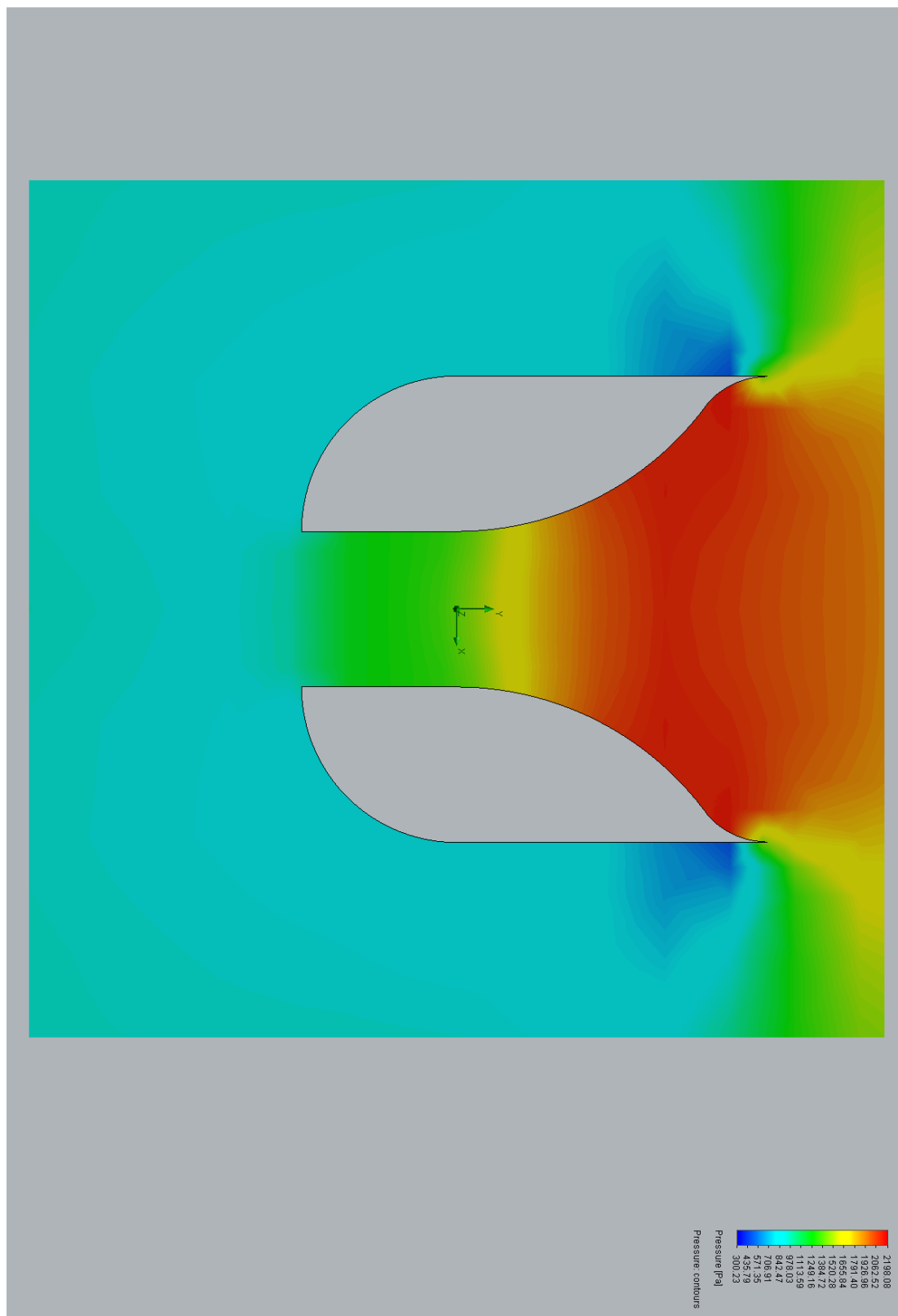
# **Appendix A - Component geometries and CFD simulation results for component analysis**



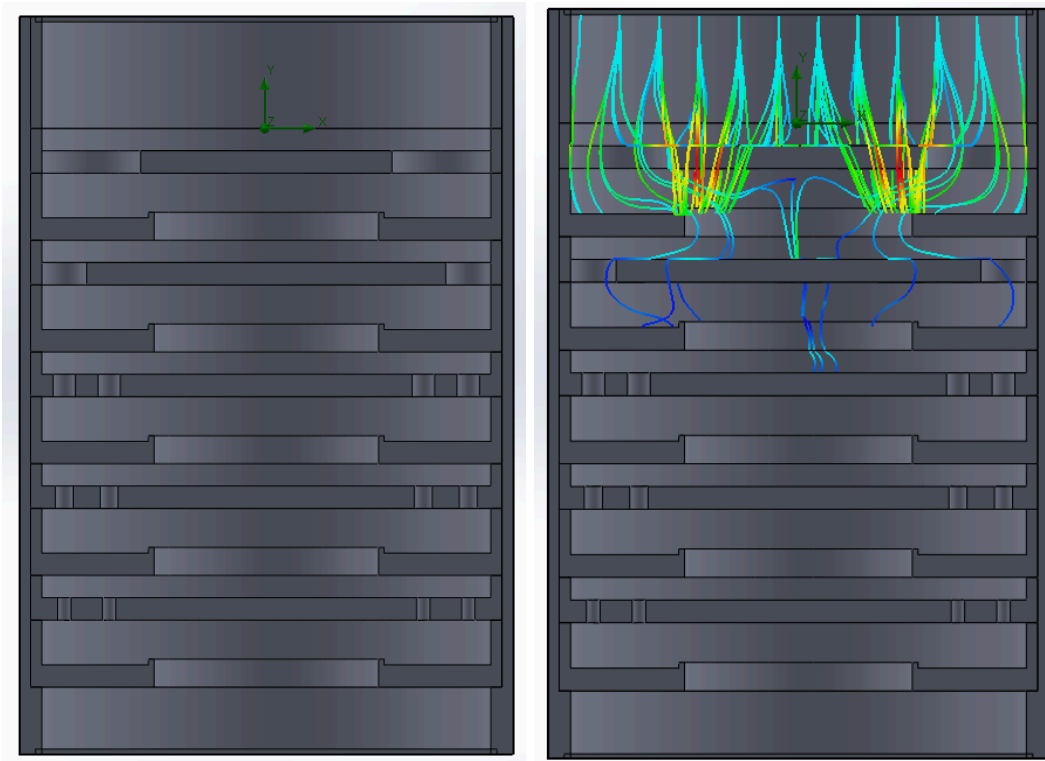
A1.1 - Micrometeorite particles for the nosecone case number 3



A1.2 - Velocity of the flow for the nosecone case 3

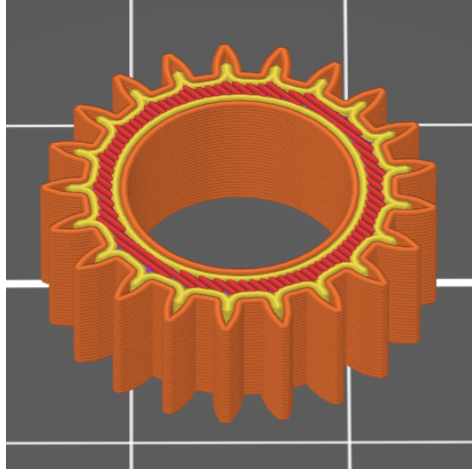


A1.3 - Pressure distribution for the nosecone case 3

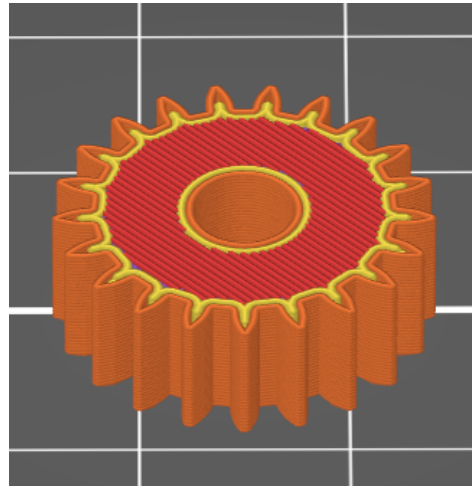


A2.1 - Iteration 1 of the cylindrical multiple openings per stage collector design

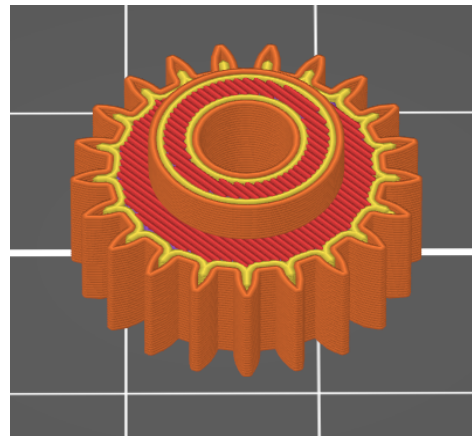
# **Appendix B - Parts in Slicer Before Manufacturing**



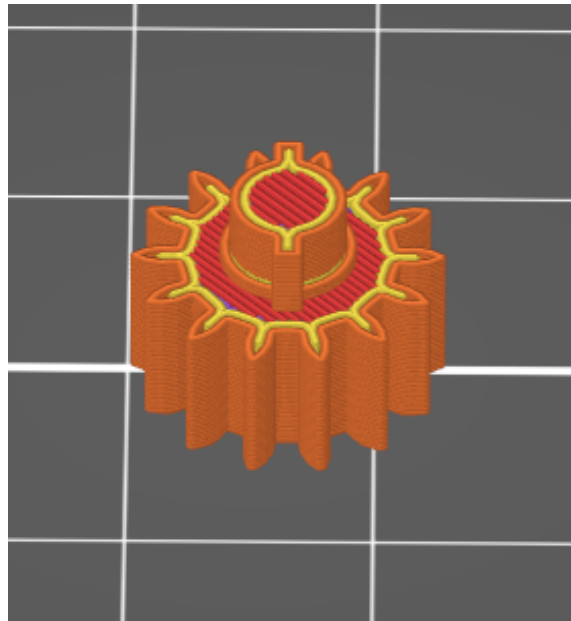
B1.1 - Planetary Gear First Stage



B1.2 - Planetary Gear Middle Stage



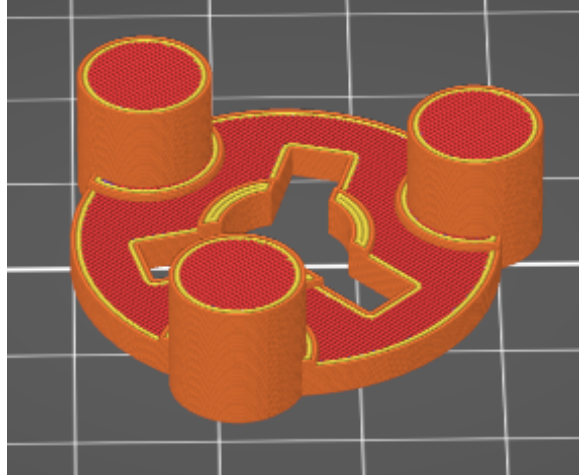
B1.3 - Planetary Gear Last Stage



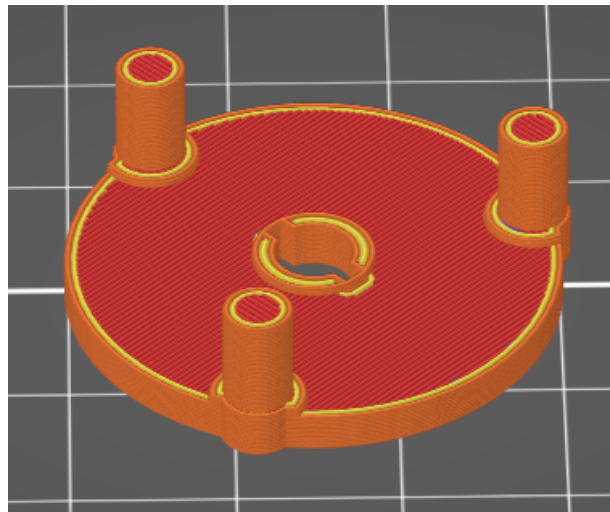
B2.1 - Sun Gear for First and Middle Stage



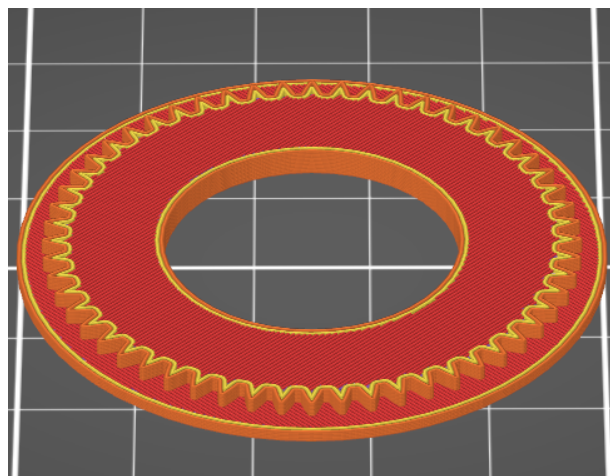
B2.2 - Sun Gear Last Stage



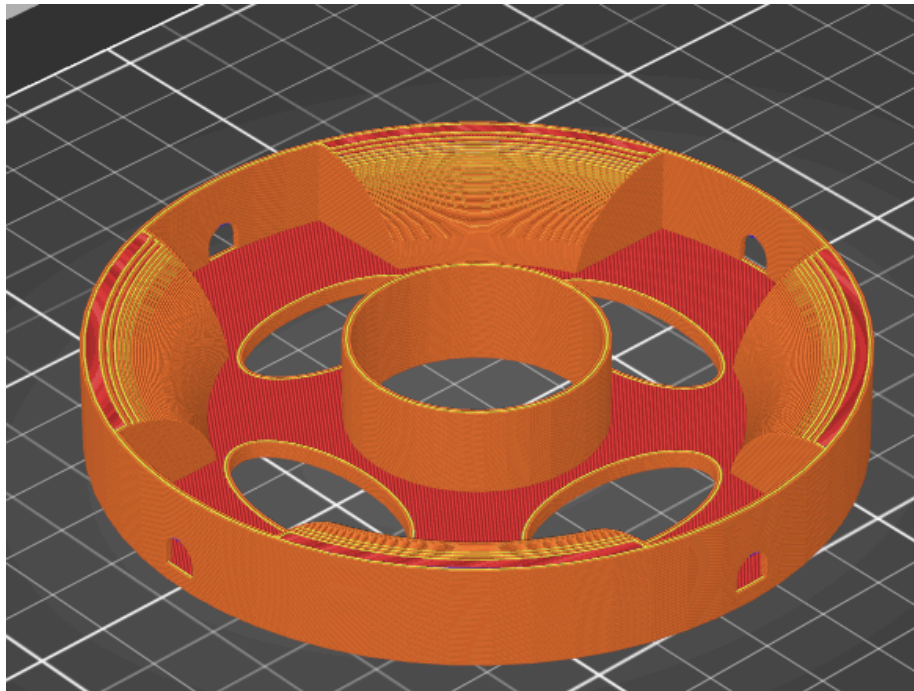
B3.1 - Planetary Gear Connector First stage



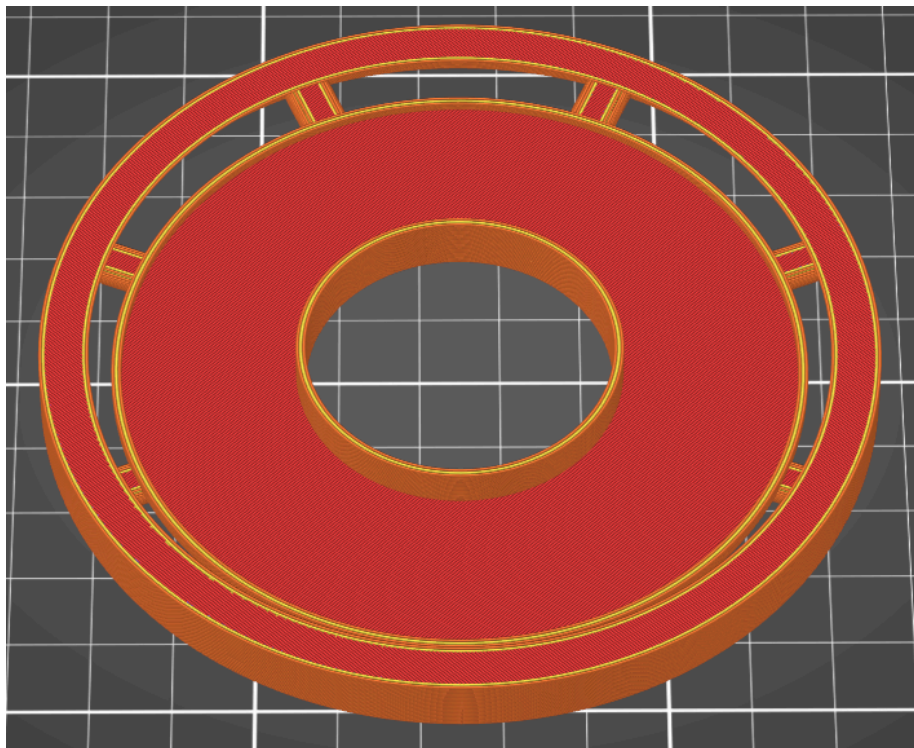
B3.2 - Planetary Gear Connector for Middle and Last Stage



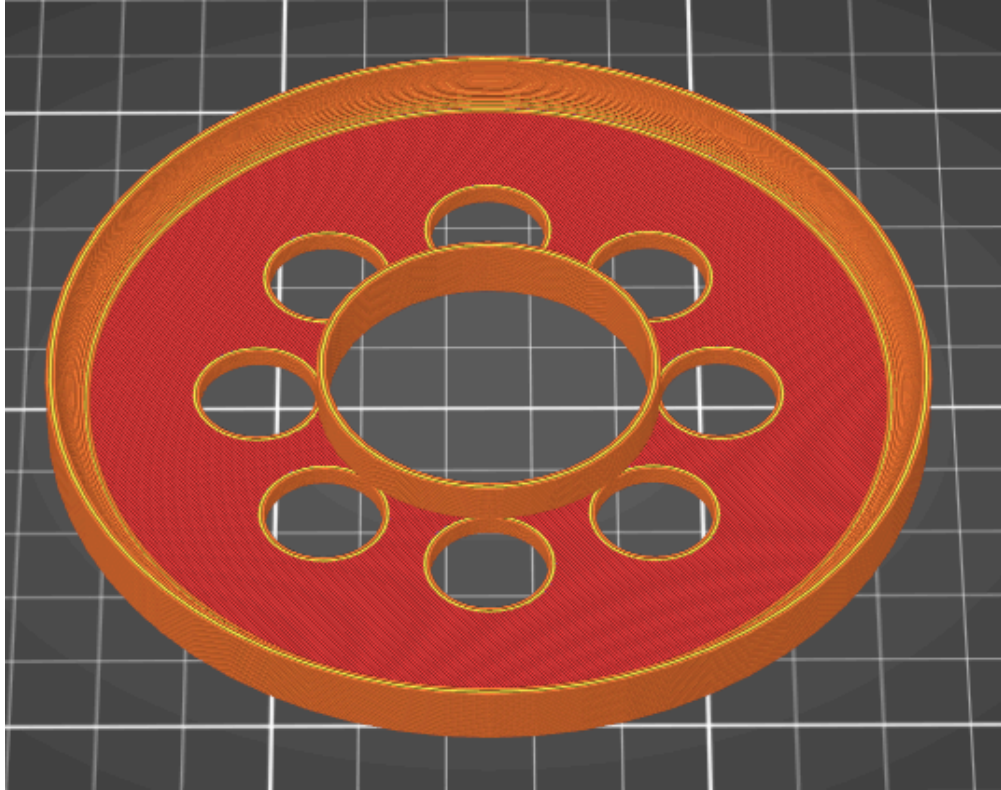
B4.1 - Ring Gear Cover



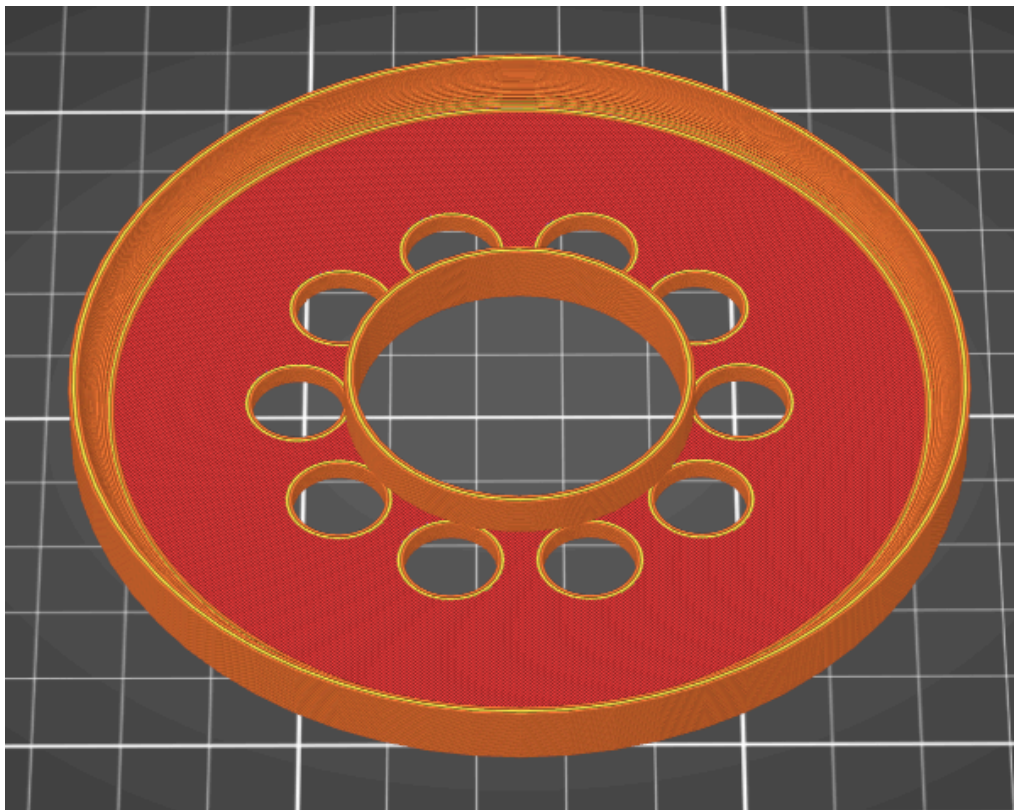
B5.1 - First Stage



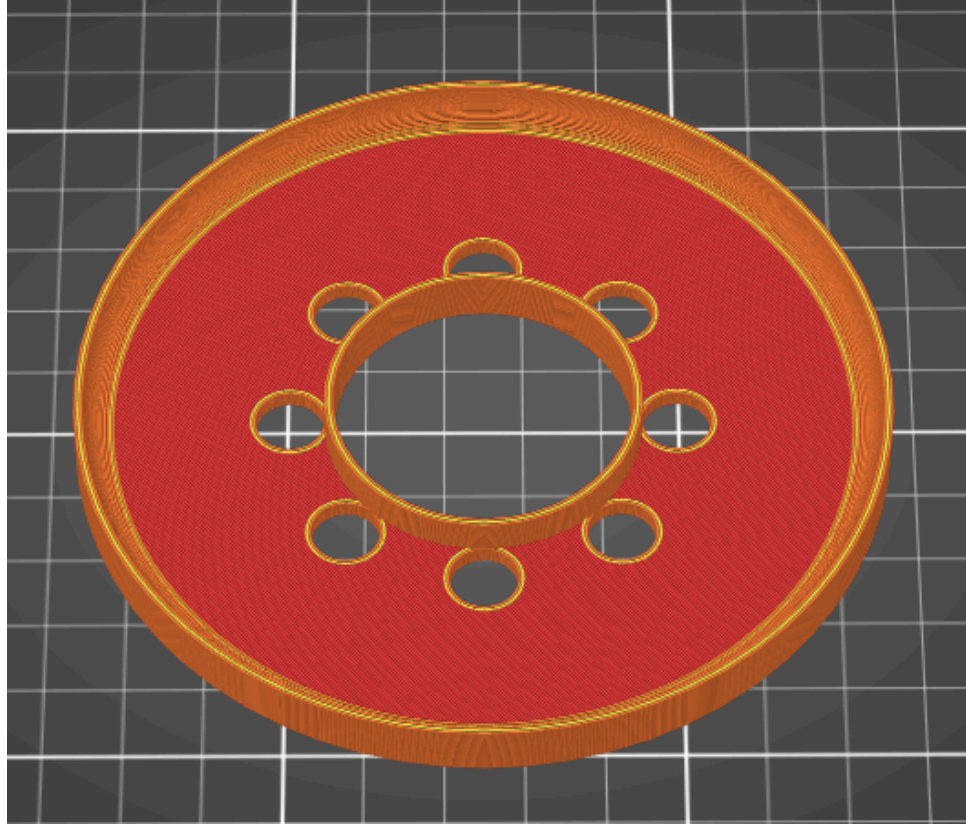
B5.2 - Collector Plate First Stage



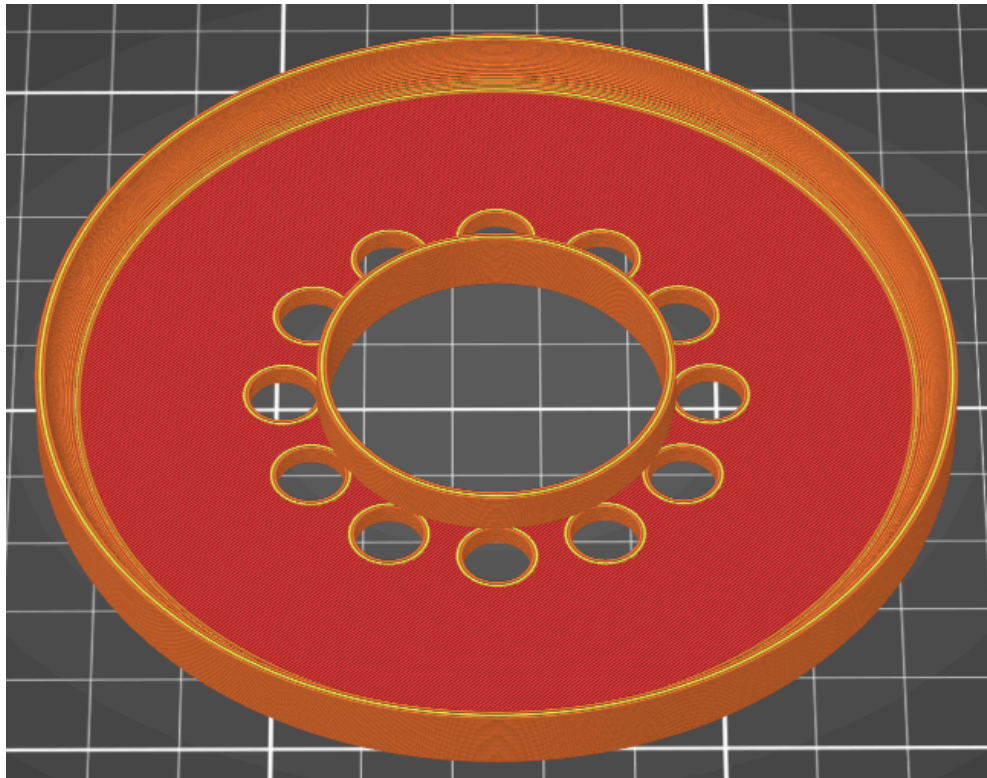
B5.3 - Second Stage



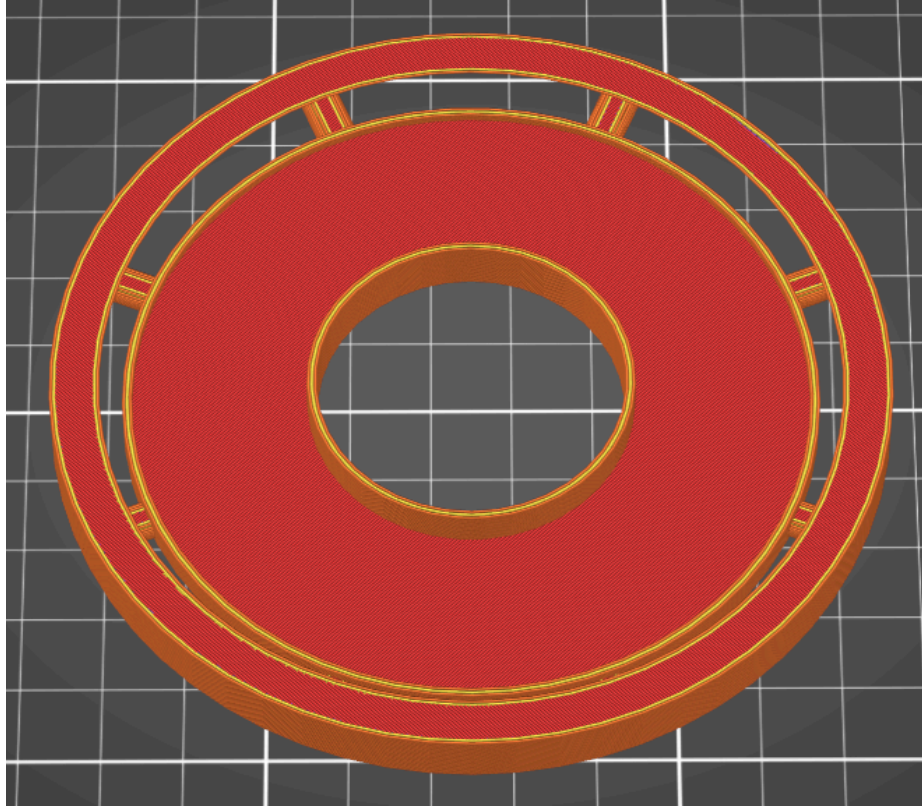
B5.4 - Third Stage



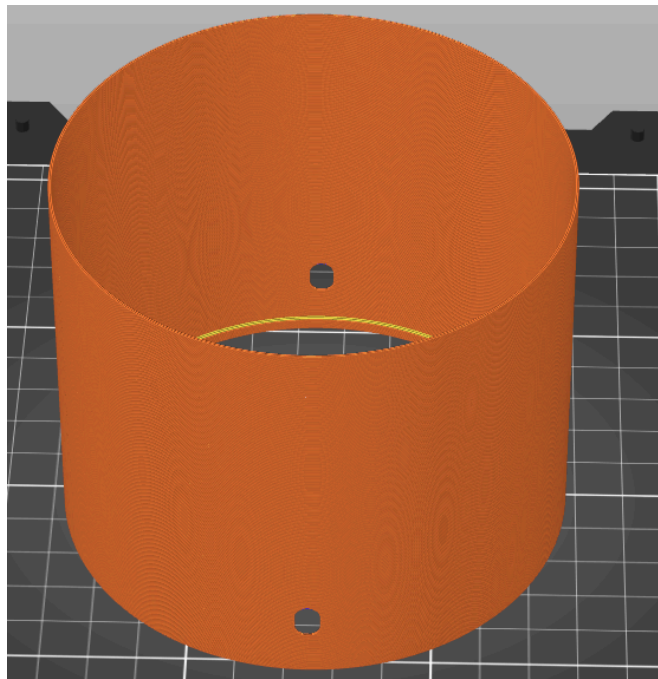
B5.5 - Fourth Stage



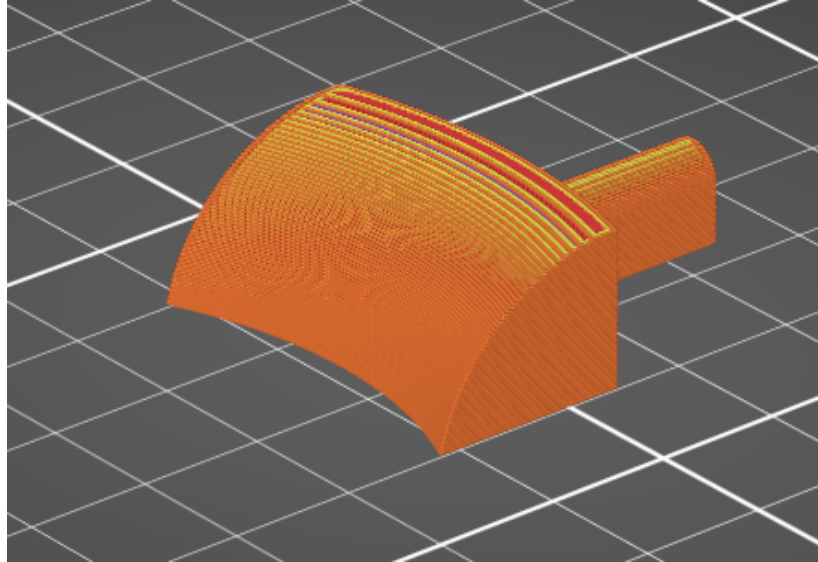
B5.6 - Fifth Stage



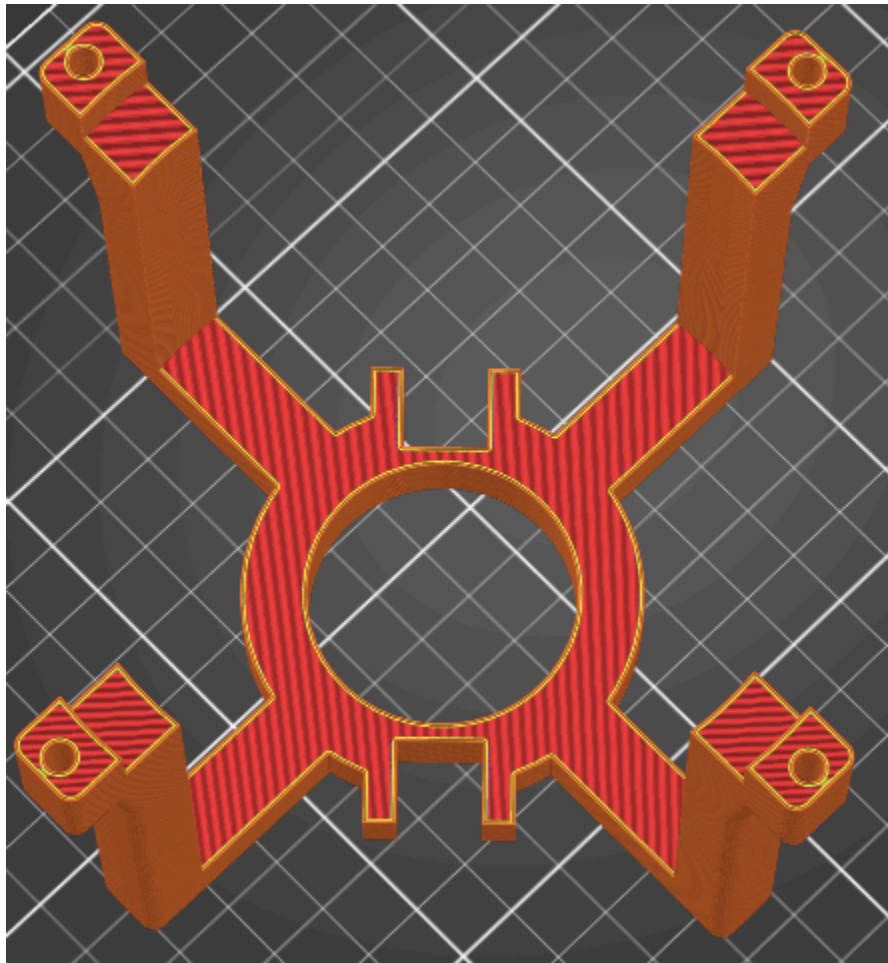
B5.6 - Stage Collector Plate



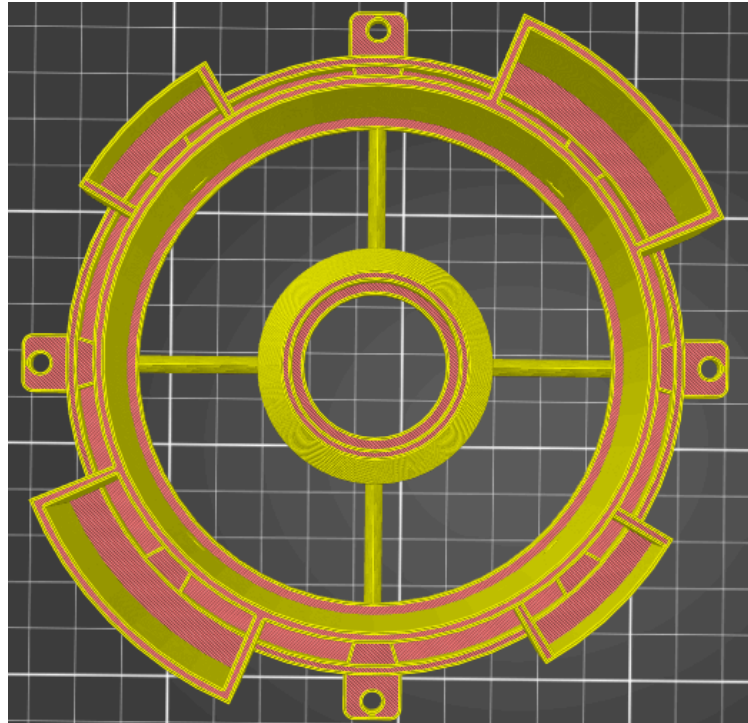
B6.1 - Outer Shell



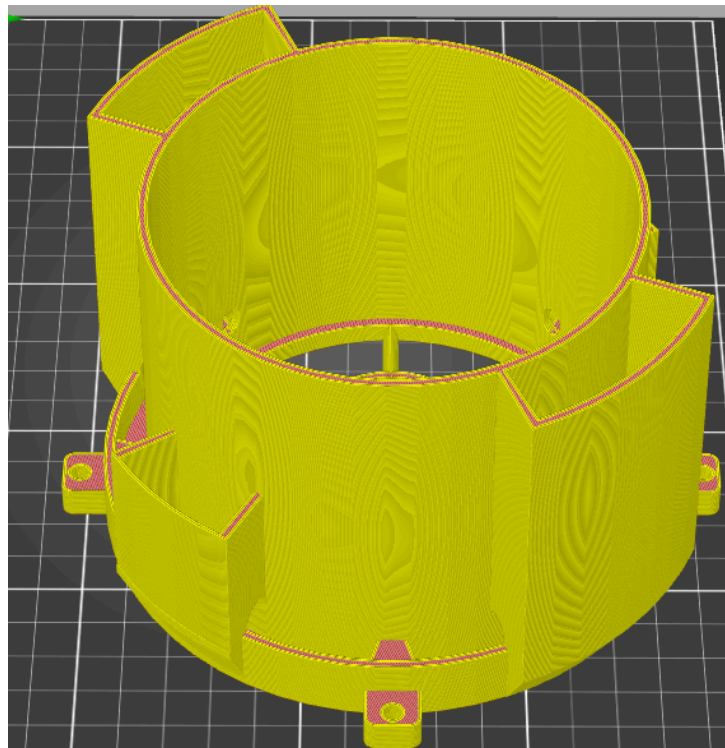
B6.2 - Collector Unit Sealer



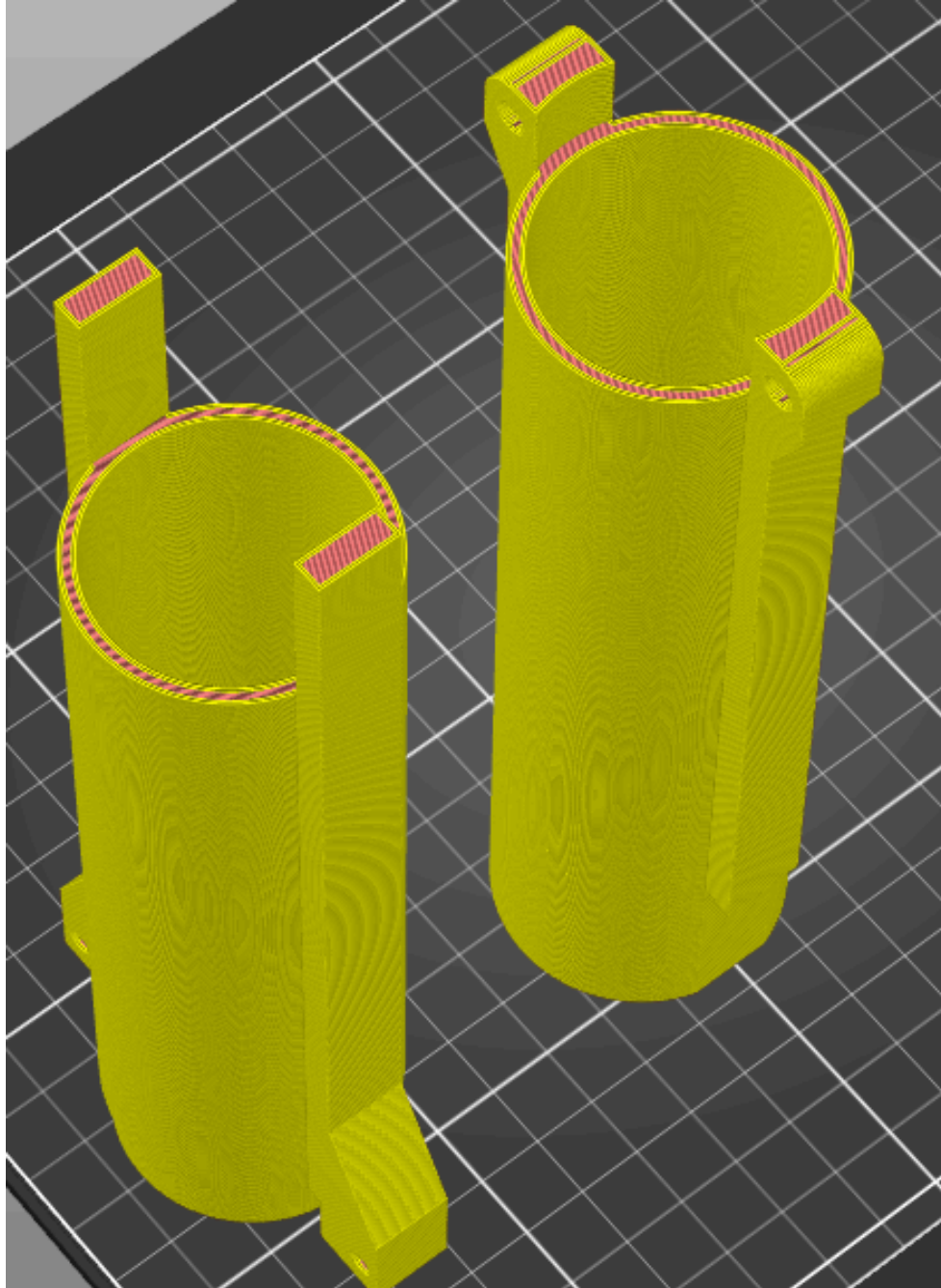
B7.1 - Tail Connector



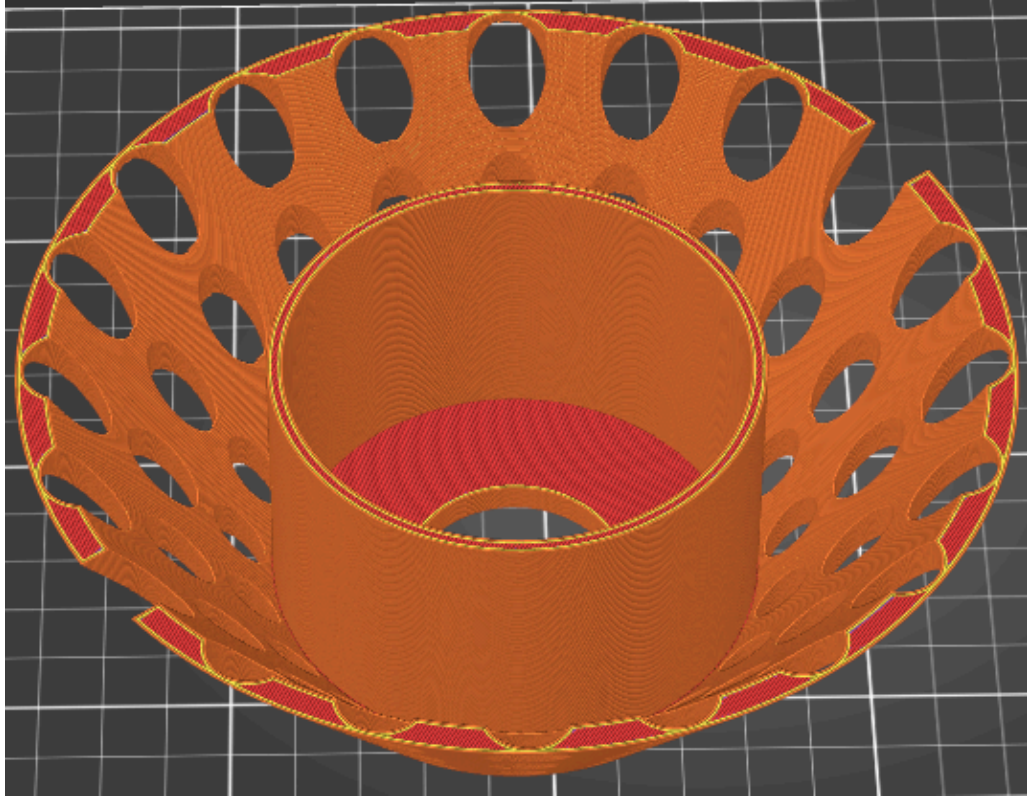
B7.2 - Main Body view from top



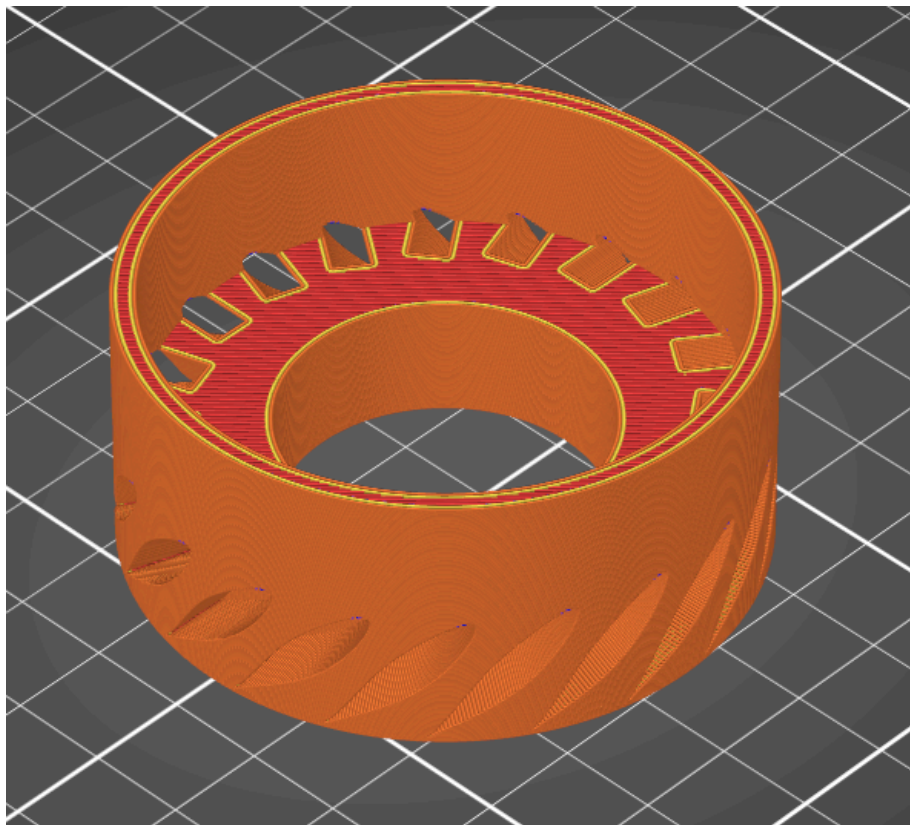
B7.3 - Main Body view from side



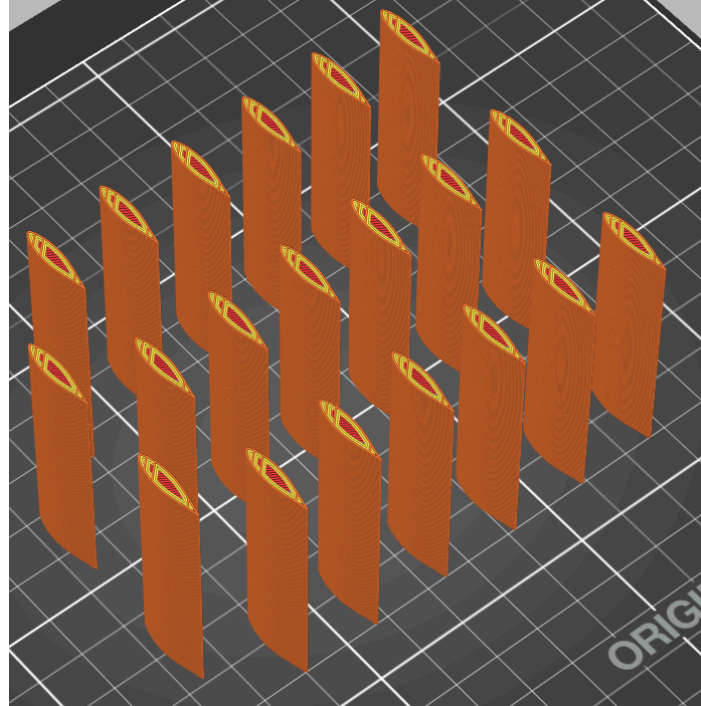
B8.1 - Tail Structure Part 1 and 2



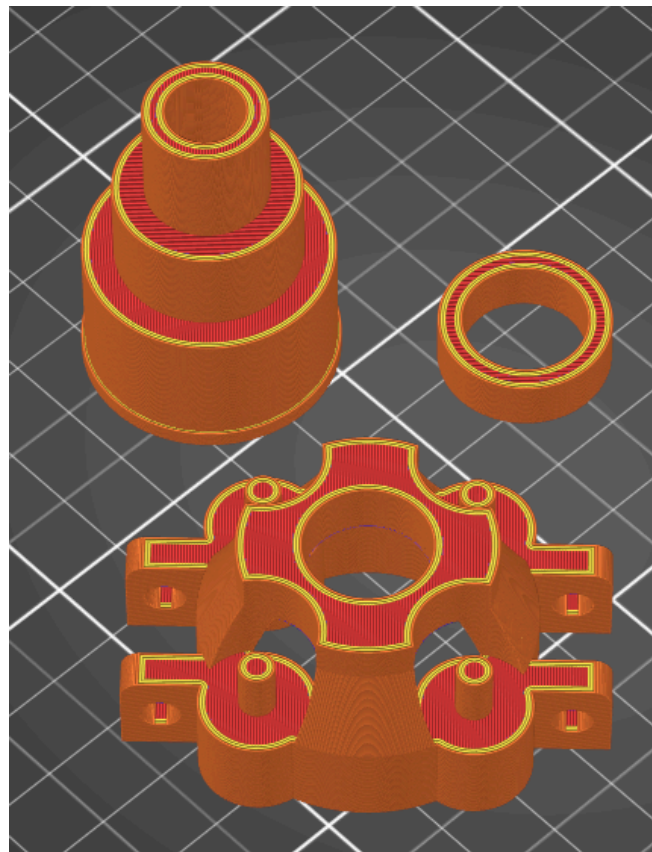
B8.2 - Tail Airbrake



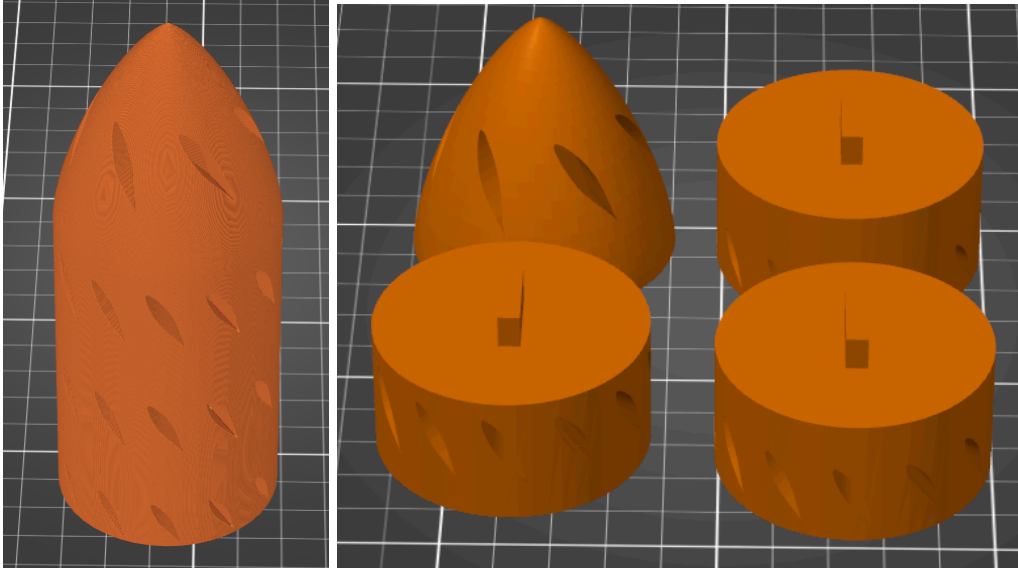
B8.3 - Tail Turbine



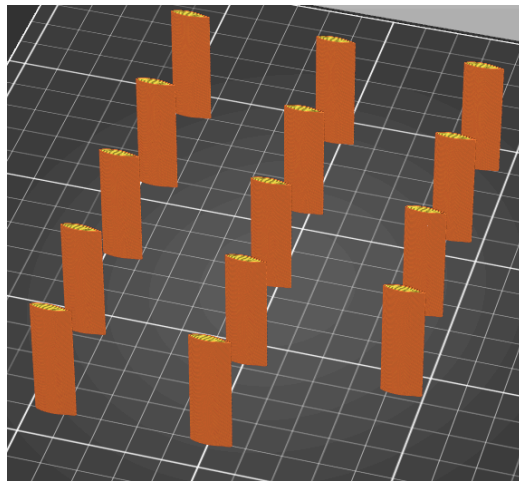
B8.4 - 20 Tail Turbine Blades



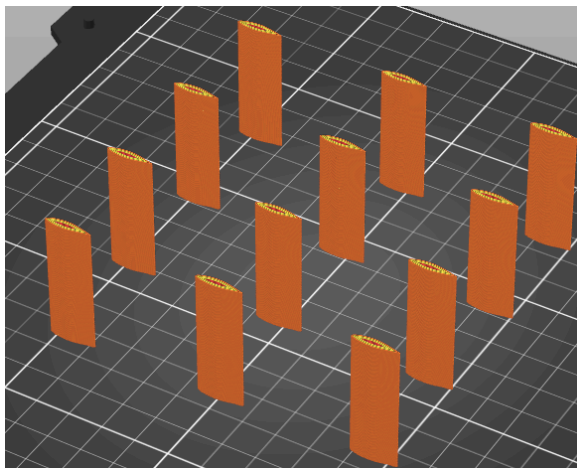
B8.5 - Tail Turbine Holder Part 1,2, and 3



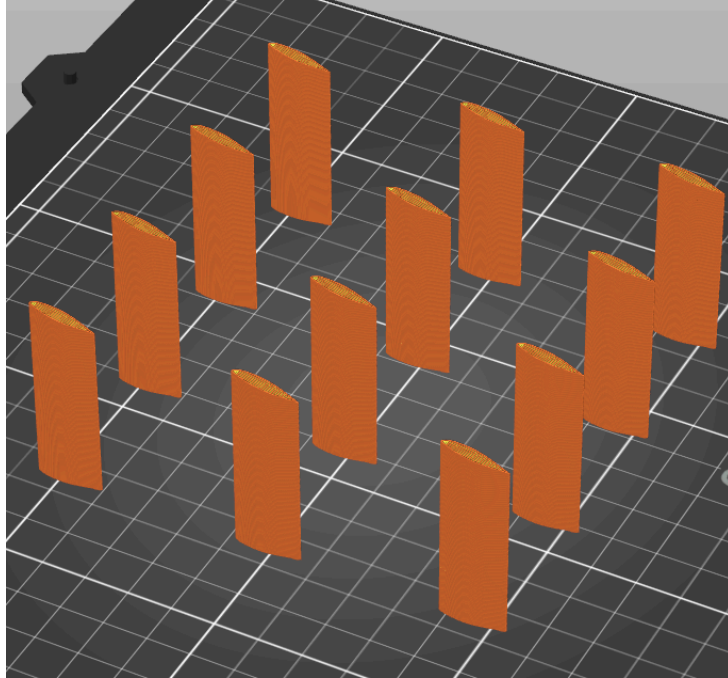
B9.1 - Compressor Von Karman Nosecone as a single part and four subparts



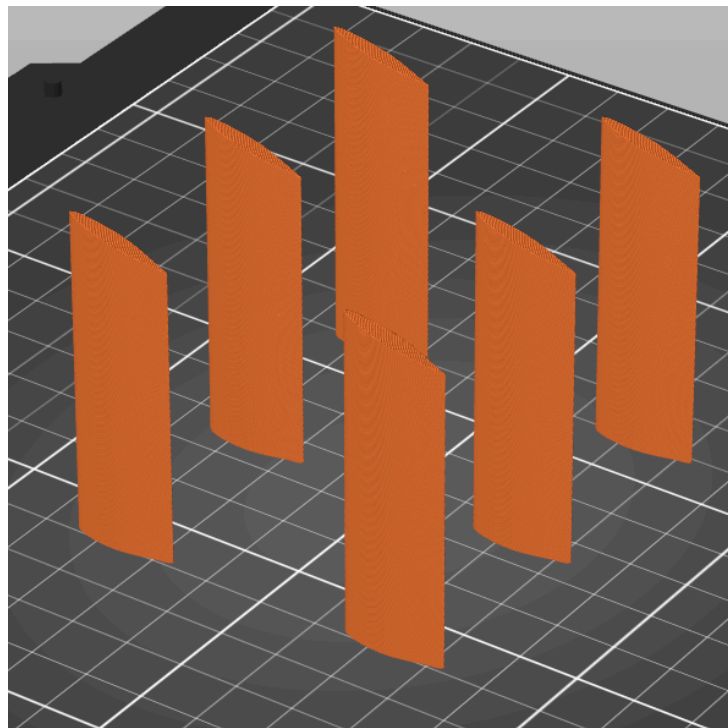
B9.2 - 14 NACA 65-221 (C=0.5 in) Rotor Blades



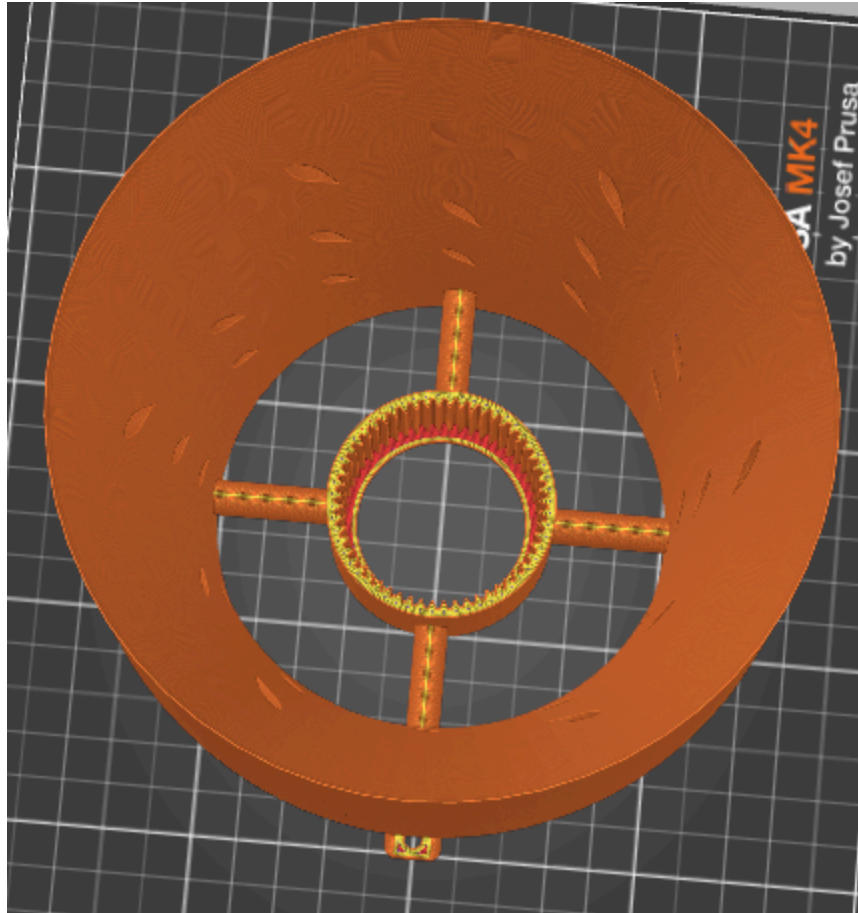
B9.3 - 12 NACA 65-221 (C=0.6 in) Rotor Blades



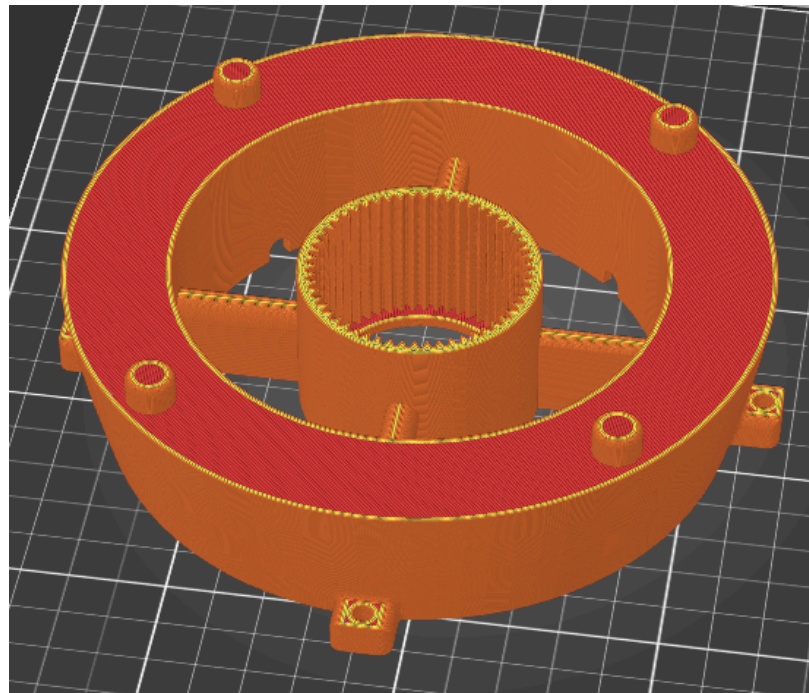
B9.4 - 12 NACA 65-221 ( $C=0.65$  in) Rotor Blades



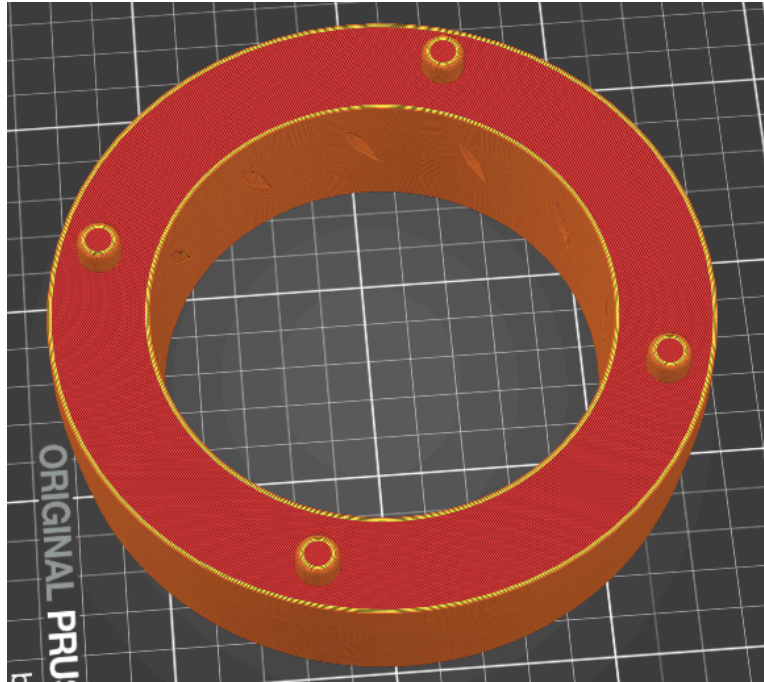
B9.5 - 6 NACA 65-221 ( $C=0.75$  in) Rotor Blades



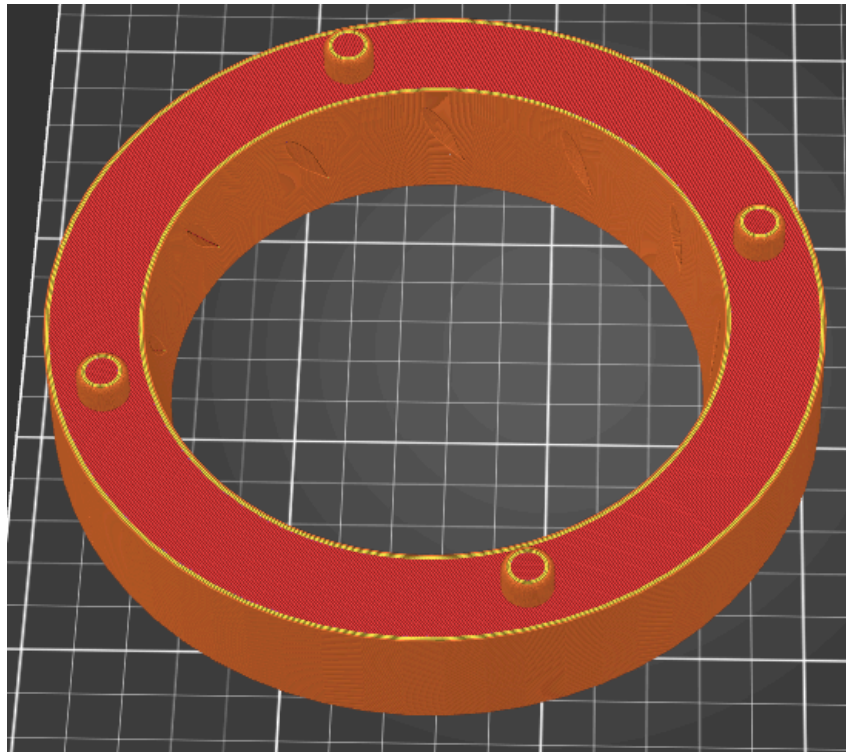
B10.1 - Nosecone with a ring gear



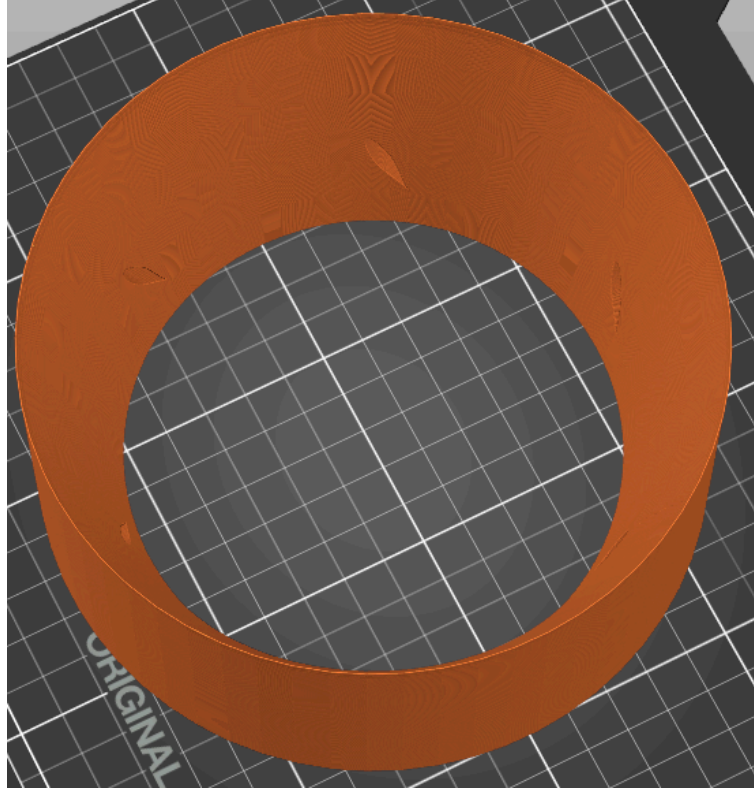
B10.2 - Nosecone with a ring gear subpart 1



B10.3 - Nosecone with a ring gear subpart 2



B10.4 - Nosecone with a ring gear subpart 3



B10.5 - Nosecone with a ring gear subpart 4

**Appendix C - Manufactured Parts  
Now Included in Chapter 8**



C1.1 - Collector unit parts



C1.2 - Gears and planetary connectors



C1.3 - Compressor subparts